IMPACT RESISTANCE OF FILLED CONCRETE BOX SECTIONS

A THESIS
SUBMITTED TO THE FACULTY OF THE GRADUATE SCHOOL
OF THE UNIVERSITY OF MINNESOTA
BY

CHRISTOPHER MICHAEL BRUHN

IN PARTIAL FULFILLMENT OF THE REQUIREMENTS
FOR THE DEGREE OF
MASTER OF SCIENCE

DR. ERIC SCOTT MUSSELMAN

August 2013

Dedication

This thesis is dedicated to my parents because it is truly them who made this and all that I do possible.

Abstract

The purpose of this research is to analyze the effects of drop-weight impact tests on filled concrete box sections. Research in other areas of soil filled container walls has proved favorable in blast loading environments suggesting a concrete system may also work well. In the experiment, thirty different box sections were cast and broken via drop weight test with six different fill materials. The testing yielded that compacted sand is the most favorable fill material for the sections. The research results indicate that further testing and applications should use compacted sand as a fill material.

Table of Contents

List of Tables

List of Figures

Chapter One: Introduction

1.1 Background

Studies of the impact resistance of concrete have been conducted since the early 1970s. The area of study provides insight into how various types of concrete and concrete structure behave under dynamic loads. A type of structure where this behavior would be important is a safe yet economical impact and blast shelter in military conflict areas.

The growing use of improvised explosive devices (IEDs) in today's warfare is of great and growing concern to the United States military. IEDs are essentially improvisational bombs that can combine destructive explosives, chemical and biological toxins, or radiological [1]. These elements can be combined in a number of ways to custom tailor weapons for different applications.

IEDs saw their first use as early as World War II when Belurussian guerillas used the devices to derail thousands of German trains during 1943-1944 [2]. Use of IEDs has continued all across the globe since WWII until the present day. During the Vietnam War, the Viet Cong used IEDs against both land and river vehicles and also against other troops [3]. In the aforementioned war, a total of twenty-eight percent of deaths were attributed to mines which also included IEDs.

A twenty-eight percent death rate in Vietnam is certainly a considerable margin, but it is shadowed in comparison to the rates of the recent Iraq War and Afghanistan War of the 2000s. As the Washington Post reported in 2007, a new high in IED use, sixty-nine percent of total United States wounded and sixty-three percent total killed in action were caused by IEDs [4].

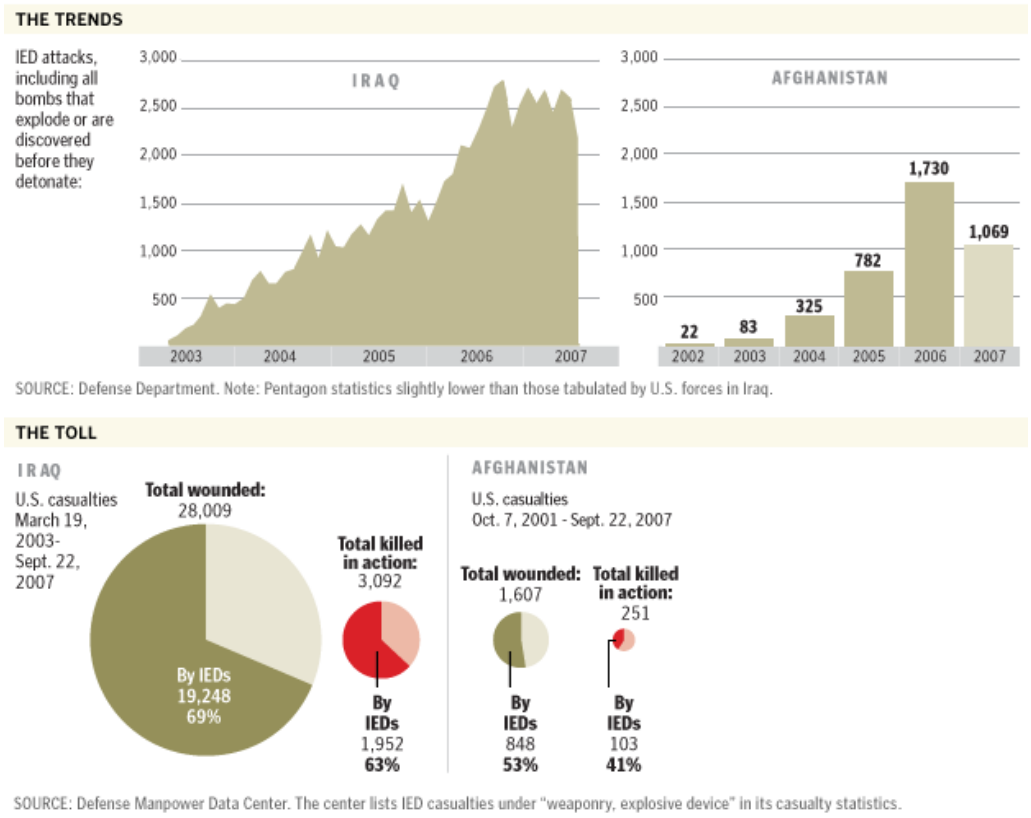

Fig. 1-1
Trends of IED deaths and injuries during the Iraq and Afghanistan conflicts of the 2000s.
Image: The Washington Post - September 30, 2007

A good portion of these deaths are not related to roadside bombs which suggest that a stationary, concrete, impact and blast resisting system would result in a reduction in the number of deaths and injuries.

1.2 Current Temporary Blast and Impact Resisting Structural Systems

There are many structures with varying degrees of economy, quickness of build, and provided strength and shelter that are used for military applications. One structural system is called HESCO bins (or bastions). A HESCO bin is essentially a welded-wire framing structure with a geo-textile material that sits inside of it (see Figure 1-2). The open volume of the container is then filled with sand. HESCO bins are popular, low-cost, safe, and fast dynamic loading resistant systems for the battlefield and other applications.

HESCO markets a system called the HAB (HESCO Accommodation Bunker) designed to provide both side and overhead protection [5]. The systems are rated for blast and fragmentation with testing being conducted with large mortar rounds [5]. The testing yielded no penetration of the fragmentation into the living space [5]. The success of HESCO bins for blast and impact suggest that a hybrid system of concrete *and* soil/aggregate could be an economical and readily available option.

Fig 1-2
Hesco bin being filled w/ front end loader
Image: http://xbradtc.wordpress.com, 2008

1.3 Research Objectives and Motivation

As discussed previously, there is a need for a safe yet quick and economical system to resist impacts, blasts, and dynamic loadings on the battlefield and the objective of this research is to determine if filled concrete box sections could fulfill this need. The project evaluates a component of a larger proposal that had been submitted to both the National Science Foundation (NSF) and the Leonard Wood Institute (LWI). The objective of the larger project was to evaluate the effectiveness of a modular, precast blast wall. The wall would be composed of box sections filled with readily available materials then post-tensioned together to create a wall of desired size. Figure 1-3 shows the modular wall system as it was presented in the original proposal.

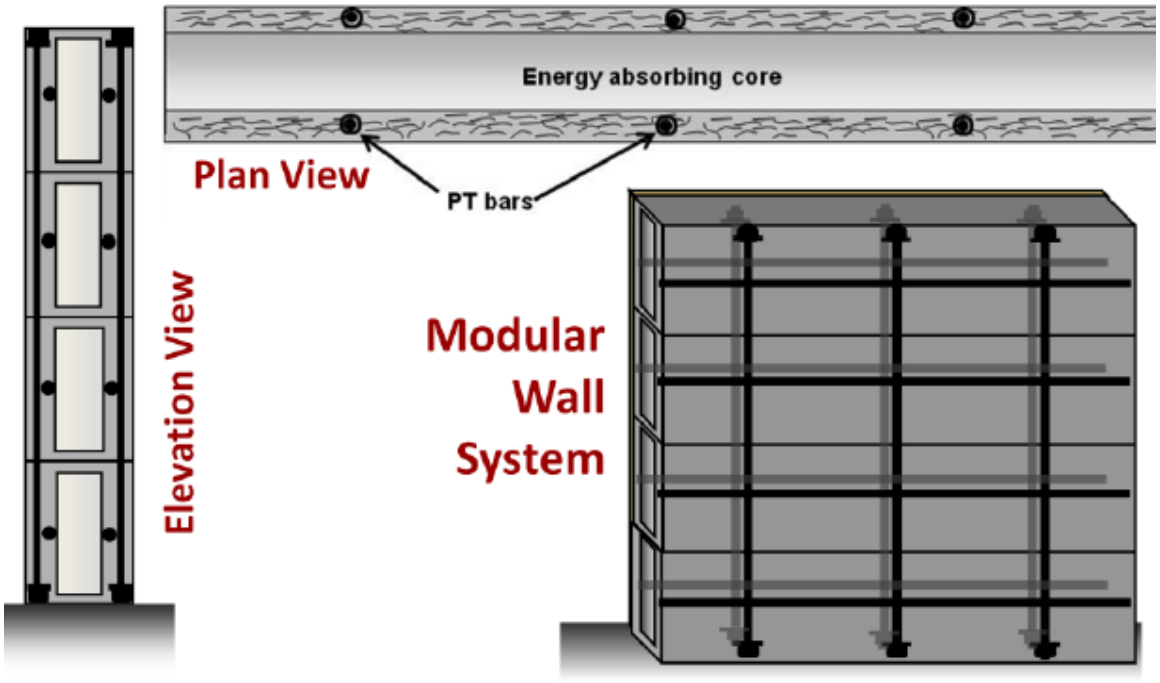

Fig 1-3
Proposed modular wall system

Research for this system in its entirety was denied funding from both institutions with one comment citing that not enough fundamental knowledge was available of the impact characteristics of filled concrete sections. This research project and thesis aims to quantify the advantages of filled concrete sections and their ability to resist dynamic loading.

1.4 Experimental Testing and Analysis

The properties of the filled concrete box sections were examined by several methods. The concrete boxes themselves were cast 12 days prior to the testing process. Seven

categories of fill material were devised for the tests based on practical availability: compacted and uncompacted soil, compacted and uncompacted sand, coarse aggregate, river gravel (rounded aggregate), and a control (empty box section). Each test specimen was tested with a 2 inch diameter, cylindrical impacting head and also a 3x6 inch rectangular plate, providing a total of 28 test specimens.

The concrete mix used was a very basic design and was constant for each box section. Mild steel reinforcement for the sections was provided by 6x6 inch conventional welded wire. Upon testing, data was taken from four, 50,000 lb capacity piezoelectric load cells measuring volts to be converted to force. High speed video was also taken with velocity and acceleration tracking capabilities of the impacting head.

1.5 Thesis Organization

The presentation of the report is broken down into five chapters and a supplementary appendix. Chapter one provides an introduction to blast and impact resistance structures and their application and aims to set up a background for the proceeding research. Chapter two explores relevant literature relating to the research and what useful data has already been collected on the topic. Chapter three outlines the procedures and methods of the experiment and gives an account of how the data, test specimens, etc were processed. The fourth chapter presents the raw visual data i.e. pictures of the test specimens at various stages of testing. Supplemental writing will accompany the visual data where applicable. The fifth chapter includes quantification of the results and

conclusions of the experiment. The appendix contains the entire load cell, velocity, and acceleration plots and any other relevant information not included in the thesis.

Chapter Two: Literature Review

There are a small collection of studies that help reinforce the main principle of this research. The field of impact resistance and dynamic loads on concrete is relatively young therefore most of the supporting papers and studies are fragments of the overall research presented in this thesis.

2.1 Effects of Strain Rate on Concrete Strength

Strain-rate or load-rate sensitivity is an important consideration for a material exposed to dynamic loads. Strain rate effects are induced in a material in the event of a high-amplitude, short-duration impulse load [6]. Typically, a material will exhibit a hardening effect when exposed to this type of impulsive load. The strain rate sensitivity of concrete was studied by Ross, Tedesco, and Kuennen [6] and will be covered in depth.

To establish a proper relationship of strain rate in concrete, a suitable testing mechanism was needed. The test setup needed to be able to accurately portray dynamic load effects in the field. The criteria for dynamic load effects aimed to be reproduced in the lab were "conventional weapons explosions, accidental explosions, and high-speed impacts" [6]. Other knowledge needed to properly analyze and model these type of load events were "dynamic material properties, response mechanisms, fracture mechanics, and constitutive relations" [6].

The testing setup chosen to best represent the field response in the lab was the split-Hopkinson pressure bar (SHPB). This test setup consists of a specimen placed between two straight bars, the incident and transmitted bar. A dynamic load is generated in the system in the form of a stress wave which travels through the incident bar into the specimen. This wave travels into the specimen but is broken into two waves upon reaching it. One wave travels through the specimen and into the transmitter bar and the other is reflected by the specimen back through the incident bar. The main underlying assumption of the SHPB test is that the "stresses in the specimen are uniformly distributed along the length and through the cross sectional area of the specimen" [6]. Schematics of this particular test setup are below in Fig 2-1.

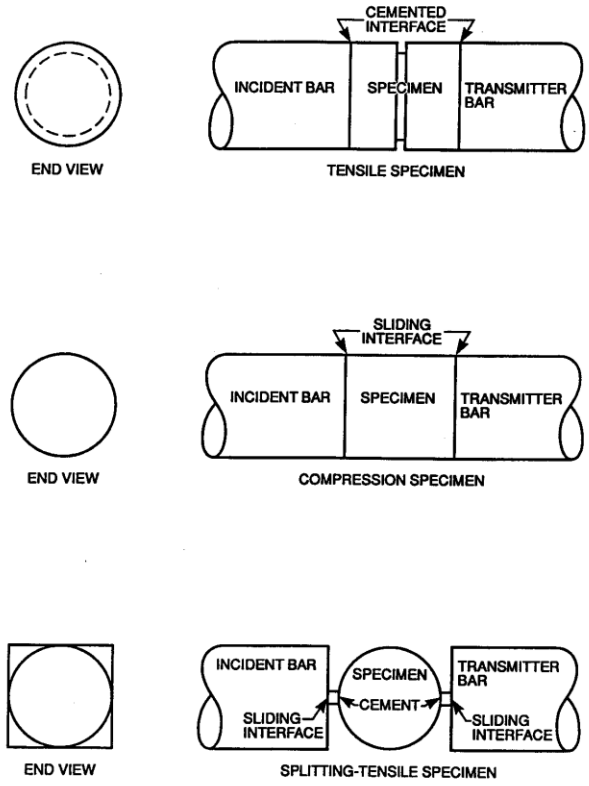

Fig 2-1
SHPB testing setup for various tests. Image: Ross, Tedesco, and Kuennen (1995)

Three experiments were conducted in the study (and pictured above): direct compression, direct tension, and splitting tensile. Specimen sizes for the experiment were right-cylindrical, 51mm diameter and length. These specimens are detailed in Fig 2-2.

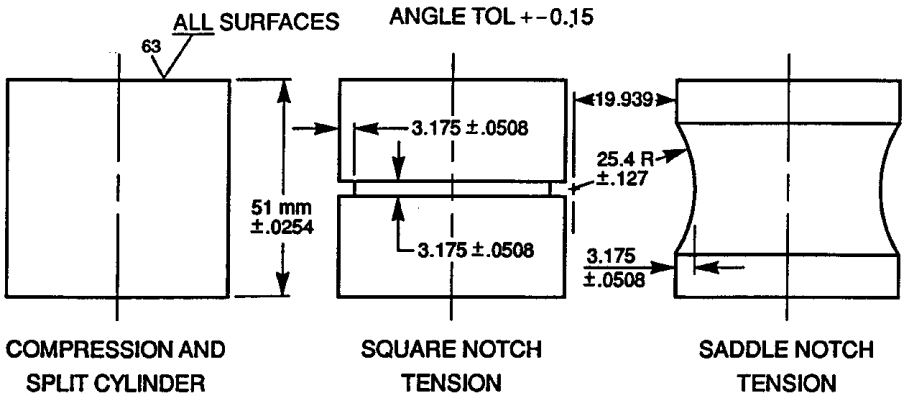

Fig 2-2
Details of SHPB concrete specimens, mm. Image: Ross, Tedesco, and Kuennen (1995)

Specimens as shown above in Fig 2-2 were also tested in a standard machine with strain rates on the order of 10^{-7}/sec to 10^{-3}/sec [6]. The SHPB was used to conduct the high strain-rate tests which ranged from 1/sec to 10^{3}/sec. A consistent concrete mix was used throughout the experiment and is detailed in Table 2-1.

Table 2-1 - Concrete Mix proportions and strengths

Water-cement ratio	0.533	—
Portland cement—Type 1	247 kg	(544.6 lb)
Fly ash—Class F	27.2 kg	(60.0 lb)
Fine aggegate—Natural silica, ASTM C 30	639.2 kg	(1409.4 lb)
Coarse aggregate—$^{3}/_{8}$ in. maximum diameter	810.4 kg	(1786.9 lb)
Anti-air-entraining limestone mixture	0.55 kg	(1.21 lb)
Water-reducing admixture	1.0 kg	(2.2 lb)
Water	131.7 kg	(290.4 lb)
Static compressive strength—152 x 305 mm cylinder	48.3 MPa	(7003 psi)
Static compressive strength—51 x 51 mm cylinder	57.1 MPa	(8279 psi)
Static splitting tensile strength—51 x 51 mm cylinder	3.86 MPa	(560 psi)
Static direct tensile strength—square notch*	4.53 MPa	(657 psi)
Static direct tensile strength—saddle notch*	3.67 MPa	(532 psi)

*51 mm diameter x 51 mm length.

Table 2-1
Concrete mix proportions and strengths. Image: Ross, Tedesco, and Kuennen (1995)

For actual testing of the specimens, a series of static and dynamic tests were conducted for each category. Wet, partially dry, and completely dry concrete specimens were tested to determine the effects of moisture on strength. This was done because it had been suggested that moisture in concrete leads to a high strain-rate response [6]. This proved to be true for dynamic loading. However, static loading strengths were lower. This was in line with other research that showed that dry concrete showed "no rate sensitivity up to strain rates of approximately 1.0/sec for direct tension, but wet concrete shows high rate sensitivity for the same region" [6].

Overall, the study clearly showed that in the range of dynamic loadings tested for, conventional weapons explosions, etc, concrete strength increase considerably. Fig 2-3 shows all strain-rate responses for tensile and compressive tests and their corresponding dynamic strength. Throughout the test, strain-rate sensitivity and large increases in strength properties are most visible for tension in the concrete but did occur visibly in compression also. The results of this test give the subject of this thesis a good basis to move forward with experimentation.

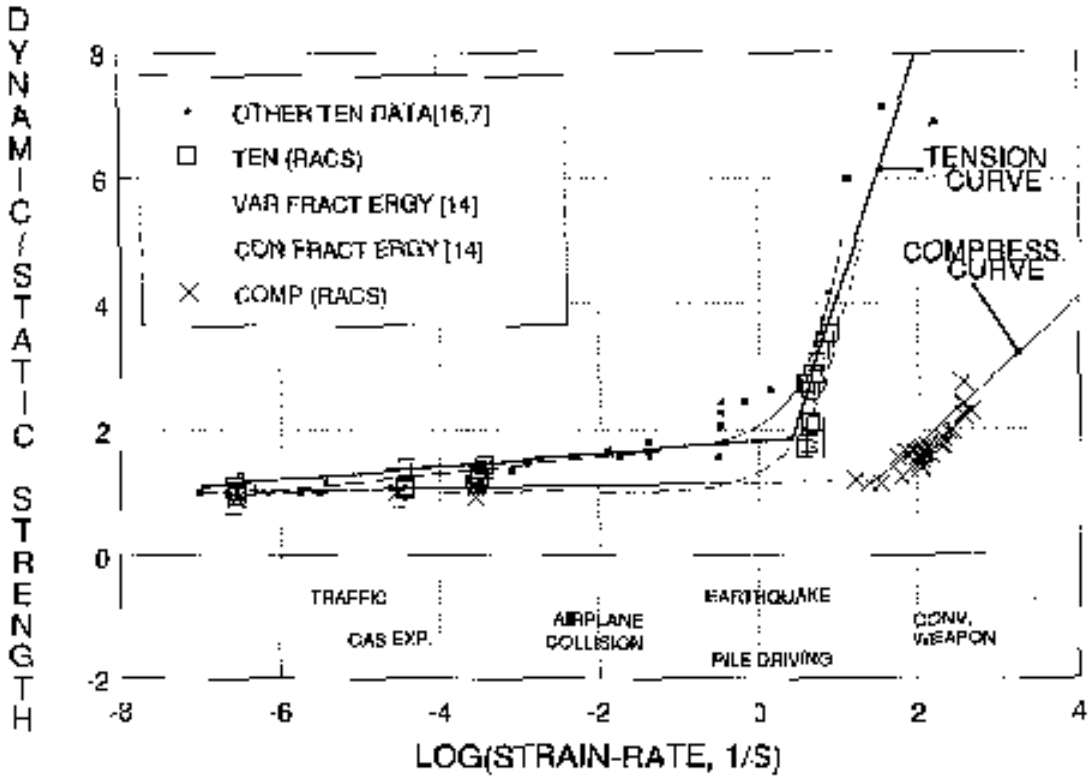

Fig 2-3
Dynamic strengths of concrete under SHPB test. Image: Ross, Tedesco, and Kuennen (1995)
Authors note: This is the best quality image available

2.2 Dynamic Loads on Soil-Filled Container Walls

While a filled, rigid blast and impact resisting structures have not been studied formally, there has been a considerable amount of research in soil-filled mesh boxes. A study involving experimental testing and then numerical modeling of blast loading on these structures will be discussed in this section.

Recall from earlier in the introduction of the thesis that a HESCO bin or bastion (will be referred to as 'units' hereafter), is a prefabricated unit comprised of a non-woven polypropylene geotextile with support from a galvanized welded steel mesh surrounding it. The transportability of the units with the possibility of virtually any fill material make the units favored in civil engineering applications and also expeditionary military applications [7]. It is mostly these military applications, where the units can be arranged in a wall or a totally enclosed structure, that blast loading is a concern for military engineers. The goal of the study of these units was to give engineers data regarding the level of blast loading that each structural form can sustain [7].

The experimental setup consisted of three HESCO bin walls. The geometric description of the tests is shown in Table 2-2. The walls were subjected to pressure loads from a blast. The mesh consisted of "8 Gauge (4 mm) diameter Galfan® coated steel wire, spaced at 75 mm both horizontally and vertically. The joints consisted of 8 Gauge (4 mm) and 10 Gauge (3 mm) diameter Galfan® coasted steel wire(s), coiled to approximately 10 mm diameter, which tie the welded wire mesh of the adjacent HB units together. The geotextile in the units is a 2 mm thick heave-duty non-woven polypropylene" [7]. Blasts waves that originated from an explosive charge detonated at a standoff generated a "substantially uniformly distributed pressure over the wall face as validated using AutoDyn software" [7]. PCB® pressure sensors generated overpressure-time histories exerted on the faces of the walls [7]. Details of charge used and distance were omitted from the report for security reasons. Displacement gauges shielded behind

steel frames measured deflection of the system from the blast. All walls were filled with a local silty-sand. This fill was compacted by means of the compactor's foot every 0.3 m to simulate actual field practice. High speed footage, before and after photos, and laser position scanning were also used for data.

Trial	HB Unit (width × depth × height) (mm × mm × mm)	Courses (wall height, m)	Filled width (m)	Average soil ρ_{wet} (kg/m^3)	Average % MC
1	Mil 3 (975×975×975)	2 (1.95)	1.20	1572	7.6
2	Mil 1 (1050×1050×1350)	1 (1.35)	1.33	1577	7.7
3	Mil 2 (600×600×600)	2 (1.2)	0.74	1646	9.5

Table 2-2
Specimen nominal size Image: Scherbatiuk et al. 2008

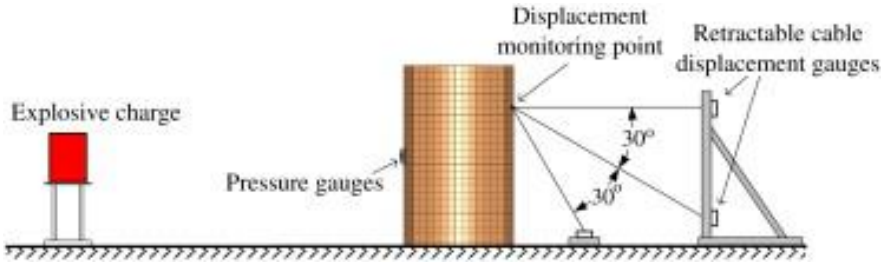

Fig 2-4
HESCO bin blast test setup. Image: Scherbatiuk et al. 2008

The main goal of this research was to reach good agreement with a finite element model. While this has limited application to the research in this thesis, the study did establish and reiterate key points about dynamic loading research.

By adding mass to this system and packing the soil as densely as possible, displacement of the wall decreases [7]. This is expected because the dense soil increases the rotational

inertia of the wall [7]. The data also shows that density of the soil is more important than other properties of the soil [7]. During the blast loading events, the soil strength and stiffness increased and had similar strain-rate sensitivity properties to that of concrete (which the researchers had problems accounting entirely for in their FE model) [7]. Other important points taken from this study were the beneficial use of the high speed footage and plenty of before and after photo analysis. Overall, this study shows great promise for using a soil fill material inside a more rigid container.

2.3 Other Concrete Composites

Much of the focus on impact resistance related to concrete has focused in the areas of plain concrete, steel fiber reinforced concrete, carbon fiber reinforced polymers, and different geometries of plain concrete. There has not been notable research yet of concrete hollow sections filled with material. However, there has been a considerable amount of research in the field of steel tubing filled with concrete by Bambach [9] and others.

Bambach et al. aimed to quantify the response of concrete filled steel hollow sections under transverse impact loading. Steel hollow sections are used extensively in practically every facet of construction and in many of these applications they are filled with concrete. The sections in the study are exposed to low velocity, large mass impacts. The sections used in the study are described below in Table 2-3.

Table 2-3 - Specimen Criterion

Specimen $b \times d \times t$ (mm)	Width to thickness ratio b/t	Slenderness to AS4100	Beam length L (mm)	Length to depth ratio L/d	Yield stress f_y (MPa)	Ultimate stress f_{su} (MPa)	Failure strain ε_f
50 × 50 × 1.6	31	40	700	14	455	504	0.16
35 × 35 × 1.6	22	28	700	20	485	501	0.17
20 × 20 × 1.6	13	15	700	35	480	508	0.17

Table 2-3
Specimen criterion. Bambach et al. 2008

These sections were chosen to represent a field of available steel ranging from slender to compact. In total, eighteen beams were tested with nine hollow and nine filled. One hollow and one filled section were tested statically for each size and two hollow and two filled tested with the low velocity, large mass impactor. Specimens were bolted to a rigid support frame via welded end plates.

The impact setup used consisted of a variable mass dropped from a height of 1.975 m (6.48 ft). A Kistler® load cell was mounted on the tip of the impacting head of the setup. Nominal velocity prior to impact was 6.2 m/s (20.34 ft/sec or 244.1 in/sec) [9]. Additional data collected included high speed footage filmed at 2000 frames per second. A painted grid on the specimen allowed displacements to be analyzed visually from the high speed footage. Fig 2-5 shows the impact setup.

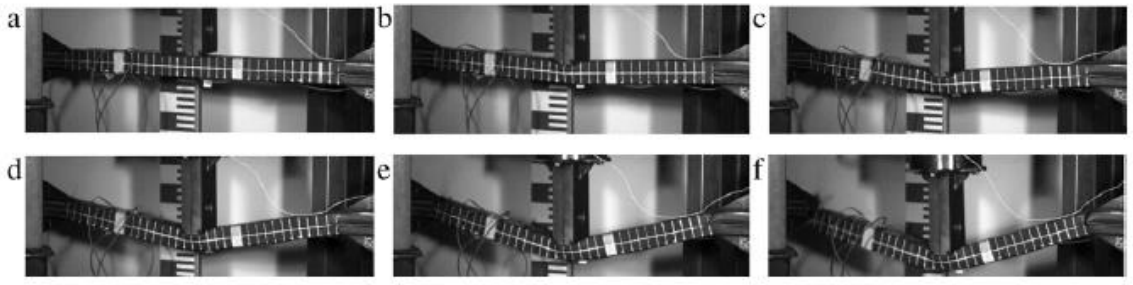

Fig 2-5
Rigid-plastic beam behavior of hollow 50SHS. Image: Bambach et al 2008

The study found substantial increases in strength and improvements in local deformations of the steel sections [9]. Concrete filling also increases the moment capacity of the sections up to 83% for slender section and reduces transverse failure defection in non-compact sections [9]. The actual results from this research do not directly benefit the study in this thesis, but the procedure and methods proved to be important. The usage of high speed footage, instrumentation of a drop weight test, and data analysis methods are also present in this research.

2.4 Summary of Literature

The literature presented in this thesis shows various studies that have already been completed that are related to the topic. Although there was not research of soil filled concrete structures available, the concepts and methodology of these past studies give confidence in this project.

Chapter Three: Procedure and Methods

3.1 Impact Testing Machine

Before any concrete specimens could be tested, a machine capable of producing the loading needed to be designed and constructed. The author produced a set of structural drawings, computer models, and calculations for the impact testing machine (Fig 3-1). The machine is capable of producing over 50,000 lbs of force (according to a classical mechanics approach) and can be equipped with various impacting tips or shapes. The machine relies solely on gravity for means of energy.

Fig 3-1
Impact testing machine with concrete box section in testing bay

The machine is equipped with four, 50,000 lb load cells mounted on two supports. An air and electric actuated quick-release system lets the operator drop the weight with a touch of a button. The quick release system is mounted between two carriages – the slave and impact carriage. The slave carriage is lowered and reconnected via the quick release to hoist the impact carriage back to the desired height for another test. These carriages are each equipped with four brass bearings gliding on two stainless steel rods. The slave (Fig 3-2) and impact (Fig 3-3) carriages are depicted below. Figure 3-4 shows both carriages mounted in the impact testing machine.

Fig 3-1
Slave carriage

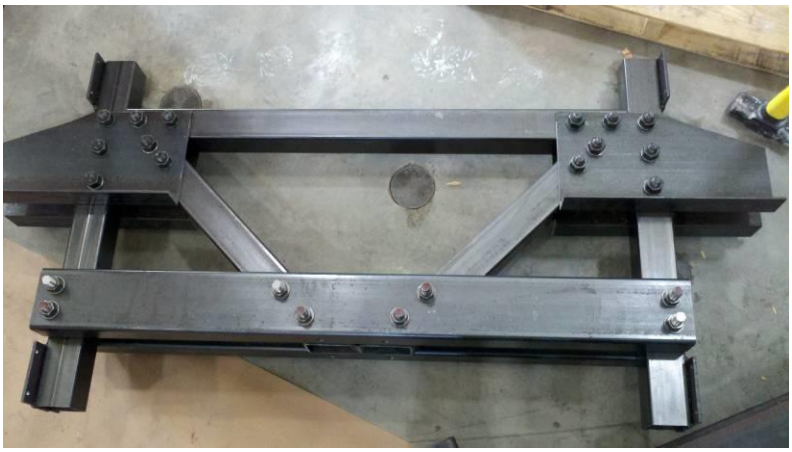

Fig 3-1
Impact carriage w/o impact head

Fig 3-4
Impact carriage mounted below slave carriage in the machine on stainless steel rods

3.2 Concrete Box Sections

The concrete box sections were all constructed with the same dimension, concrete mixture, and reinforcement layout. Fig 3-5 below shows the nominal shape of the concrete box sections.

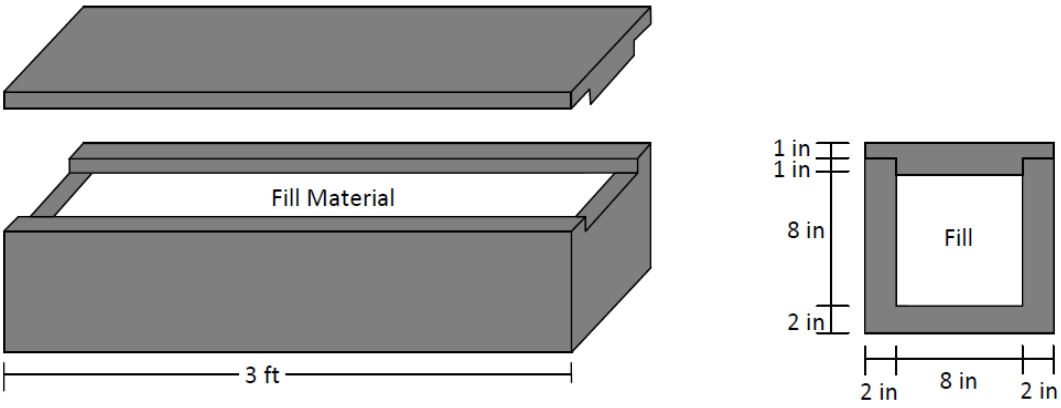

Fig 3-5
Nominal shape of concrete box sections

For the concrete, a simple mix design was followed for each cast. Coarse aggregate consisted of 3/8" sieve pass basalt. The properties of the concrete were not as important as the fill material so admixtures were omitted. The parameters of this design are depicted from a spreadsheet in Fig 3-6. Average compressive strengths for the test specimens were near 3300 psi at the time of testing, 12 days (See appendix for complete strengths table).

Table 3-1

Mix Design			
	cu ft	**cu yd**	
Total batch size	5.65	0.240648	
Water/Cement Ratio	0.45		
Item	**lb/cu yd** (at SSD)*	**lb/cu yd** (at MC)**	**lb/batch**
cement	758.00		**182.41**
fine aggregate	1216.00	1216.00	**292.63**
coarse aggregate	1652.00	1652.00	**397.55**
water	341.10	341.10	**82.09**
Total Weight (lbs)	3967.10	3209.10	954.68

Table 3-1
Mix Design

The box sections initially were designed to have a mild steel reinforcement cage of #3 flexural bars and shear stirrups. This design was used for a test round of three specimens and proved to be over reinforced to get enough distinction of the behavior of the fill materials. Instead, a 6x6 inch welded wire mesh with diameter of 10 gauge (0.102 in) was used in both the lid and the box. This provided just enough reinforcement to keep the box sections intact after impacts.

3.3 Casting

Three wooden forms were built for both the lid section and the main box section. The casting process consisted of rebuilding the forms after the previous cast first. Then the forms were oiled then the welded wire was placed. The concrete was mixed and poured/shoveled into the forms. A vibrating tool was used to consolidate the mix. The specimens were then covered with a plastic and moist cured for at least 24 hours before removal. It should be noted that all box sections have a sacrificial strip of plywood left in them after the casting process. This piece is located in the bottom of the fill material bay. The reason for this is that the forms were built to be the easiest to assemble and pull out and the bottom piece of plywood was virtually impossible to remove.

Fig 3-6
Concrete box sections and lids in forms

3.4 Fill Material

Four different fill materials were used in the experiment. The coarse aggregate used was a ¾" basalt based stone. River gravel is a rounded stone found on the shores of Lake Superior for this study. The soil used is an organic, nutrient-rich top soil. The sand used was the same sand used in the concrete mix. The unit weights are listed below in Table 3-2.

Table 3-2 Unit Weights of Fill Material

Category	Unit Weight (lb/ft^3)
Coarse Aggregate	101.1
Uncompacted Sand	102.4
Compacted Sand	113.5
Uncompacted Soil	63.2
Compacted Soil	85.1
River Gravel	91.9

Table 3-2
Unit weights of fill materials

3.5 Data Acquisition

The real time data acquisition system consisted of four, 50,000 lb capacity load cells measuring reaction force at four corners of the test setup. The load cells used were PCB 200C50 Dynamic Force Sensors. The mounting of the load cells consisted of two supports with two load cells each. A 1 inch thick steel plate was placed over both load cells to distribute load equally into both sensors. The setup is depicted in Fig 3-7. The

load cells led to a powered signal conditioning which was then routed to an oscilloscope. The oscilloscope was run directly into the field computer via USB cable.

Fig 3-7
Load cell support setup

Once this chain was running into the field computer, the program PicoScope 6 by Pico Technology was used to capture the raw data from the USB signal capturing 500,000 data points per second per load cell. The software reads the load in terms of volts which can be converted to force. This will be covered further in the Data Analysis chapter.

For visual data, a Memerex GX camera was used to record high speed footage of each test specimen. The camera recorded at 2000 frames per second. Playback can be varied from as low as 5 fps to 60 fps. This recording speed shows significant detail of the impact including crack propagation. In addition to quantifying force from the load cell data, the high speed footage can extract data from the videos that can be presented in

graphical form. Using the HotShot SC Link program, a point in the video (in our case a small white dot against a black background) can be tracked and from that, position, velocity, and acceleration data can be extracted. Again, this will be covered more in the Data Analysis chapter.

3.6 Testing Procedure

After 12 days of hydrating, the concrete box sections were ready to be tested. Three boxes were tested on a given day since only three could be cast at a time. Prep work was done before setup to ensure smooth operation. This included inspection of the impact testing machine and operation of the of the load cells. After this was done, the specimen was loaded on to the supports over the load cells.

Once the specimen was placed on the load cells, the high speed camera was armed to start recording. This consisted of getting as much light on the impact area as possible. Three halogen spot lights were used to light the area. The camera was then focused and armed for a short, triggered response so that the footage could be take only at the impact and shortly before and after.

After it was confirmed the camera was ready, the box section was prepared by adding a fill material (or empty for a control specimen). Once the box had the appropriate fill inside of it, the lid was put on and fastened using two steel clamps that wrap around the

perimeter of the box. The box was then laid on its side to emulate an impact in the field rather than penetrate the lid.

For round impacting head use, the drop height was 5 ft and velocity before impact was around 90 in/sec. For rectangular plate drops, the height was increased to 6 ft and velocity was around 95 in/sec. The drop heights were determined by means of trial and error on sample, empty boxes. Impacting heads were dropped from various heights until the level of damage became satisfactory. For the round impacting head, a punching shear failure was desired. The plate impactor was used to generate a flexural failure in the box.

After determining the height and fill of the test and that the data acquisition was working, it was time to conduct the test. The safety pin could then be removed from the quick release, the carriages would be raised, and the weight would be released.

Fig 3-8
Test setup

Chapter Four: Visual Data

In this section a visual analysis will be presented of each test specimen. The pictures of the aftermath of the impact test may present the most compelling data for arguments of a certain fill material. Below is a picture of a typical, finished box section prior to fill material.

Fig 4-1
Unfilled box sections

The chapter will be broken in to two larger sections categorized by impacting head shape. Those categories will be further subdivided into fill material. Each test specimen is summarized below in Table 4-1

Important note:

All round impacting heads are **5 ft** drop heights and all plate drops are **6 ft**.

Table 4-1 Testing Categories

Test #	Test Category	Impact Head	Date Cast	Date Broken
1	Control	Plate	2/17/2012	3/1/2012
2	Control	Plate	2/17/2012	3/1/2012
4	Control	Round	2/19/2012	3/2/2012
5	Control	Round	2/19/2012	3/2/2012
3	Crushed Stone	Plate	2/17/2012	3/1/2012
10	Crushed Stone	Plate	2/24/2012	3/7/2012
6	Crushed Stone	Round	2/19/2012	3/2/2012
7	Crushed Stone	Round	2/22/2012	3/5/2012
11	Uncompacted Sand	Plate	2/24/2012	3/7/2012
12	Uncompacted Sand	Plate	2/24/2012	3/7/2012
8	Uncompacted Sand	Round	2/22/2012	3/5/2012
9	Uncompacted Sand	Round	2/22/2012	3/5/2012
13	Compacted Sand	Plate	3/9/2012	3/21/2012
14	Compacted Sand	Plate	3/9/2012	3/21/2012
15	Compacted Sand	Round	3/9/2012	3/21/2012
16	Compacted Sand	Round	3/23/2012	4/9/2012
17	Uncompacted Soil	Plate	3/23/2012	4/4/2012
18	Uncompacted Soil	Plate	3/23/2012	4/4/2012
21	Uncompacted Soil	Round	3/28/2012	4/9/2012
20	Uncompacted Soil	Round	3/28/2012	4/9/2012
24	Compacted Soil	Plate	3/29/2012	4/10/2012
23	Compacted Soil	Plate	3/29/2012	4/10/2012
19	Compacted Soil	Round	3/28/2012	4/9/2012
22	Compacted Soil	Round	3/29/2012	4/10/2012
25	River Gravel	Plate	3/30/2012	4/11/2012
26	River Gravel	Plate	3/30/2012	4/11/2012
27	River Gravel	Round	3/30/2012	4/11/2012
28	River Gravel	Round	3/31/2012	4/12/2012
29	Control	Plate	3/31/2012	4/12/2012
30	Control	Plate	3/31/2012	4/12/2012

Table 4-1
Impact Testing Categories

4.1 Round Impacting Head

4.1.1 Round Control I

Fig 4-2
Test 4 - Round Control I Post Impact

4.1.2 Round Control II

Fig 4-3
Test 5 - Round Control II Post Impact

The round control specimens showed the importance of having a fill material immediately. Without the fill material, the impactor was able to penetrate fully on both tests thus letting the broad part of the impacting carriage contact the box producing a second wave of damage. The slow motion footage of the test shows only a modest amount of cracking from the impactor penetration but very large amounts of flexural damage from the carriage. As force traveled through the box into the simple supports, there was considerable damage to the ends which responded poorly to the impulse and

cracked. Fig 4-3.1 and fig 4-3.2 show the progression of damage of specimen #5 from the impactor.

Fig 4-3.1
Test 5 – Impactor penetration from high speed footage

Fig 4-3.2
Test 5 – Carriage Impact from high speed footage

4.1.3 Round Coarse Aggregate I

Fig 4-4
Round Coarse Aggregate Fill

Fig 4-5
Test 6 - Round Coarse Aggregate I Post Impact

4.1.4 Round Coarse Aggregate II

Fig 4-6
Test 7 - Round Coarse Aggregate 2 Post Impact

As expected, a fill material improved the response of the box from the impact. However, just as with the control specimen, full penetration of the impactor occurred causing considerable flexural cracking after the carriage impact. Response at the ends improved and less damage occurred as the coarse aggregate mass was able to absorb more energy. Both coarse aggregate tests seemed comparable and consistent in results.

4.1.5 Round Sand Uncompacted I

Fig 4-8
Test 8 – Round Sand Uncompacted 1 Before Impact

Fig 4-9
Test 8 – Round Sand Uncompacted I Post Impact

Fig 4-10
Test 8 - Round Sand Uncompacted I Post Impact 2

Fig 4-11
Test 8 - Round Sand Uncompacted I Post Impact Penetration

4.1.6 Round Sand Uncompacted II

Fig 4-12
Test 9 – Round Sand Uncompacted II Post Impact

Fig 4-13
Test 9 – Post Impact Fill Removed

Again, just as in the control and coarse aggregate tests, the round impactor fully penetrated and caused significant flexural cracking. However, this seemed to be the most critical damage in the specimen and rigidity was maintained after the test. Little to no end cracking or damage was observed and the impacted side was limited to just the punching shear hole caused by the impactor. Both specimens appeared to respond very similarly. Upon impact, the uncompacted sand was settled by the impact and a reduction of volume can be seen in Fig 4-9 and 4-10.

4.1.7 Round Sand Compacted I

Fig 4-15
Test 15 – Round Sand Compacted Impactor Penetration

Fig 4-16
Test 15 – Side Penetration

Fig 4-17
Test 15 – Sand Fill Post-Impact

Fig 4-18
Test 15 - Emptied

4.1.8 Round Sand Compacted II

Fig 4-19
Test 16 – Round Sand Compacted II Emptied

The compacted sand performed very well as the impactor was not able to fully penetrate for the first test (Fig 4-15). The second specimen did penetrate fully but was evidently slowed by the compacted sand and produced little extra damage upon carriage impact. Interestingly, no evidence of flexural cracking was produced on either specimen. True shear cracking showed up most prevalently in the first test in one crack and none in the second test. Ends of the boxes were preserved very well.

4.1.9 Round Soil Uncompacted I

Fig 4-20
Test 20 – Round Soil Uncompacted I Post Impact

Fig 4-21
Test 20 – Soil Fill Post Impact

Fig 4-22
Test 20 – Emptied Post Impact

2.1.10 Round Soil Uncompacted II

Fig 4-23
Test 21 – Round Soil Uncompacted II Post Impact

Fig 4-24
Test 21 – Emptied Post Impact

Fig 4-25
Test 21 – Soil Fill Post Impact

Both uncompacted soil specimens performed relatively poorly. Full penetration of the impactor caused extended flexural damage that failed the reinforcement considerably. The soil used has the lowest unit weight of any fill material in the study. The ends of the sections held up surprisingly well consider the amounts of flexural and shear damage in both specimens.

4.1.11 Round Soil Compacted I

Fig 4-26
Test 19 – Round Soil Compacted I Post Impact

Fig 4-27
Test 19 - Round Soil Compacted I Emptied

Fig 4-28
Test 19 – Soil Fill Post Impact

4.1.12 Round Soil Compacted II

Fig 4-29
Test 22 – Round Soil Compacted 2 Post Impact

Fig 4-30
Test 22 – Side Hole Penetration

Compacted soil performed better than uncompacted soil but could not match performance of sand. Full penetration of the impactor caused extended flexural damage from carriage impact. Flexural cracks propagated slower than in the uncompacted test. The ends showed damage after fill material was extracted as corners fell off completely.

4.1.13 Round River Gravel I

Fig 4-31
Test 27 – Round River Gravel I Post Impact

4.1.14 Round River Gravel II

Fig 4-32
Test 28 – Round River Gravel II Post Impact

The round river gravel fill performed somewhat similarly to the angular coarse aggregate fill. Most of the failure was localized around a main flexural crack with a few shear cracks nearby. Ends were mostly preserved in both tests. Both tests showed full penetration of the impactor causing extended damage from the carriage impact.

4.2 Plate Impacting Head

4.2.1 Plate Control I

Fig 4-30
Test 1 – Plate Control I Post Impact

4.2.2 Plate Control II

Fig 4-31
Test 2 – Plate Control II Post Impact

4.2.3 Plate Control III

Fig 4-32
Test 29 – Plate Control III Post Impact

4.2.4 Plate Control IV

Fig 4-33
Test 30 – Plate Control IV Post Impact

The plate control specimens all exhibited similar behavior. Upon impact, a small flexural crack, if any, would form. But just as with the round controls and other tests, the impactor fully penetrated causing the carriage to impact. At this point the plate had already cause a considerable amount of damage to the face of the specimen. Upon carriage impact, a flexural crack would evidently propagate along with shear cracking. Fig 4-33.1 and 4-33.2 shows the differences before and after impactor penetration. Aside from test #1, ends stayed intact during testing and fill extraction, but were cracked

evidently. The reason for four plate control tests is explained in the results and conclusions chapter.

Fig 4-33.1
Test 29 – Initial Penetration from High Speed Footage

Fig 4-33.2
Test 29 – Full Penetration from High Speed Footage

4.2.5 Plate Coarse Aggregate I

Fig 4-34
Test 3 – Plate Coarse Aggregate I Post Impact

4.2.6 Plate Coarse Aggregate II

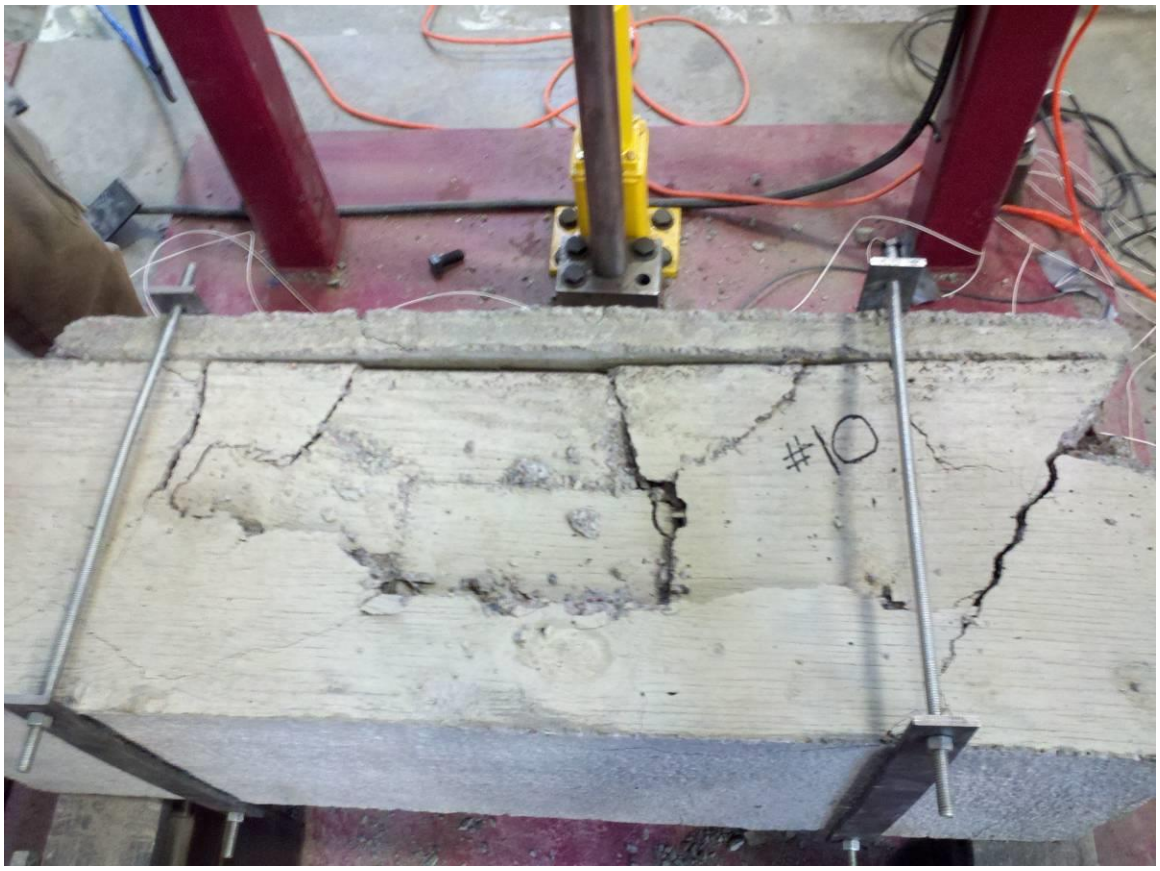

Fig 4-35
Test 10 – Plate Coarse Aggregate II Post Impact

Fig 4-36
Test 10 – Plate Coarse Aggregate II Emptied

Fig 4-37
Test 10 – Plate Coarse Aggregate II Bottom Cracking

For both coarse aggregate tests, the impactor was stopped from fully penetrating by approximately one inch. Flexural and shear cracking were significantly reduced from that of the control specimens. However, considerable damage to the ends of the specimen occurred causing chunks of concrete to barely be held on by the welded wire reinforcement after fill extraction.

4.2.7 Plate Sand Uncompacted I

Fig 4-38
Test 11 – Plate Sand Uncompacted w/ Impactor Head

Fig 4-39
11 – Plate Sand Uncompacted Emptied

4.2.8 Plate Sand Uncompacted II

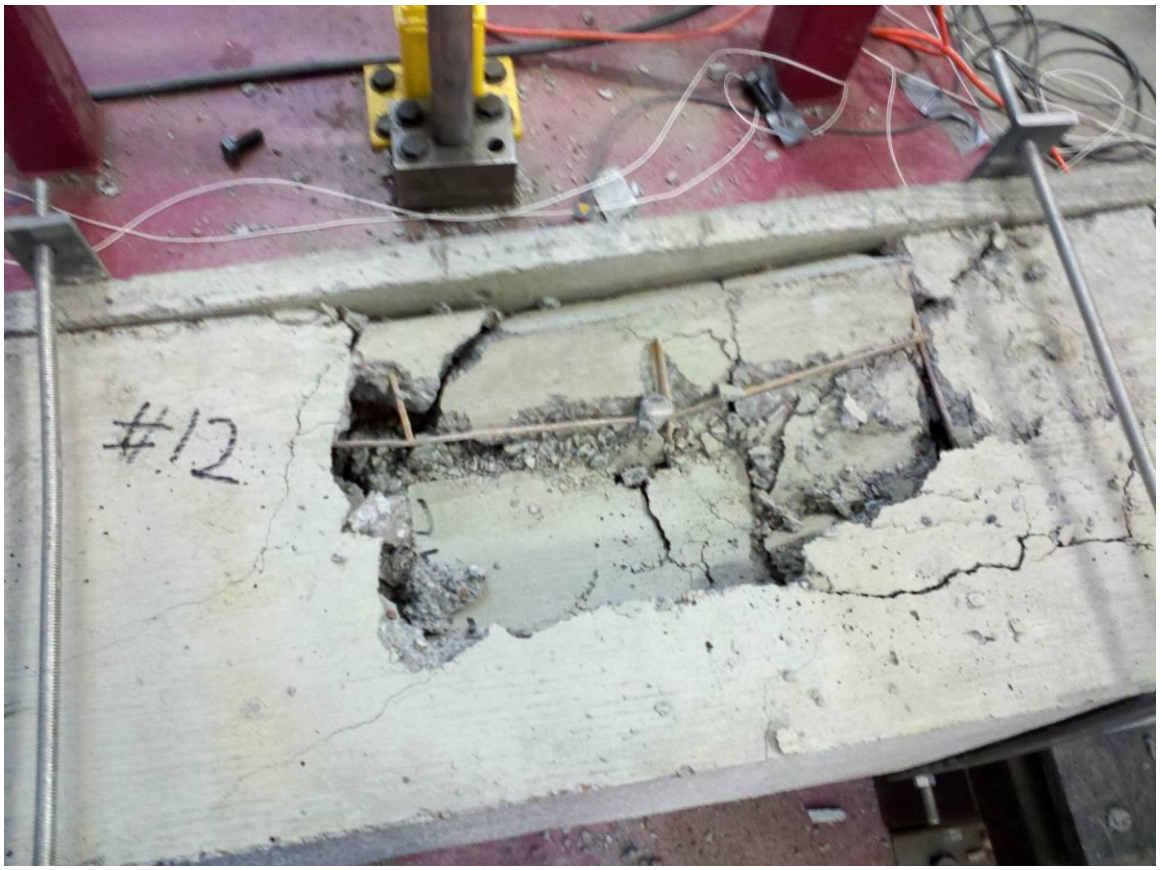

Fig 4-40
Test 12 – Plate Sand Uncompacted II Post Impact

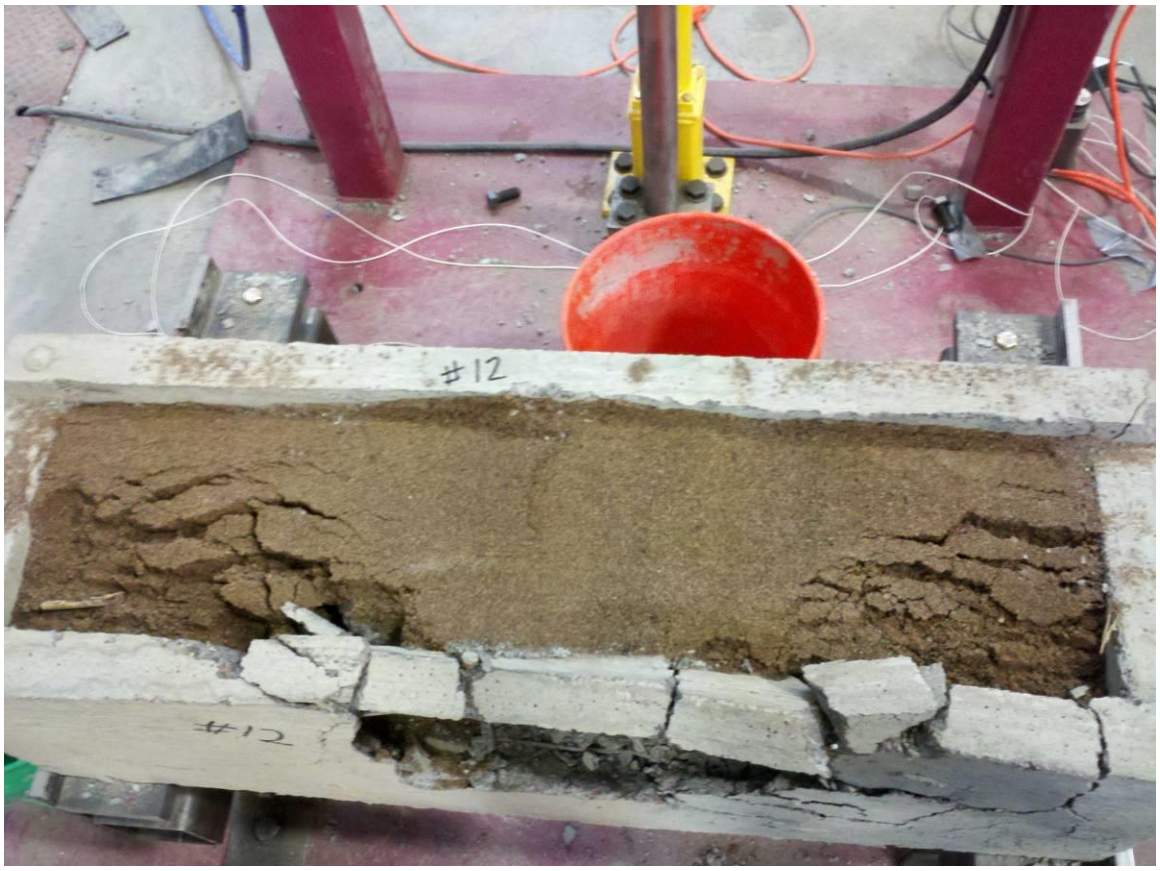

Fig 4-41
Test 12 – Sand Fill Post-Impact

Fig 4-42
Test 12 – Plate Sand Uncompacted II Emptied

The first uncompacted sand test, #11, showed no signs of flexural or shears cracking upon impact. The second test did crack both in flexure and shear but the cracks did not cause nearly the amount of damage of the controls. The impacting head did not fully penetrate on either test and ends were reasonably well preserved. On both tests, the damage was confined mostly to the impacted face of the box section.

4.2.9 Plate Sand Compacted I

Fig 4-43
13 – Plate Compacted Sand Pre-Impact

Fig 4-44
Test 13 – Plate Sand Compacted Post Impact

Fig 4-45
Test 13 – Plate Sand Compacted Emptied

Fig 4-46
Test 13 – Sand Post-Impact

4.2.10 Plate Sand Compacted II

Fig 4-47
14 – Plate Sand Compacted II Sand Fill Post Impact

Fig 4-48
Test 14 – Plate Sand Compacted II Post-Impact

Fig 4-49
Test 14 – Plate Sand Compacted II Emptied

Fig 4-49.1
Test 13 – Plate Sand Compacted Bottom cracking

Plate impact on compacted sand fill showed some flexural and shear cracking. This was more evident on the first test, #13 where the impact created significant bursting forces. Ends were preserved but again, #13 shows a significant crack on one side. The boxes were well intact. An interesting behavior noticed here was the significant cracking about one inch down from the face. After looking at the compaction of each specimen, #14 seems to have had a more thorough compacting. The cracking shown above did not occur in #14. It appears that the lack of good compaction caused a fixed end moment failure but the sand prevented a further total flexural failure.

4.2.11 Plate Soil Uncompacted I

Fig 4-50
Test 17 – Plate Soil Uncompacted I Post Impact

Fig 4-51
Test 17 – Soil Fill Post-Impact

Fig 4-52
Test 17 – Plate Soil Uncompacted I Emptied

4.2.12 Plate Soil Uncompacted II

Fig 4-53
Test 18 – Plate Soil Uncompacted II Post Impact

Fig 4-54
Test 17 – Plate Soil Uncompacted I Bottom Cracking

The plate soil uncompacted performed poorly as expected. The damage to the impacted side was significant as well as end damage. Interestingly, the same fixed end moment failure as seen with compacted sand occurred. The first test, #17, did not have full impactor penetration but still exhibited significant flexural cracking. The second specimen did allow full impactor penetration which led to carriage impact. The carriage impact caused a very significant flexural crack to form and propagate .

4.2.13 Plate Soil Compacted I

Fig 4-55
Test 23 – Plate Soil Compacted I Post Impact

Fig 4-56
Test 23 – Plate Soil Compacted I Emptied

4.2.14 Plate Soil Compacted II

Fig 4-57
Test 24 – Plate Soil Compacted II Post Impact

Fig 4-58
Test 24 – Soil Fill Post-Impact

Fig 4-59
Test 24 – Plate Soil Compacted II Emptied

The two tests showed the most variability among duplicates. The first specimen, #23, saw the same fixed end moment failure as before but concrete was spalled from this location. Flexural and shear cracks appeared and propagated down the side. Ends were split at the joint of the side and the ends on both sides. The second specimen did not appear to have any flexural or shear cracks but did sustain significant end damage and total loss of concrete is some areas of the corners.

4.2.15 Plate River Gravel I

Fig 4-60
Test 25 – Plate River Gravel I Post Impact

4.2.16 Plate River Gravel II

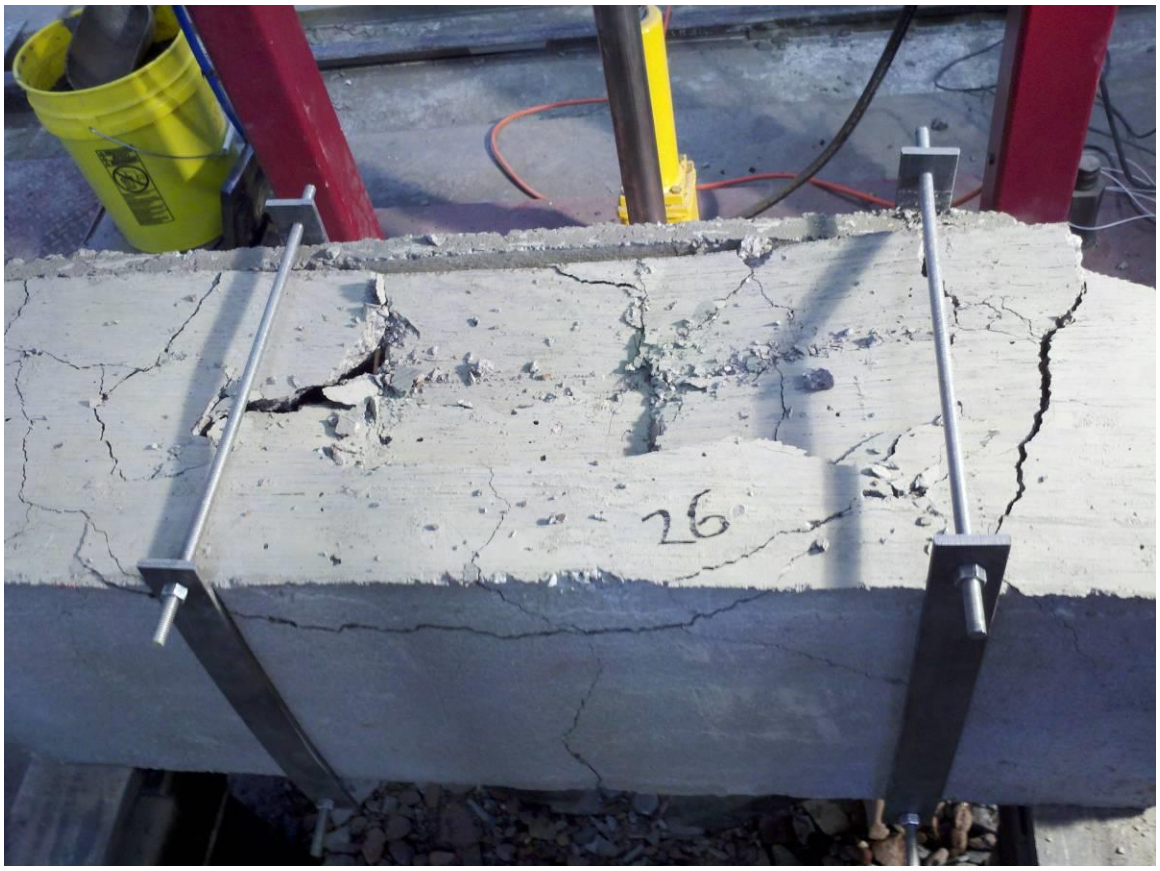

Fig 4-61
Test 26 – Plate River Gravel II Post Impact

The second specimen shown above showed more significant flexural and shear damage than the first specimen. Ends were damage in both tests but more severely in the first test. The first specimen saw a large crack propagate from the impact right through the middle of the end causing the end to fall off. The second specimen also lost concrete off the ends from the impact but not as severely.

Chapter Five: Results and Conclusions

Visual inspection showed both results that were expected and unexpected. Still, going into the testing process, it was known that the addition of mass to a system improves its response to dynamic loading. The simple equation below applies to the system:

$$\omega = \sqrt{k/m}$$

Eq. 5-1

Where ω is frequency, k is the spring constant, and m is mass. By adding more mass to the system the natural frequency is lowered. Less vibration is beneficial for controlling dynamic loads. Taking into account that the box sections were constructed to be uniform, the fill material's mass should be an important factor. However, the stiffness of the material will change, affecting the response. The addition of mass to the system is better understood with Eq. 5-2 below. This equation ignores damping as this research is focused on the peak response, and the dampening does little to affect the peak behavior.

$$F_t = ma_t + kx_t$$

Eq. 5-2

The F_t term represents the applied load to the box and can be quantified using the following equation:

$$F_t = m_i * a_i$$

Eq. 5-3

For Equation 5-3, mass, m_i, represents the mass of the impactor. The acceleration term, a_i, was derived from a second-order polynomial best-fit curve of the velocity graphs, which is explained in depth later in the report.

As the impactor penetrates the concrete and the fill material resists the load, the stiffness will vary and change dramatically for each fill material. Spring constants were not evaluated for each fill material or concrete box. It is expected that with the addition of mass to the system from the fill materials, the ma_t term in the equation will become greater and result in a reduction in the reaction term, R_t. The acceleration, a_t, and variable position, x_t, are very difficult to discretely determine and this was not attempted. The exact numerical correlation of F_t and the other terms in Eq. 5-2 is not the objective of the analysis. The important focuses are the total peak load, impulse, and decelerations of the impacting head as these represent the force and energy transmitted to the supports by the box, and total energy applied to each box, respectively.

5.1 Analysis Methods and Data Extraction

For numerical analysis, three sets of data are used. These data are total load, reaction impulse, and impactor deceleration. From the impact event recorded in the PicoScope software, a force-time plot was generated in Excel for each impact event when available (ex. Fig 5-2). The data from this software corresponds to the four different load cells used in the project. The load recorded originally is in volts and is then converted based on

the manufacturer's specifications to pounds. Force values were then sorted taking every seventy-fifth data entry to narrow the field down from over 265,000 data points to around 3,500 each incrementing by 0.001 seconds. From these, the peak loads were sorted from each channel after conversion and combined for one total load observed. Total load for all tests can be observed in Table 5-1.

After the total load was calculated, area under the force-time curve from the load cells was calculated to produce impulse values. It should be noted that all impulse values represent the initial impact event in the system. For example, many round impactor head tests had the similar event of the impactor head fully penetrating allowing the carriage to impact the box as well. Only the impact of the round head would be analyzed in this situation. Impulse was calculated by applying a trapezoidal sum of the area under the force-time curve to obtain an answer in lbs-sec. Impulse values from the reaction are tabulated below in Table 5-2.

The acceleration data for the impactor was not taken from any load cell data but rather from the velocity data from the high speed video footage. The velocity graphs (ex. Fig 5-4) are broken down into impact events (i.e. round head hitting but not entire carriage, ex. Fig 5-5). This impact velocity was modeled with a second order best-fit curve with corresponding R^2-value which gave describes the accuracy of the curve. Although the HotShot SC program gave acceleration data corresponding to the velocity, it was far too noisy to make any conclusions from.

Average values of the total load and impulse are presented Table 5-3. The results of the impactor deceleration are described in Section 5.2 and 5.3.

Table 5-1 Total Load

Test #	Impact Head	Test Category	Total Load (lbs)
1	Plate	Control	-
2	Plate	Control	-
4	Round	Control	21945.09
5	Round	Control	33895.74
3	Plate	Coarse Aggregate	-
10	Plate	Coarse Aggregate	19189.35
6	Round	Coarse Aggregate	20048.83
7	Round	Coarse Aggregate	20798.44
11	Plate	Uncompacted Sand	17875.72
12	Plate	Uncompacted Sand	13392.75
8	Round	Uncompacted Sand	25405.93
9	Round	Uncompacted Sand	31715.30
13	Plate	Compacted Sand	20888.78
14	Plate	Compacted Sand	21977.78
15	Round	Compacted Sand	16271.52
16	Round	Compacted Sand	-
17	Plate	Uncompacted Soil	38166.29
18	Plate	Uncompacted Soil	16498.60
21	Round	Uncompacted Soil	16205.59
20	Round	Uncompacted Soil	18205.35
24	Plate	Compacted Soil	21880.11
23	Plate	Compacted Soil	25486.51
19	Round	Compacted Soil	14767.43
22	Round	Compacted Soil	17375.17
25	Plate	River Gravel	27803.69
26	Plate	River Gravel	23113.17
27	Round	River Gravel	28353.07
28	Round	River Gravel	-
29	Plate	Control	-
30	Plate	Control	-

Table 5-1
Total Load

Table 5-2 Total Impulse and Average Deceleration

Test #	Impact Head	Test Category	Total Impulse	Average Deceleration (in/sec^2)
1	Plate	Control	-	-42
2	Plate	Control	-	-533
4	Round	Control	67.92	-
5	Round	Control	38.10	-107
3	Plate	Coarse Aggregate	-	-7
10	Plate	Coarse Aggregate	204.66	-406
6	Round	Coarse Aggregate	42.11	-248
7	Round	Coarse Aggregate	87.15	-533
11	Plate	Uncompacted Sand	188.43	-184
12	Plate	Uncompacted Sand	203.99	-
8	Round	Uncompacted Sand	41.97	-368
9	Round	Uncompacted Sand	31.11	-317
13	Plate	Compacted Sand	230.15	-288
14	Plate	Compacted Sand	226.35	-520
15	Round	Compacted Sand	208.22	-306
16	Round	Compacted Sand	-	-198
17	Plate	Uncompacted Soil	256.47	-
18	Plate	Uncompacted Soil	87.57	-611
21	Round	Uncompacted Soil	42.74	-249
20	Round	Uncompacted Soil	43.92	-71
24	Plate	Compacted Soil	234.39	-357
23	Plate	Compacted Soil	234.20	-143
19	Round	Compacted Soil	82.68	-336
22	Round	Compacted Soil	53.71	-44
25	Plate	River Gravel	219.39	-256
26	Plate	River Gravel	218.21	-169
27	Round	River Gravel	52.29	-100
28	Round	River Gravel	-	-508
29	Plate	Control	-	-
30	Plate	Control	-	-

Table 5-2
Total Impulse and Average Deceleration

Table 5-3 Averages of Testing Data

Table 5-3 Averages of Test Data					
Test	**Category**	**Unit Weight (lb/ft^3)**	**Total Peak Load (lbs)**	**Total Impulse (lbs-sec)**	**Decel. (in/sec^2)**
Round	Control	N/A	27920.41	53.01	-107.00
	Coarse Aggregate	101.1	20423.64	64.63	-390.50
	Uncompacted Sand	102.4	28560.62	36.54	-342.50
	Compacted Sand	113.5	16271.52	208.22	-306.00
	Uncompacted Soil	53.1	23683.31	43.33	-160.00
	Compacted Soil	74.5	16071.30	68.20	-190.00
	River Gravel	91.9	28353.07	52.29	-100.00
Plate	Control	N/A	N/A	N/A	-287.50
	Coarse Aggregate	101.1	19189.35	204.66	-406.00
	Uncompacted Sand	102.4	15634.23	196.21	-184.00
	Compacted Sand	113.5	21433.28	228.25	-404.00
	Uncompacted Soil	53.1	27332.44	172.02	-611.00
	Compacted Soil	74.5	23683.31	234.29	-250.00
	River Gravel	91.9	25458.43	218.80	-212.50

Table 5-3
Averages of Tables 5-1 and 5-2

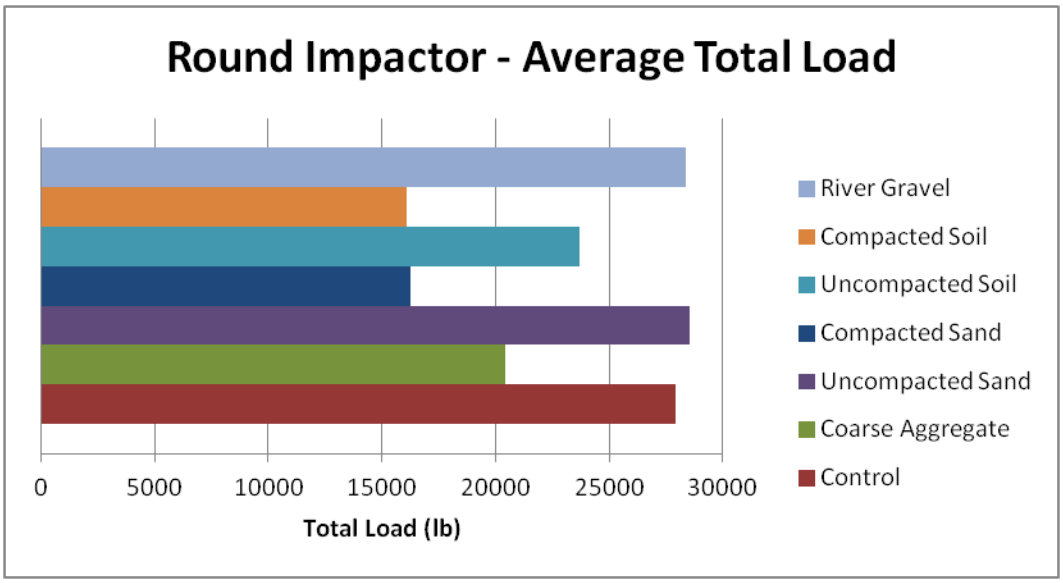

Fig 5-2
Round Impactor Total Load

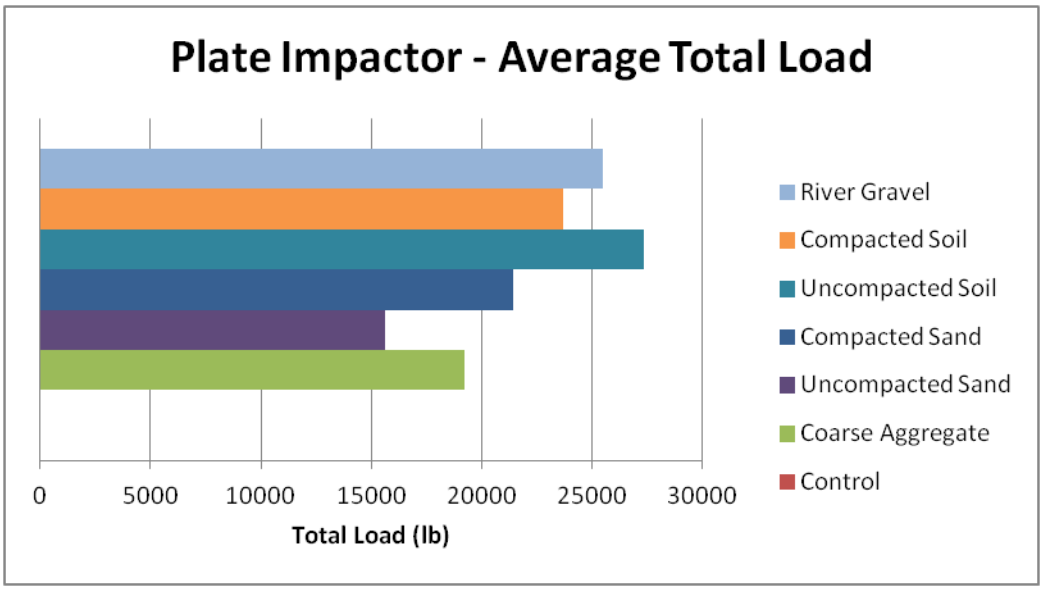

Fig 5-3
Plate Impactor Total Load

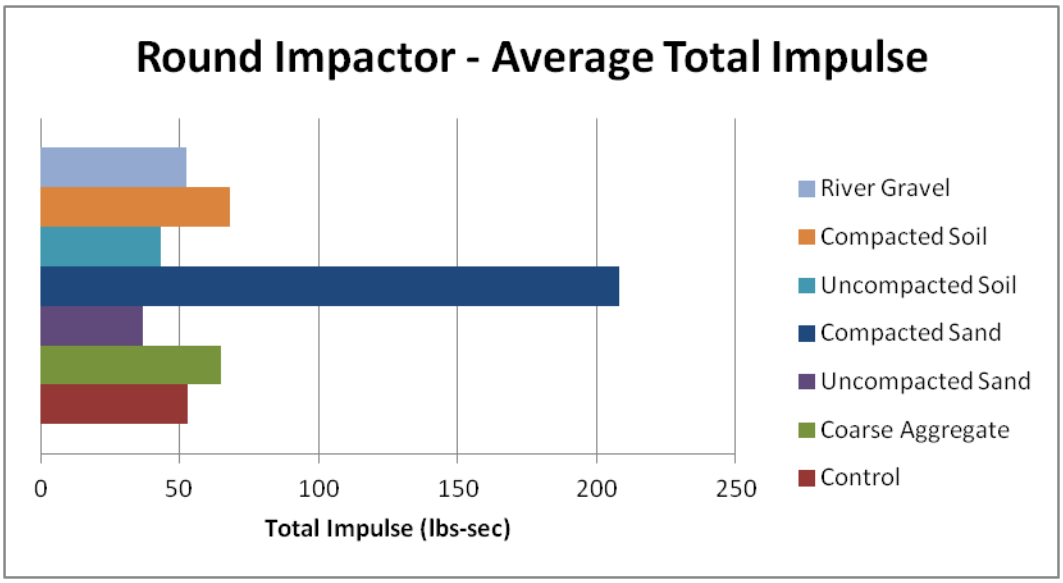

Fig 5-4
Round Impactor Total Impulse

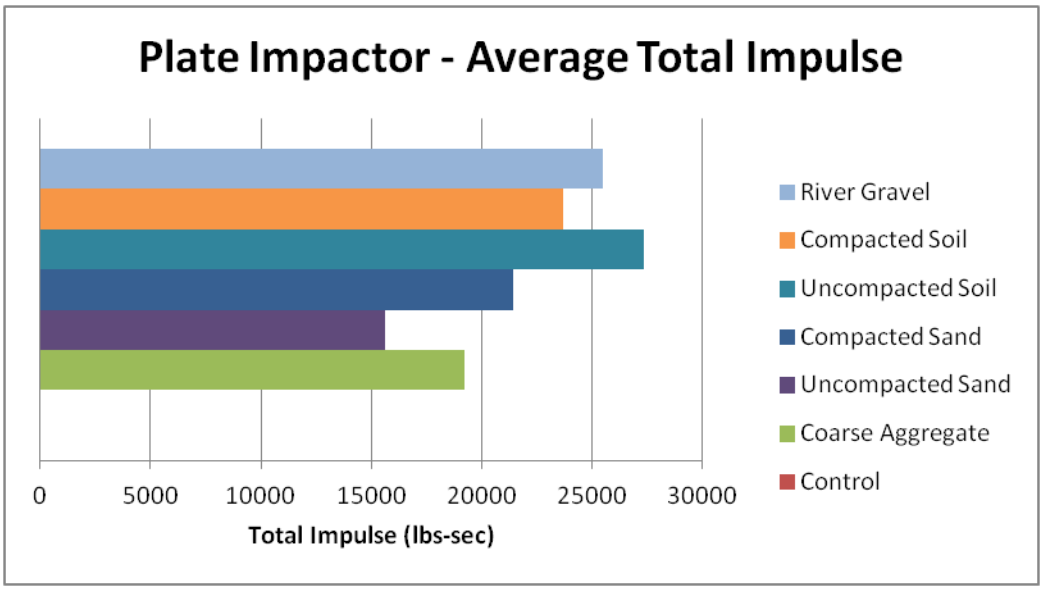

Fig 5-5
Plate Impactor Total Impulse

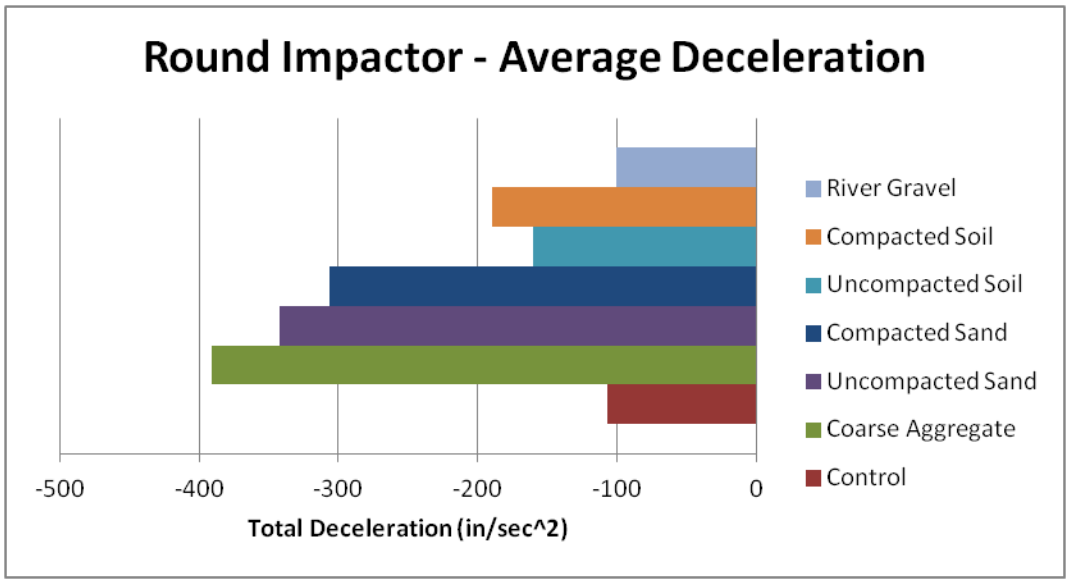

Fig 5-6
Round Impactor Average Acceleration

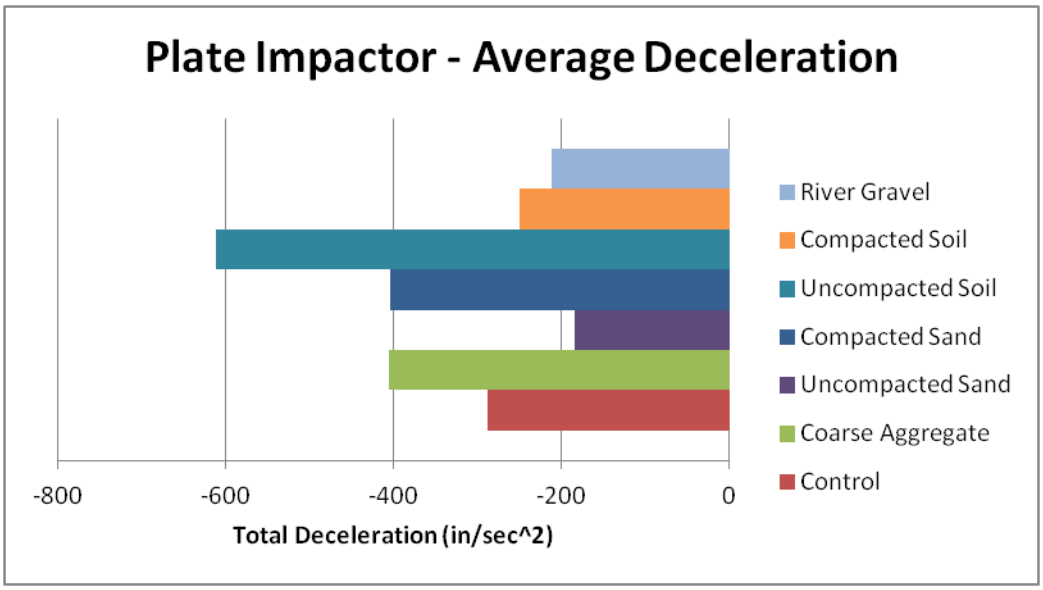

Fig 5-7
Plate Impactor Average Acceleration

5.2 Round Impacting Head Analysis

Before testing took place, it was expected that sand would most likely be the best fill material and particularly compacted sand as it added the most mass to the system. Below is a comparison of data from load cells and velocity tracked of the round control specimens and the compacted sand specimens.

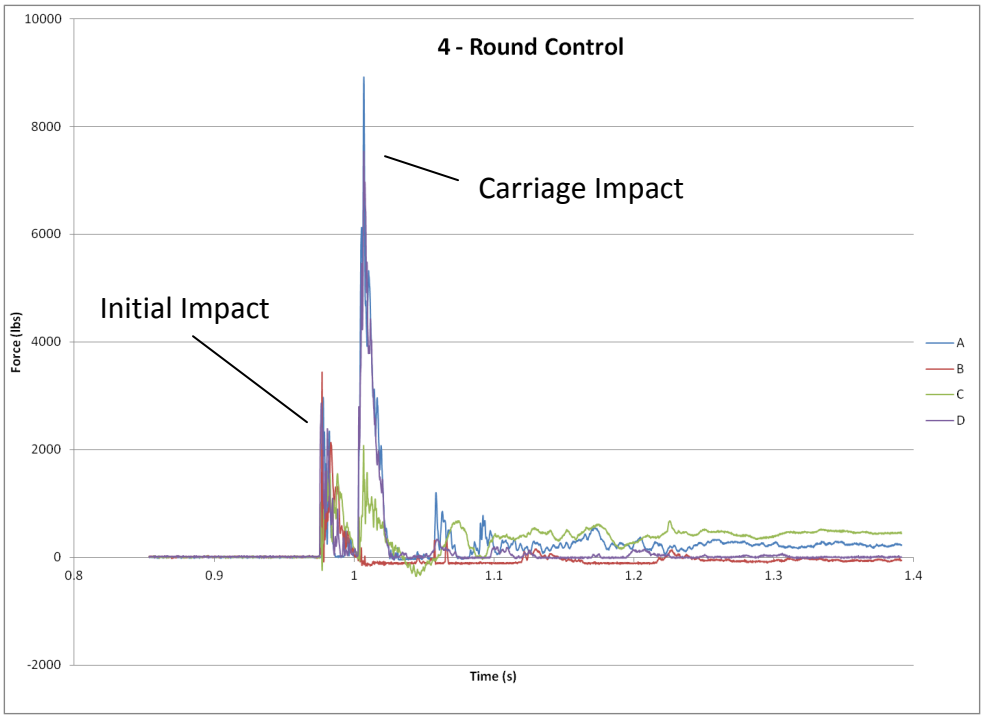

Fig 5-8
Round Control I Load Cell Response

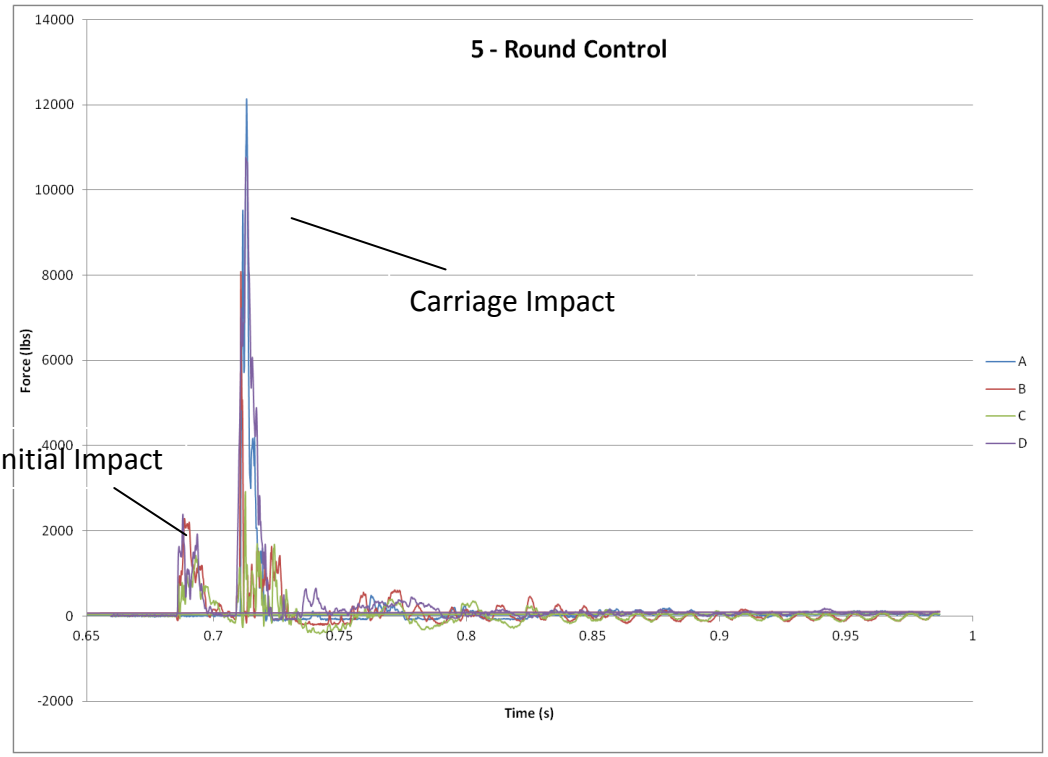

Fig 5-9
Round Control II Load Cell Response

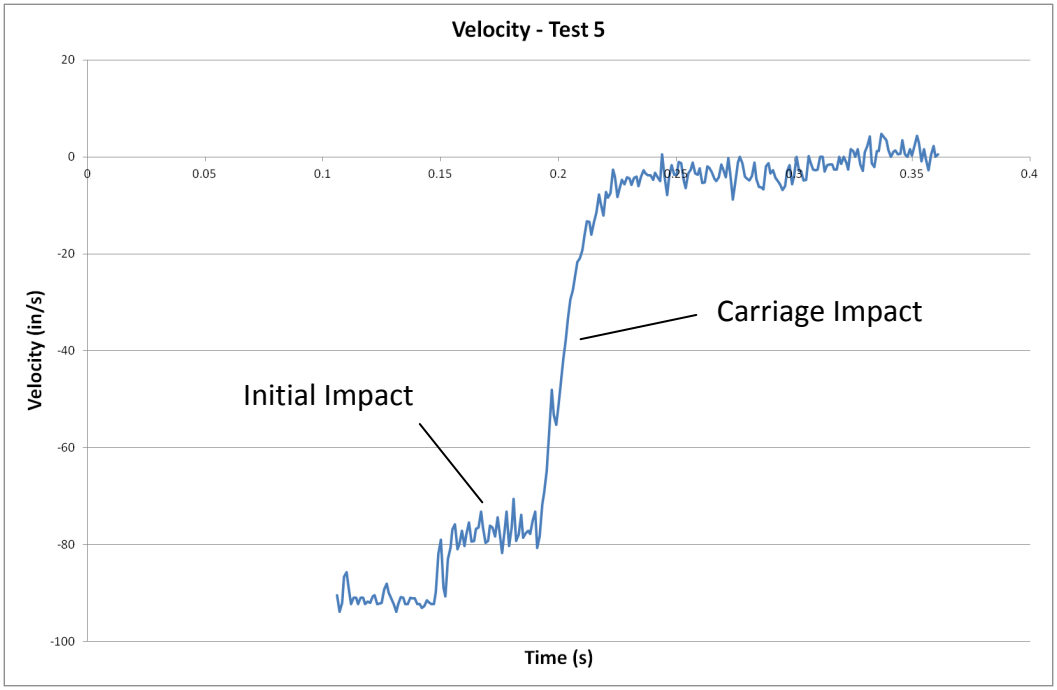

Fig 5-10
Velocity of carriage before, during, and after impacts for Test 5

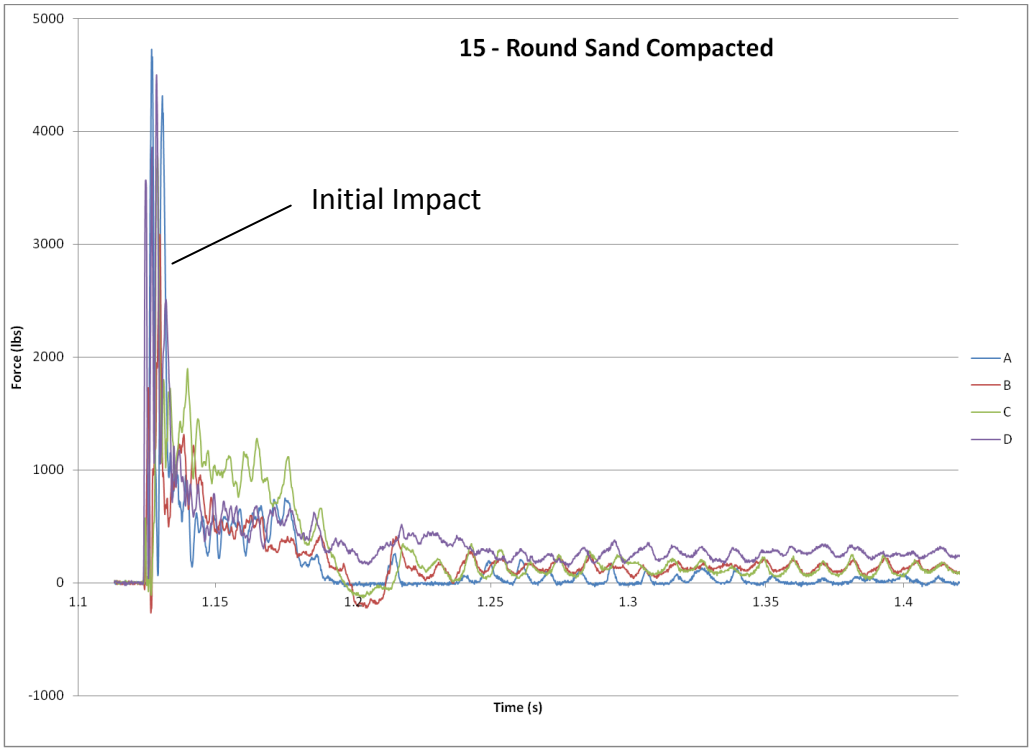

Fig 5-11
Round Sand Compacted Load Cell Response

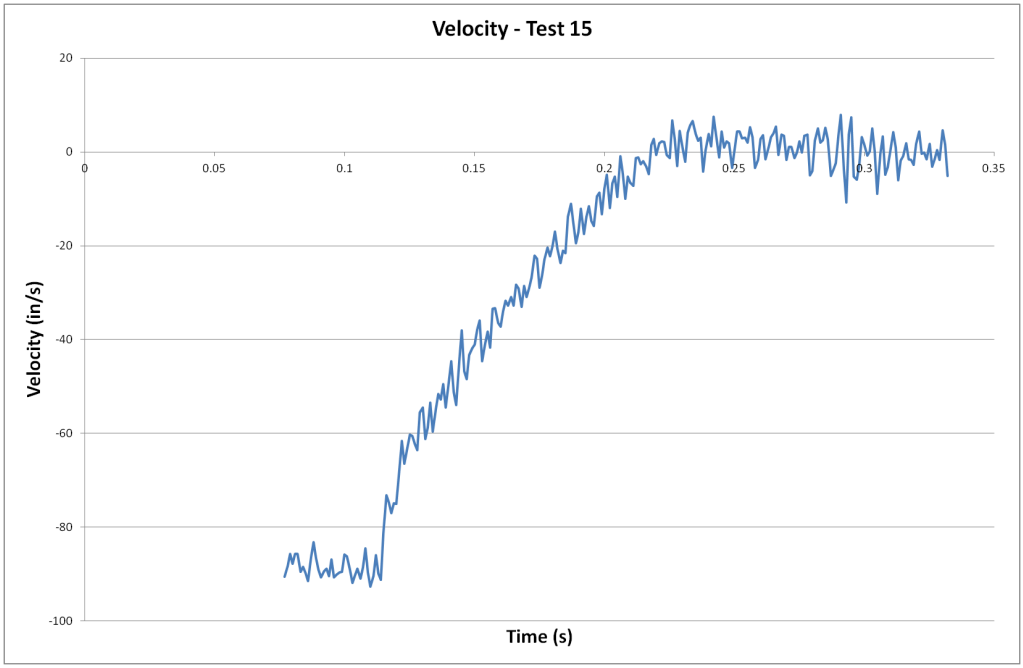

Fig 5-12
Velocity of carriage before, during, and after impacts for Test 15

Two impact events are seen in the load cell data in figures 5-1 and 5-2. These correspond to the initial penetration of the impactor and then the impact of the carriage. Total load registered in the control specimens averaged 27920 lbs while compacted sand fill was recorded at 16271 lbs, a reduction of 41.7%. It is important to note that despite *individual* load cells registering higher loads on some specimens, a total of *all* load cells and their data for each test is the true measure. Higher spikes on individual load cells are caused due to small changes in geometries of the box sections and how they are situated on the plate which distributes the load into the load cells.

Impulse data from the load cell graphs also supports the performance of compacted sand over the control specimen. In general, a greater impulse value means more energy dissipation and increased response time. Impulse data is likely the most telling data in the experiment because it better represents the energy applied and dissipated. Total peak load is useful but it does not incorporate the time component of the impact which is a very important factor since dynamic loads happen very quickly. Since no additional impact was made in the compacted sand test, one impulse value was recorded so it is obviously larger than the control value (refer to Table 5-3). Compacted soil and coarse aggregate also produced impulse values that were greater than the control.

It was expected that all impulse values should be greater than the control. However, three fills failed to do this for the round impactor head: river gravel, uncompacted sand, and uncompacted soil based on the load cell data. This behavior can be explained

considering the reaction of the supports, the mass added for each fill in the box, and the force of the impactor head. If an assumption is made that the test setup is constant, the behavior described above can be summarized as a change in mass. Applied force remains the same and needs to be reacted by the supports and the box. The addition mass in the box drives the reaction forces in the supports. Thus, when everything else is held constant, it is expected the impulse at the supports will be lower as mass is added even if the resistance is otherwise unchanged. The extra material is not adding resistance in the cases above, just mass. Without the acceleration data from the box, this is not able to be quantified. Still, visual data from tests such as uncompacted sand show an obvious improvement in overall damage to the box sections.

It should be noted that in the control specimens, there is some 10000 lbs of force of difference between the two. The higher force value seems consistent with the behavior in the system after viewing the high speed footage. Specimen #5 has much more damage than #4, so much so that it had broken in half after extraction from the machine. A variation in stiffness of the box sections at this point seems evident. Regardless, the performance of compacted sand is unquestionable in reducing impact force. It should also be noted however that load cell data for test #16, another round compacted sand test is not available. The data had been corrupted during transfer.

Another parameter to examine aside from the load cells is the initial impact velocity and extracted acceleration data. For this, the graphs of control versus the compacted sand are

first presented below. Velocity data for test #4 is not available due to errors in the program while extracting that data.

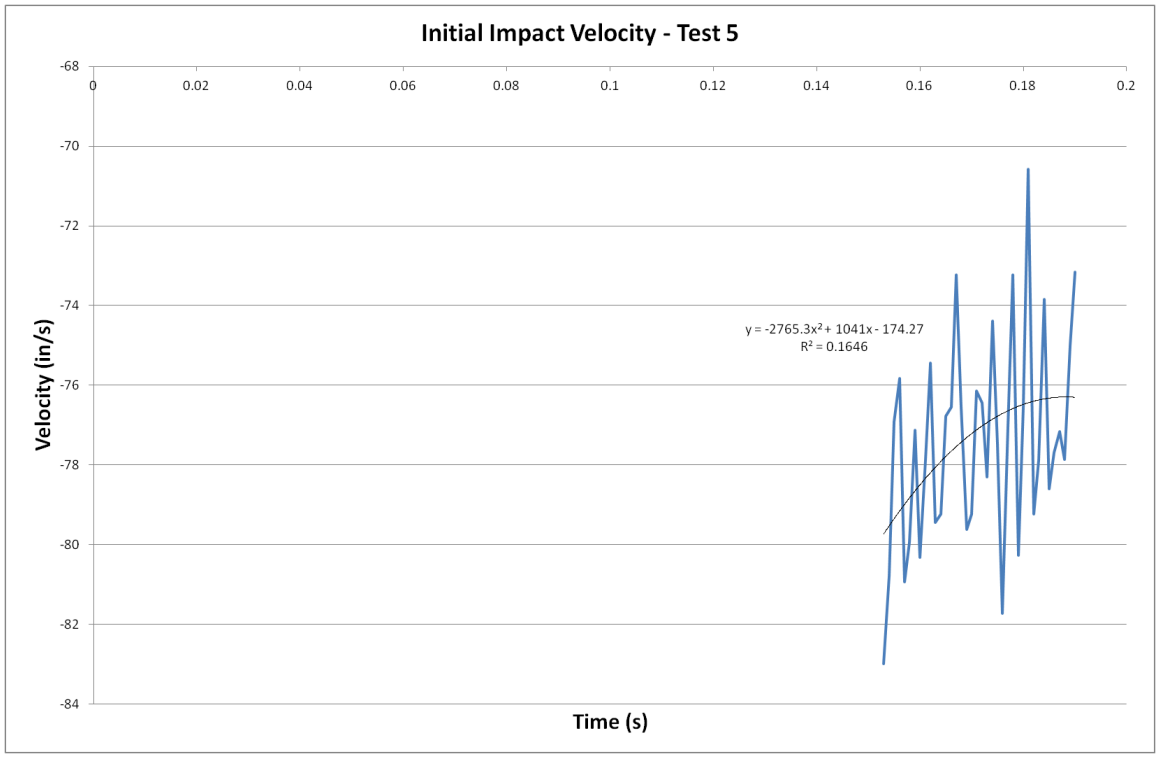

Fig 5-13
Round Control Initial Impact Velocity

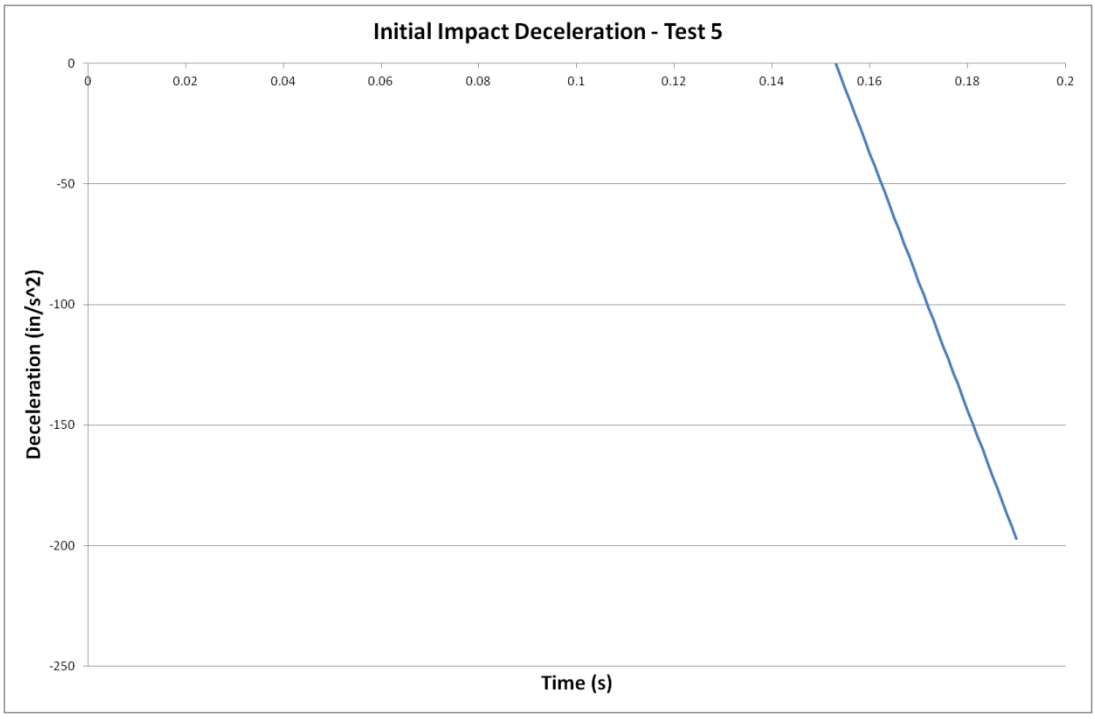

Fig 5-14
Round Control Initial Impact Acceleration

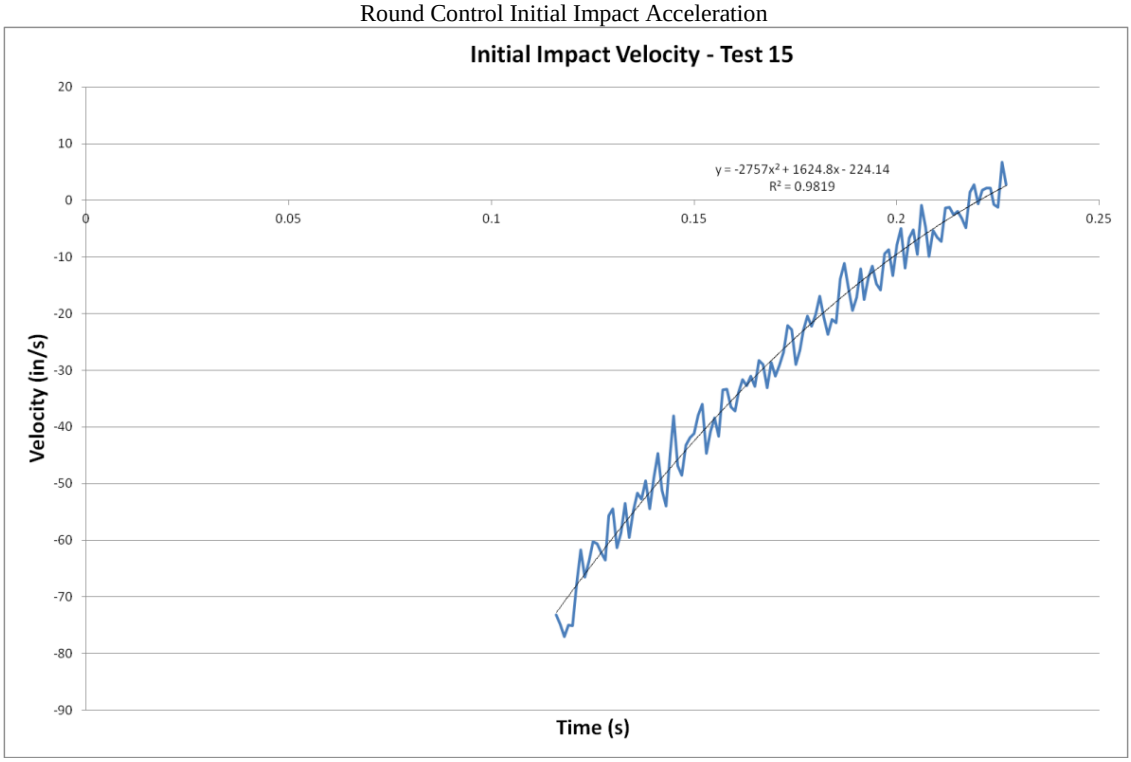

Fig 5-15
Round Sand Compacted Initial Impact Velocity

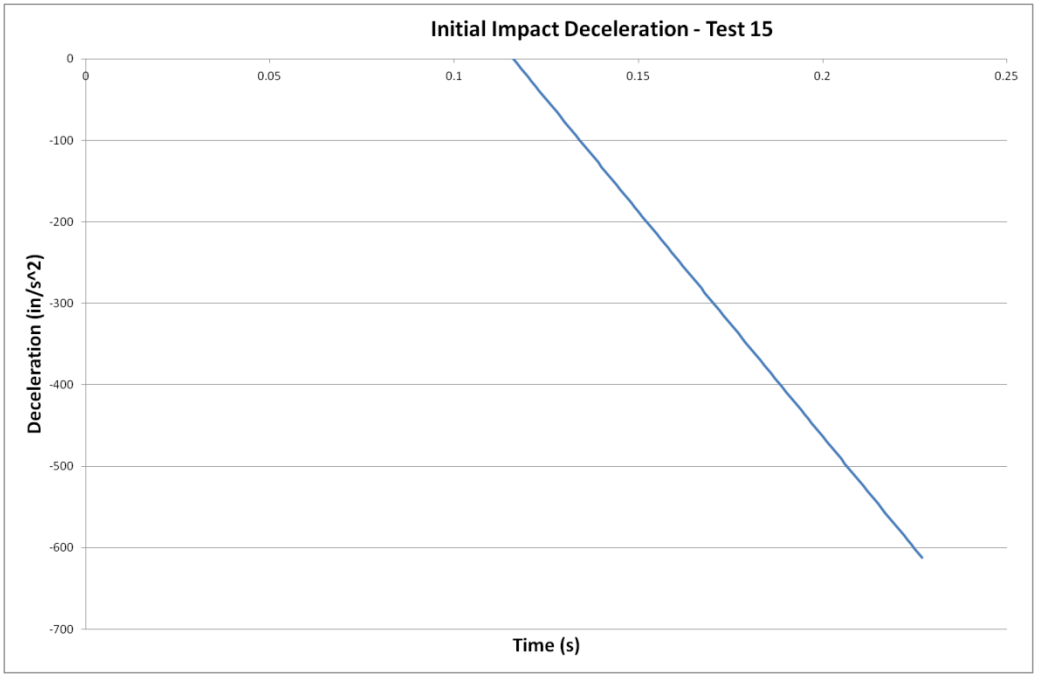

Fig 5-16
Round Sand Compacted Initial Impact Acceleration

After reviewing the plots for initial impact velocities and accelerations, the compacted sand fill provides a much more controlled deceleration of the impactor head. It provided enough mass to the system for this as well as additional stiffness, preventing the impactor from penetrating fully.

5.3 Plate Impacting Head Analysis

The plate impactor tests produced data that was more difficult to analyze. A problem with the plate impactor data set is the lack of any control data. Control data for the plate impactor was all unusable, corrupted, or lost. For tests 1 and 2, the force parameter and time parameter for the load cell data program were set too low. This caused a gap in the data and missed any peak loadings. An attempt to reclaim lost control data was made by

making two additional plate control specimens, 29 and 30. These sets of data were lost when a computer was reformatted without having the data pulled from them properly. Visual data of the control specimens showed considerable damage where the impacted face of the box was caved in, severe flexural cracking, and ends blowing out. However, these failures seen by visual inspection repeat themselves in fill materials that the data suggests performed well.

The plate impacting head did not typically experience a multiple impact event meaning that anytime an impact occurred, it was only the impactor head. The load cell graphs pictured in the appendix for the plate impactor reinforce this as no double-spikes are typically seen for the exception of the control. Since load cell data is not available to analyze directly with a control specimen, acceleration can be used instead. Below, the acceleration plots of the best numerically-performing fill materials, compacted soil and compacted sand are compared with a control specimen.

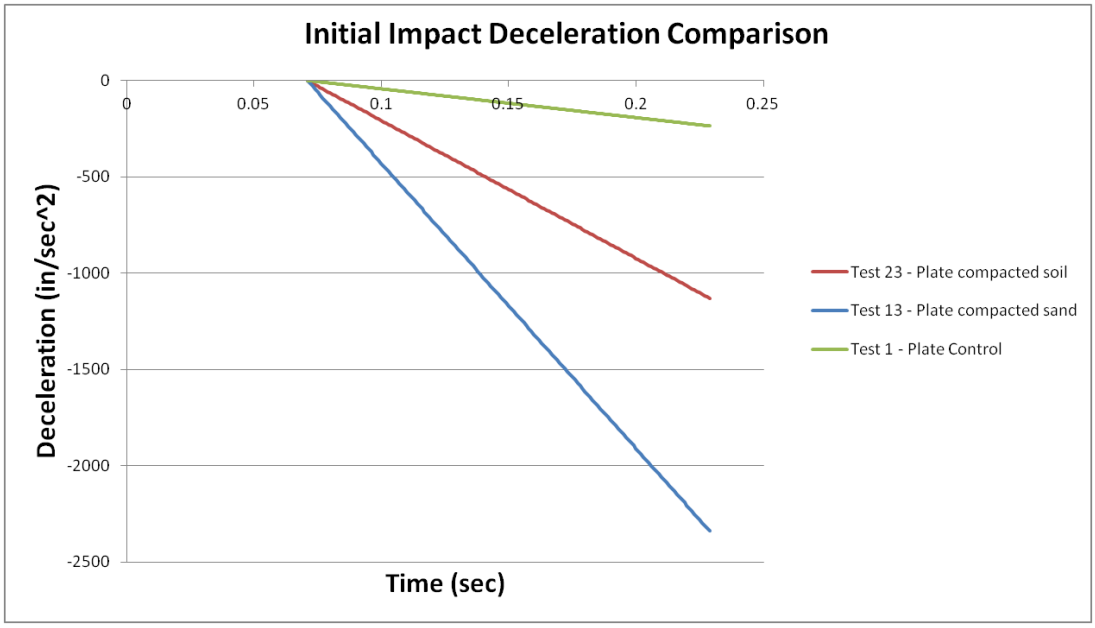

Fig 5-17
Initial impact comparison of tests, 1, 13, and 23

As the data shows, both compacted soil and sand decelerated the impactor much more effectively than the control. Compacted sand improved deceleration another 200 in/sec^2 over compacted soil.

Referring to Table 5-3 again, impulse values from the tests suggest that compacted soil performed better than compacted sand. However, based on the visual inspection and acceleration data, compacted sand fill seems to perform better. Despite not being effective in the round impactor head tests, river gravel also produced favorable impulse values with visual inspection being better than compacted soil. Both compacted soil tests, although producing favorable and consistent impulse values, failed considerably more than compacted sand and river gravel. In total, all fill materials gave what seems to be consistent, favorable impulse response minus that of uncompacted sand which had

nearly 200 lbs-sec difference between test duplicates. High speed footage seems to support the fact that the first plate uncompacted soil test outperformed the second plate uncompacted soil test, but only relatively. Both boxes have more than moderate damage but the second having lower impulse value definitely sustained more.

5.4 Conclusions and Recommendations

Upon visual inspection after each test during the testing phase, it was clear that compacted sand performed the best. This visual data was backed by impulse figures, total load data, and deceleration data obtained and analyzed afterwards. While the round impactor head data was clearer for the specific case, the benefit of compacted sand as a fill material applies to both impact events. It should be noted that sand was a good fill material, but extra emphasis should be placed on it being compacted. This allowed more mass to be added to the system and increases the resistance to penetration. Overall, visual inspection appeared to be the most telling of how the specimens performed. Load cell data and accelerations did help reinforce some key points, but it was usually obvious upon removing specimens after an experiment which fill materials performed well.

Should further research be conducted, the author has a few remarks on what can be improved for this type of study. One of the most important things to reconsider in future testing is the concrete forms. In this study, the wooden forms used to cast all 30 specimens were deteriorating by the end. While these forms worked decently for this application, a more long-term study would benefit from metal forms with some sort of exterior bolting mechanism. The forms would have a higher upfront cost, but would save

a significant amount of labor rebuilding the forms and extracting the cured boxes. As the forms deteriorated, splintering caused the wood to become more difficult to reassemble and also concrete cured around these splintering locations to make extraction very difficult. The deterioration of the forms would often make new pieces needed thus delaying original scheduling for the day. Additionally, the wooden forms were susceptible to deforming when poured with concrete and no two box sections had *exactly* the same dimensions. Uniform, rigid metal forms would help the above issues considerably.

In addition to using more substantial forms for casting concrete, it is believed that the method of attaching the lids to the box sections could be improved. The current method constrained the fill material within the box well, but a system in which the load transfer through the box would be more desirable. The lids were weak already, but being attached in the way they were created even more asymmetry in the system.

The drop heights used in this study seemed to work for the impactor heads. A 5 ft drop height for the round impactor worked effectively since the compacted sand test was not able to penetrate. The plate most likely could have been dropped from 5 ft as well but the goal was a more flexural-type failure. It was believed more energy would be needed to produce those results which *did* happen. It may have been beneficial to have equal energy applied to each system.

The research is not limited to just impact testing however. Future studies could include larger box structures, more similar to the original study proposed to the Leonard Wood Institute and Nation Science Foundation. These larger scale tests could focus primarily on better fill materials such as compacted sand. Also, the studies could branch out in terms of applied dynamic loads. Real projectiles from military-grade weapons could be used during the tests as well blast loading. These additional test ideas would help progress the development of a potential life-saving concrete system.

Works Cited

1. Pike, John. "Improvised Explosive Devices (IEDs) / Booby Traps." GlobalSecurity.org - Reliable Security Information. 7 May 2011. Web. 27 Jan. 2012.

2. Stockfish, David: Yariv Eldar, Daniella HarPaz Mechnikov (1970). Dokszyc-Parafianow Memorial Book – Belarus (Sefer Dokshitz-Parafianov). Tel Aviv: Association of Former Residents of Dokszyce-Parafianow in Isreal. p. 274.

3. Marolda, Edward J. "Mine Warfare in South Vietnam." Naval History and Heritage Command. 26 Aug. 2003. Web. 27 Jan. 2012.

4. "More Attacks, Mounting Casualties." Washington Post: Breaking News, World, US, DC News & Analysis. 30 Sept. 2007. Web. 27 Jan. 2012.

5. "HAB 1 Specifications." HESCO. Web. 01 Feb. 2012. <http://www.hesco.com/prod_hab1.asp>.

6. Ross, Tedesco and Kuennen, "Effects of Strain Rate on Concrete Strength." ACI Materials Journal 92, no. 1 (1995): 1-11.

7. Scherbatiuk, K, and N Rattanawangcharoen. "Experimental testing and numerical modeling of soil-filled container walls." *International Journal of Engineering Structures* . 30. no. 12 (2008): 3545-54.

8. Scherbatiuk, K, and N Rattanawangcharoen. "A hybrid rigid body rotation model for predicting a response of a temporary soil-filled wall subjected to blast loading." *International Journal of Impact Engineering*. no. 37 (2010): 11-16.

9. Bambach, M.R.; Jama, H.; Zhao, X.L.; Grzebieta, R.H.; “Hollow and Concrete Filled Steel Hollow Sections Under Transverse Impact Loads,” Engineering Structures, v 30, n 10, p2859-2870, October 2008.

Appendix

The appendix is broken down much like the raw visual data section of the thesis. Each impactor will have a section with relevant graphs associated with the type of tests. Graphs included are load cell data graphs (force), velocity, and acceleration from the HotShot Link SC program.

After the first graphs presented, any important interpretations in how the graphical data appears and what it is believed to mean will be covered. The rest of the plots will be included. As mentioned in the thesis, the concrete static compressive strengths is listed in Table A-1. All cylinders were 6”x12”.

Test #	Test Category	Impact Head	Date Cast	Date Broken	Comp Strength (lb)	Comp Strength (psi)
1	Control	Plate	2/17/2012	3/1/2012	83730	2961
2	Control	Plate	2/17/2012	3/1/2012	83730	2961
4	Control	Round	2/19/2012	3/2/2012	81980	2900
5	Control	Round	2/19/2012	3/2/2012	81980	2900
3	Coarse Aggregate	Plate	2/17/2012	3/1/2012	83730	2961
10	Coarse Aggregate	Plate	2/24/2012	3/7/2012	96770	3423
6	Coarse Aggregate	Round	2/19/2012	3/2/2012	81980	2900
7	Coarse Aggregate	Round	2/22/2012	3/5/2012	92400	3268
11	Uncompacted Sand	Plate	2/24/2012	3/7/2012	96770	3423
12	Uncompacted Sand	Plate	2/24/2012	3/7/2012	96770	3423
8	Uncompacted Sand	Round	2/22/2012	3/5/2012	92400	3268
9	Uncompacted Sand	Round	2/22/2012	3/5/2012	92400	3268
13	Compacted Sand	Plate	3/9/2012	3/21/2012	92500	3272
14	Compacted Sand	Plate	3/9/2012	3/21/2012	92500	3272
15	Compacted Sand	Round	3/9/2012	3/21/2012	92500	3272
16	Compacted Sand	Round	3/23/2012	4/9/2012	82960	2934
17	Uncompacted Soil	Plate	3/23/2012	4/4/2012	82960	2934
18	Uncompacted Soil	Plate	3/23/2012	4/4/2012	82960	2934
21	Uncompacted Soil	Round	3/28/2012	4/9/2012	78500	2776
20	Uncompacted Soil	Round	3/28/2012	4/9/2012	78500	2776
24	Compacted Soil	Plate	3/29/2012	4/10/2012	67470	2386
23	Compacted Soil	Plate	3/29/2012	4/10/2012	67470	2386
19	Compacted Soil	Round	3/28/2012	4/9/2012	78500	2776
22	Compacted Soil	Round	3/29/2012	4/10/2012	67470	2386
25	River Gravel	Plate	3/30/2012	4/11/2012	124040	4387
26	River Gravel	Plate	3/30/2012	4/11/2012	124041	4387
27	River Gravel	Round	3/30/2012	4/11/2012	124042	4387
28	River Gravel	Round	3/31/2012	4/12/2012	150710	5330
29	Control	Plate	3/31/2012	4/12/2012	150710	5330
30	Control	Plate	3/31/2012	4/12/2012	150710	5330

Table A-1
Concrete Static Compressive Strengths

A.1 Round Impacting Head

A.1.1 Round Control I

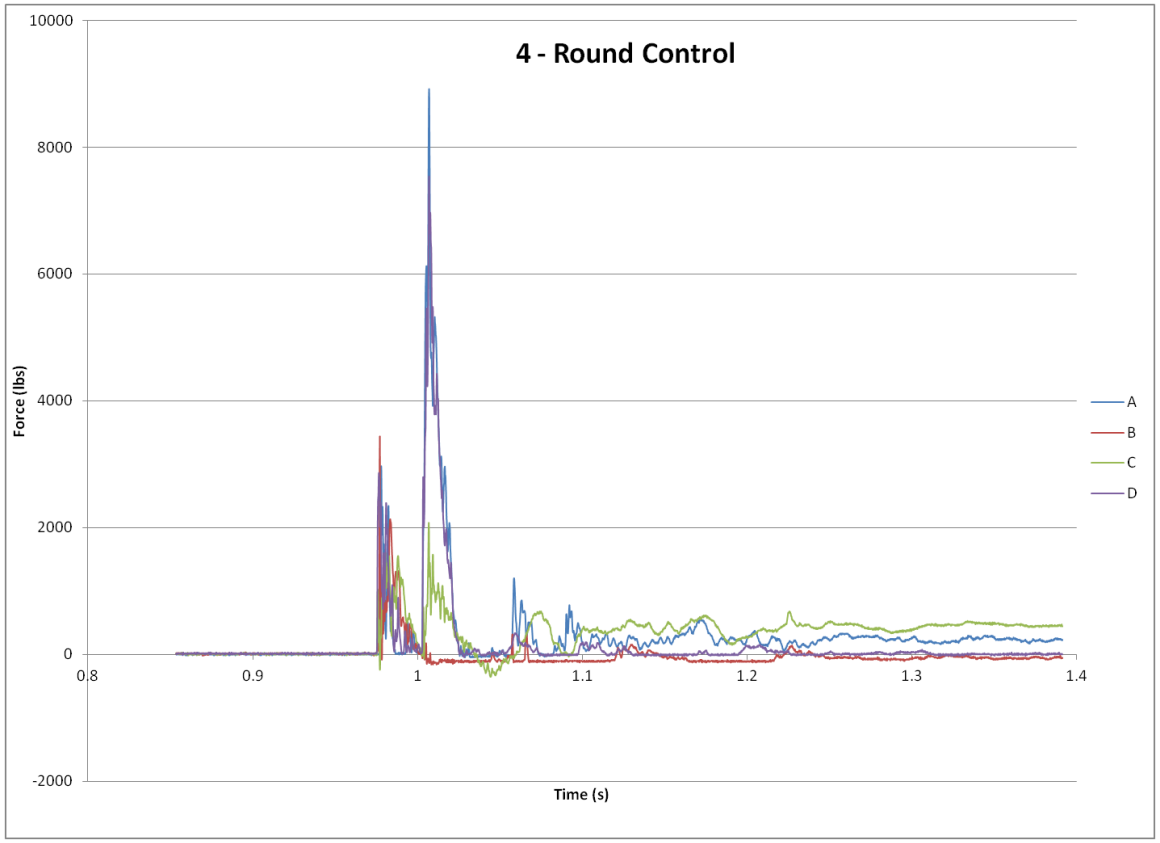

Velocity and acceleration data for test #4 are not included due to extraction error from the HotShot program.

A.1.2 Round Control II

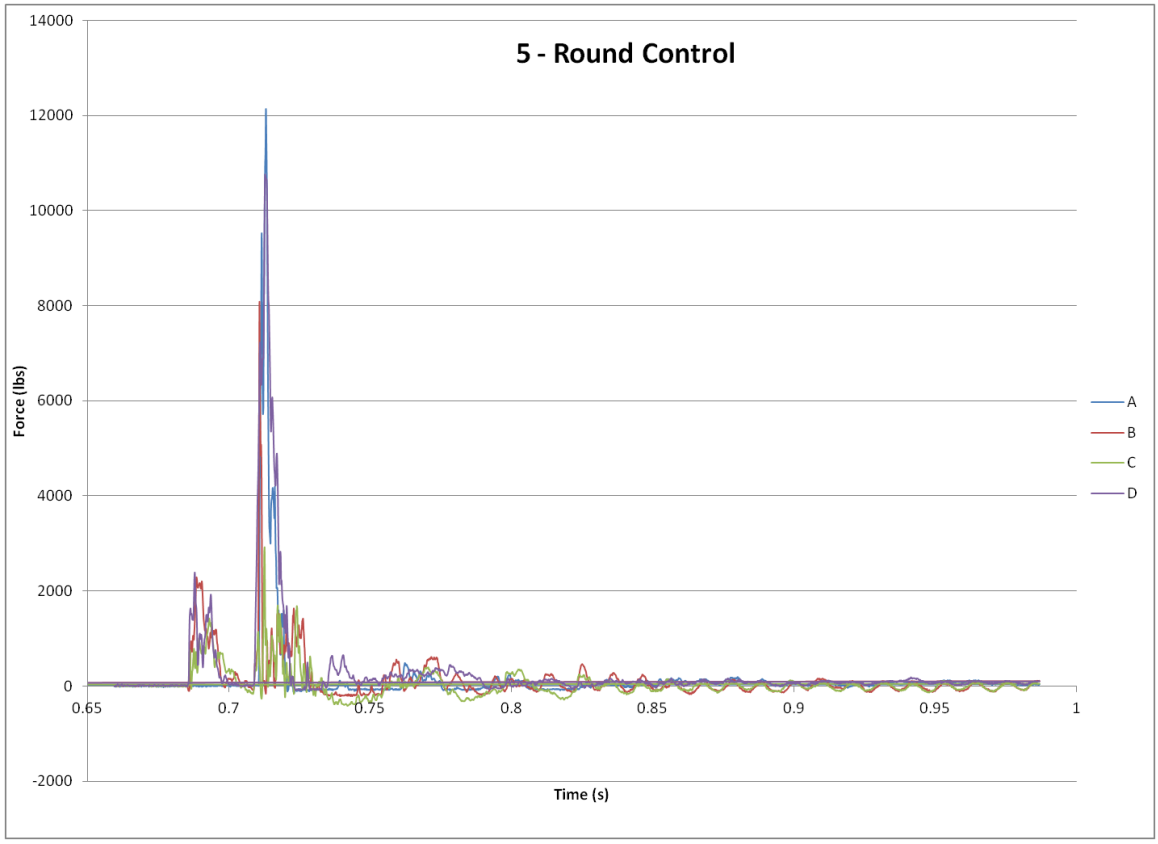

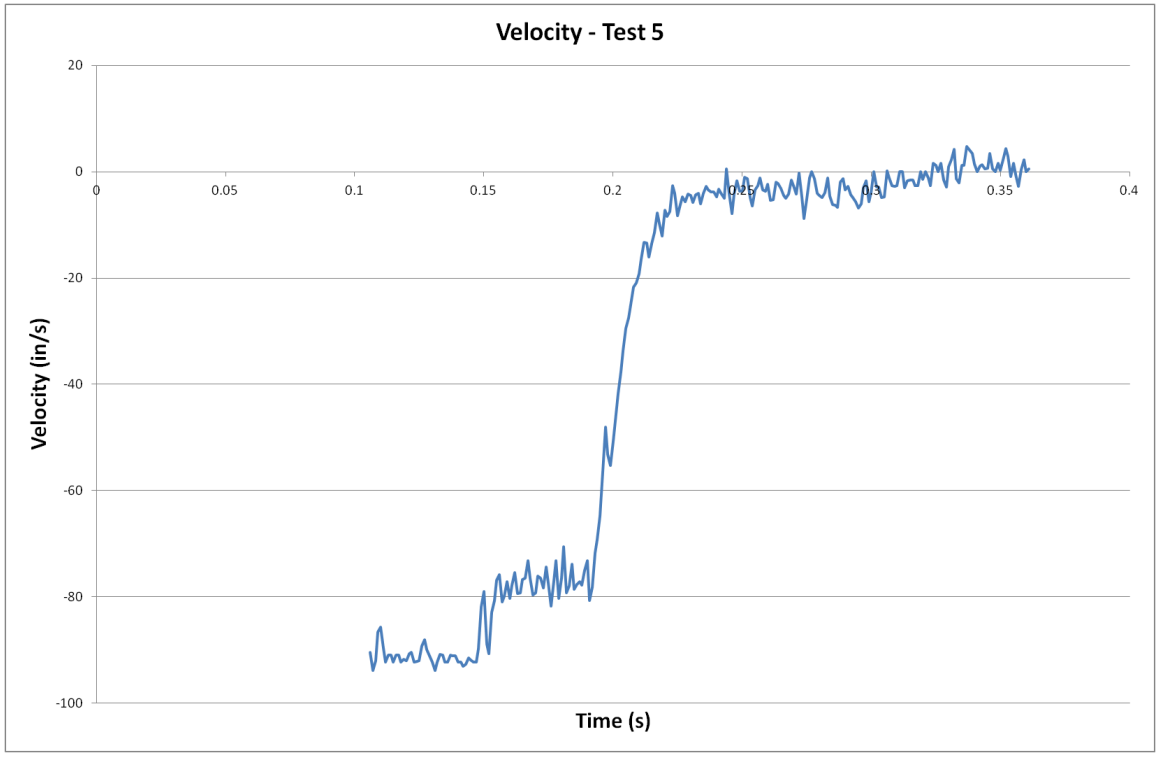
Velocity - Test 5
Velocity (in/s)
Time (s)
20
0
-20
-40
-60
-80
-100
0
0.05
0.1
0.15
0.2
0.25
0.3
0.35
0.4

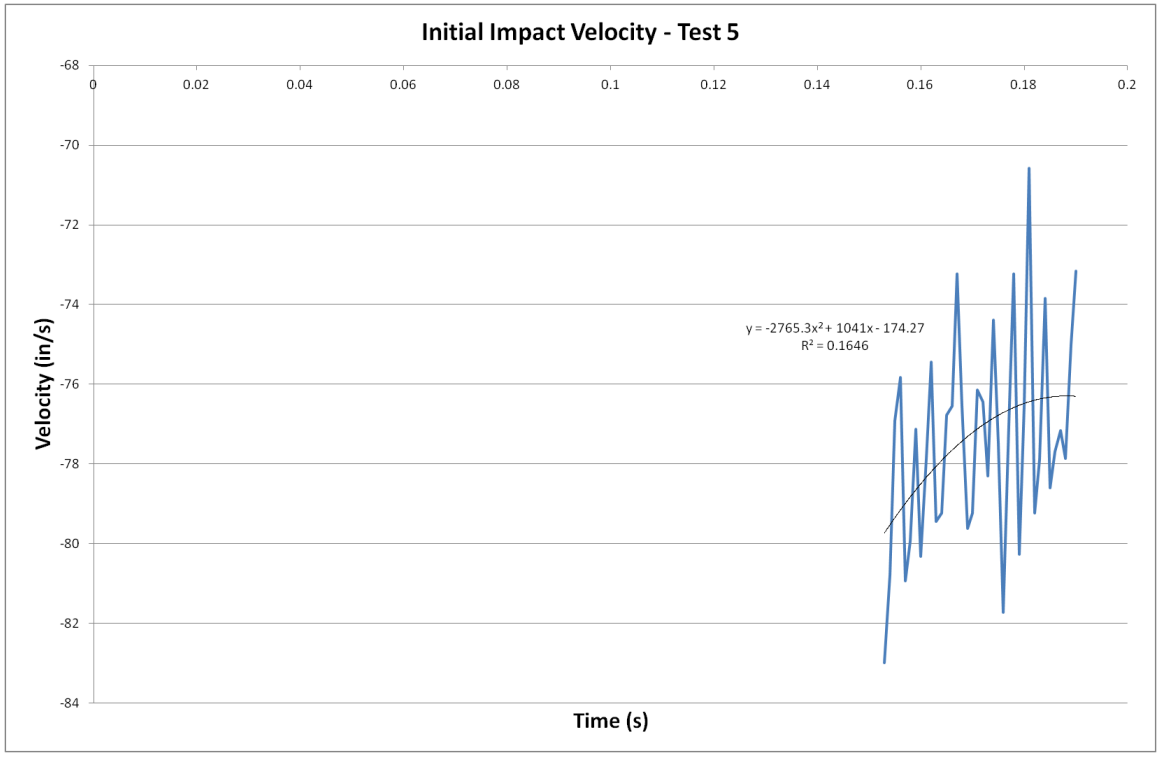
Initial Impact Velocity - Test 5
Velocity (in/s)
Time (s)
y = -2765.3x² + 1041x - 174.27
R² = 0.1646
-68
-70
-72
-74
-76
-78
-80
-82
-84
0
0.02
0.04
0.06
0.08
0.1
0.12
0.14
0.16
0.18
0.2

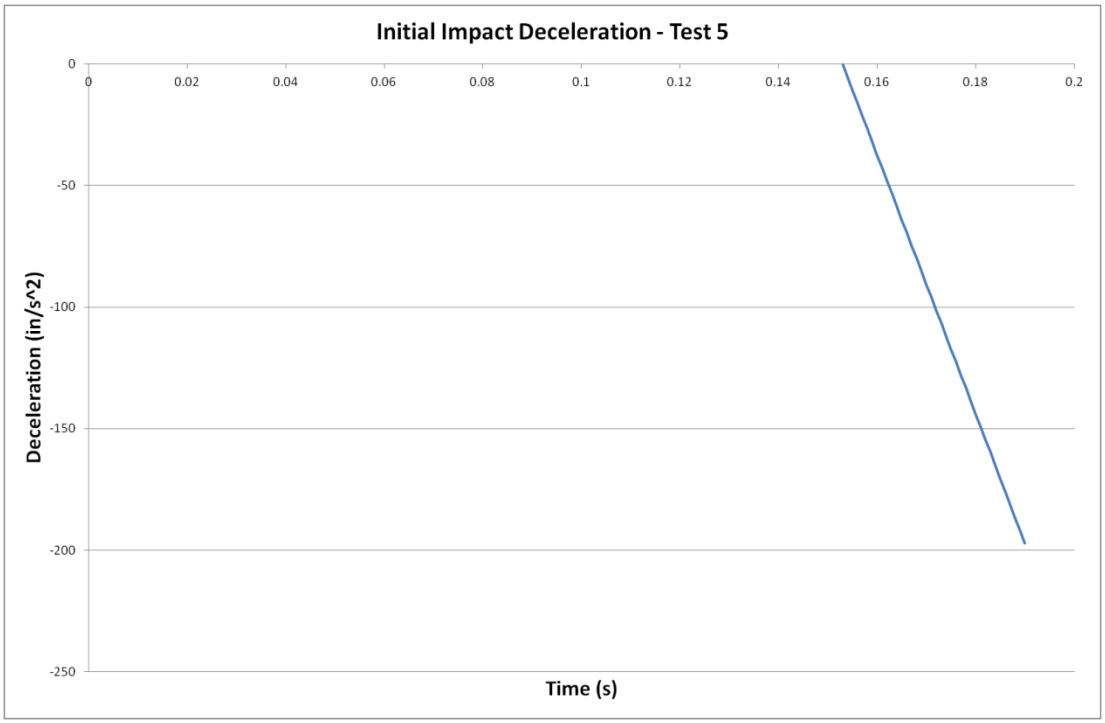

The two spikes in load cell data correspond to the impactor full penetrating then the impact carriage making contact with the specimen. In every velocity graph, there is an inherent amount of noise because of the tracking software. The software produces this noise because of the percent match of light to the white dot that it is tracking. The software will then jump slightly to a different pixel given its interpretation of what the dot is. This also explains the "jump" in every velocity graph after it has impacted the specimen. It is assumed to be caused by the flexural response to the impact in the impact carriage. The sudden point load into the carriage bends the carriage enough to register a small change in velocity thus a deceleration and reacceleration in the system. The acceleration graphs are significantly noisy, so much so that they do not provide a lot of useful data. It can be seen that deceleration values do have less large peaks in cases such as the round compacted sand, but the graphs still do not provide much useful data.

A.1.3 Round Coarse Aggregate I

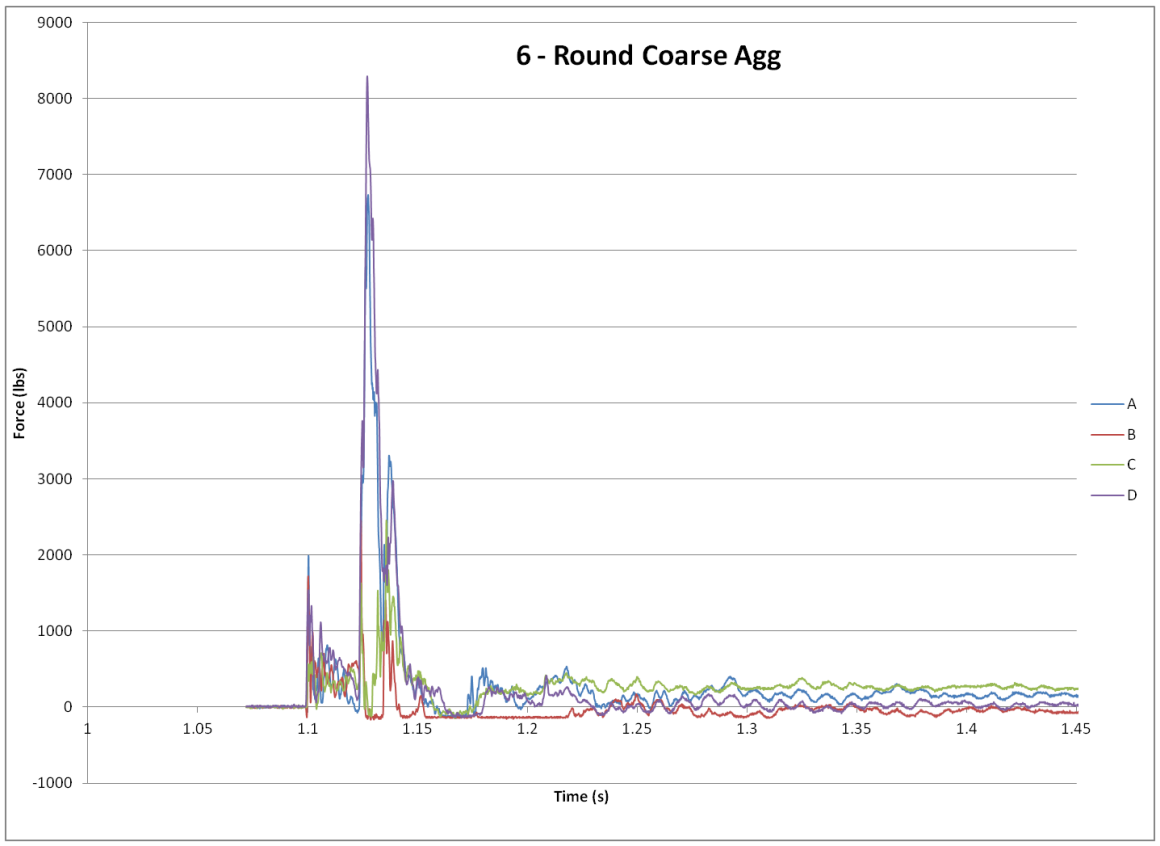

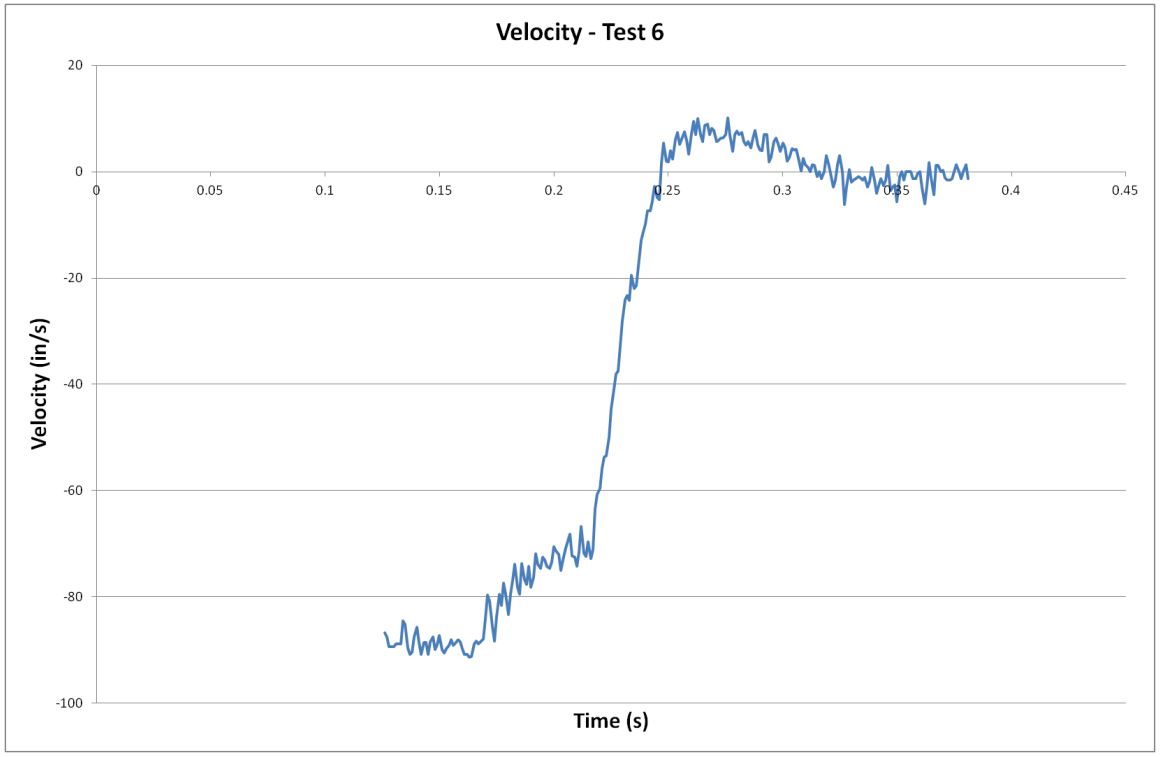
Velocity - Test 6
Velocity (in/s)
Time (s)
20
0
-20
-40
-60
-80
-100
0
0.05
0.1
0.15
0.2
0.25
0.3
0.35
0.4
0.45

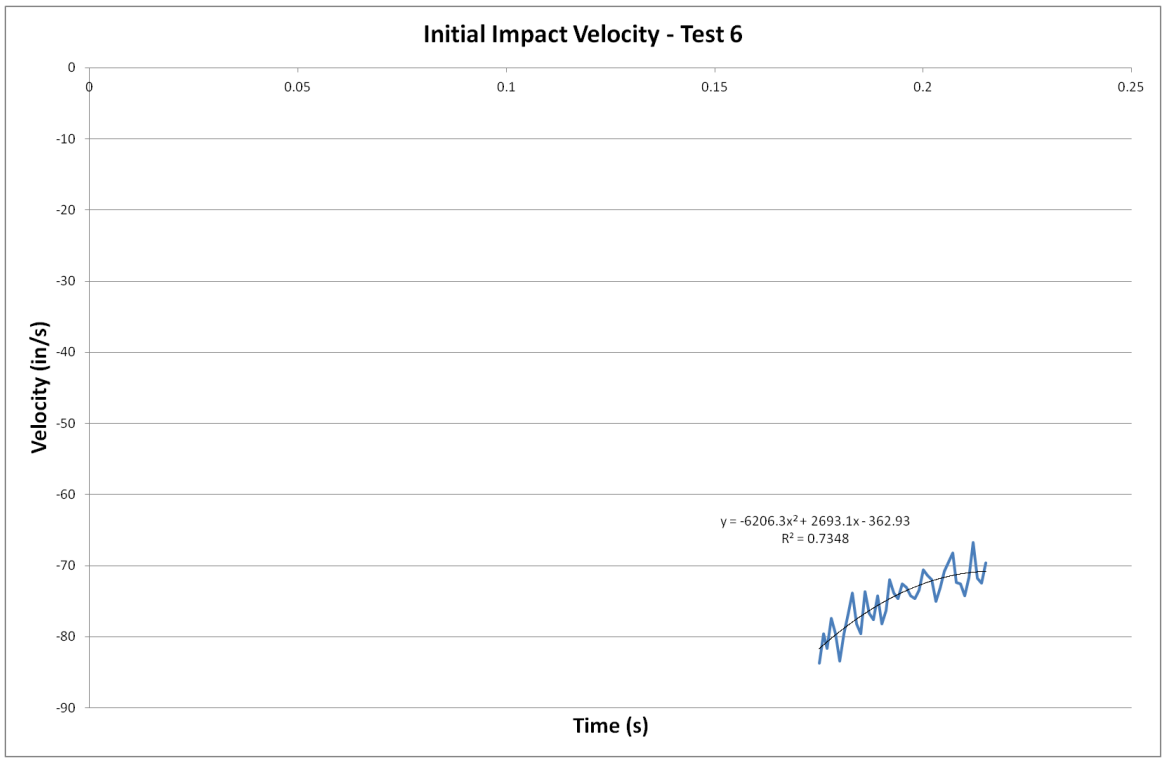
Initial Impact Velocity - Test 6
Velocity (in/s)
Time (s)
y = -6206.3x² + 2693.1x - 362.93
R² = 0.7348
0
-10
-20
-30
-40
-50
-60
-70
-80
-90
0
0.05
0.1
0.15
0.2
0.25

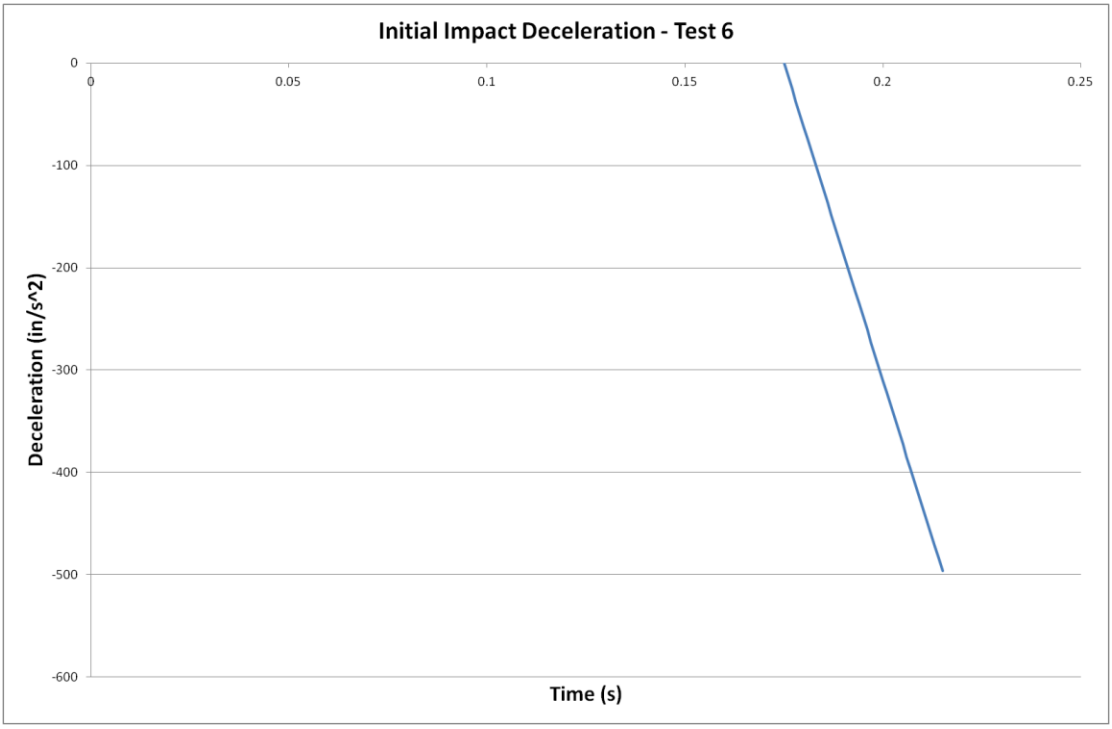
Initial Impact Deceleration - Test 6
0
-100
-200
-300
-400
-500
-600
0
0.05
0.1
0.15
0.2
0.25
Deceleration (in/s^2)
Time (s)

A.1.4 Round Coarse Aggregate II

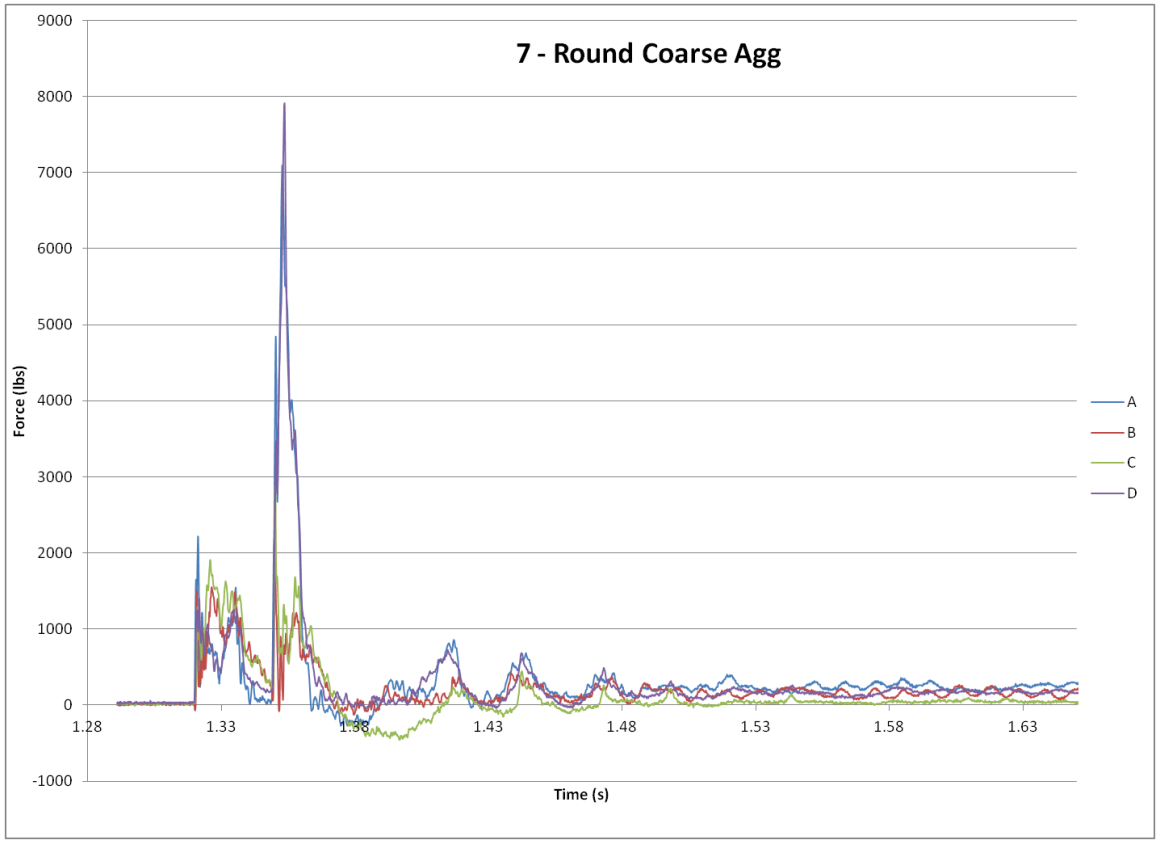

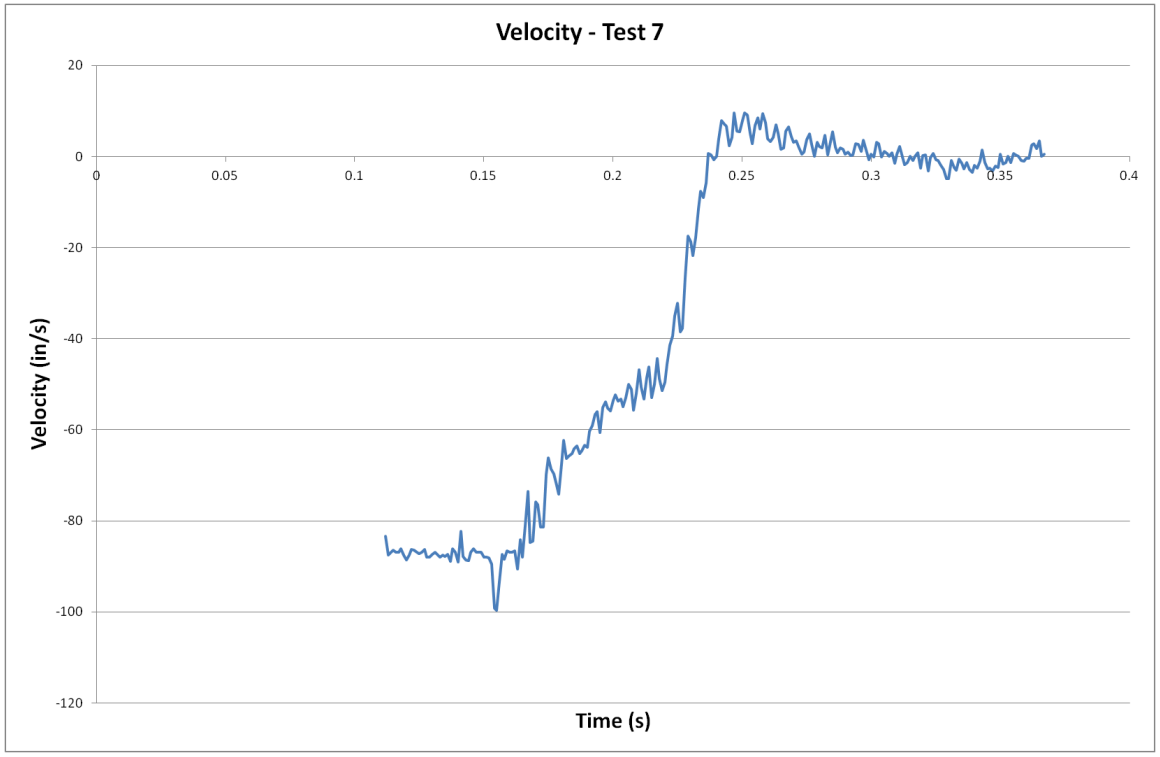
Velocity - Test 7
Velocity (in/s)
Time (s)
20
0
-20
-40
-60
-80
-100
-120
0
0.05
0.1
0.15
0.2
0.25
0.3
0.35
0.4

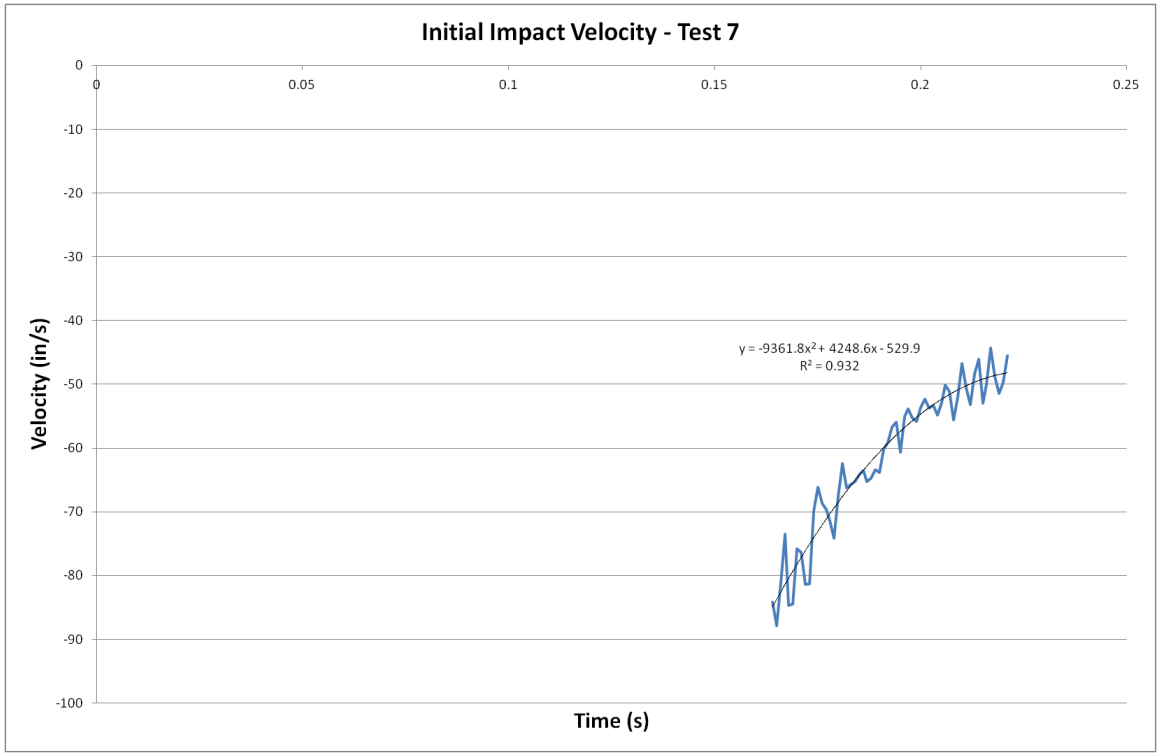
Initial Impact Velocity - Test 7
Velocity (in/s)
Time (s)
y = -9361.8x² + 4248.6x - 529.9
R² = 0.932
0
-10
-20
-30
-40
-50
-60
-70
-80
-90
-100
0
0.05
0.1
0.15
0.2
0.25

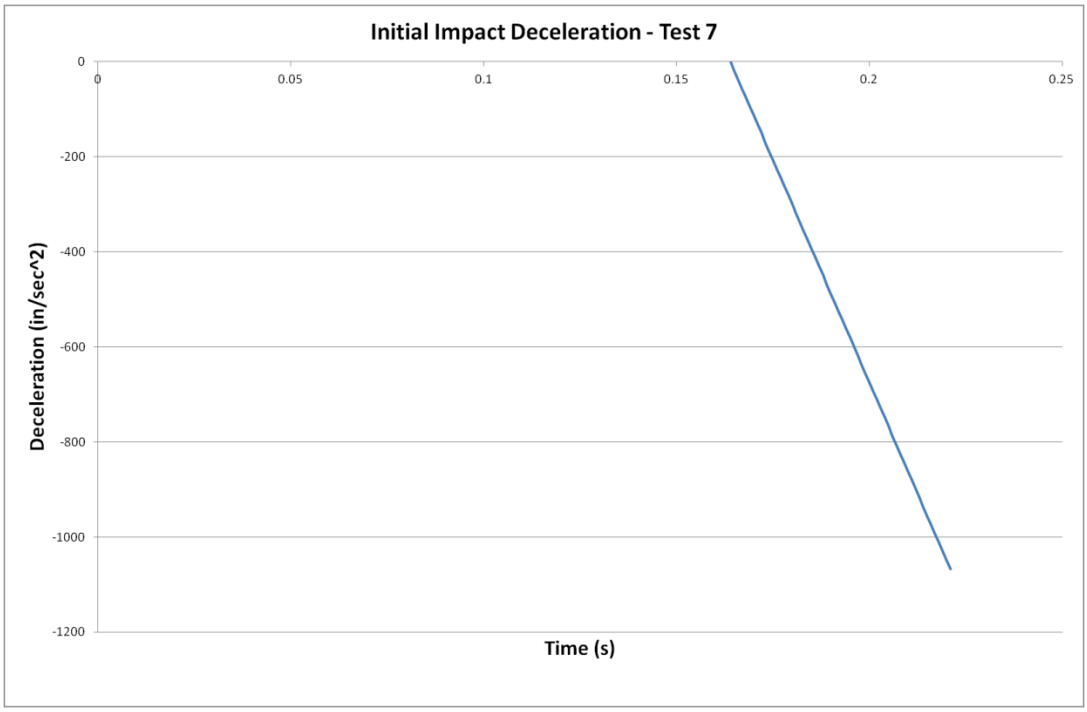
Initial Impact Deceleration - Test 7
0
-200
-400
-600
-800
-1000
-1200
Deceleration (in/sec^2)
0
0.05
0.1
0.15
0.2
0.25
Time (s)

A.1.5 Round Sand Uncompacted I

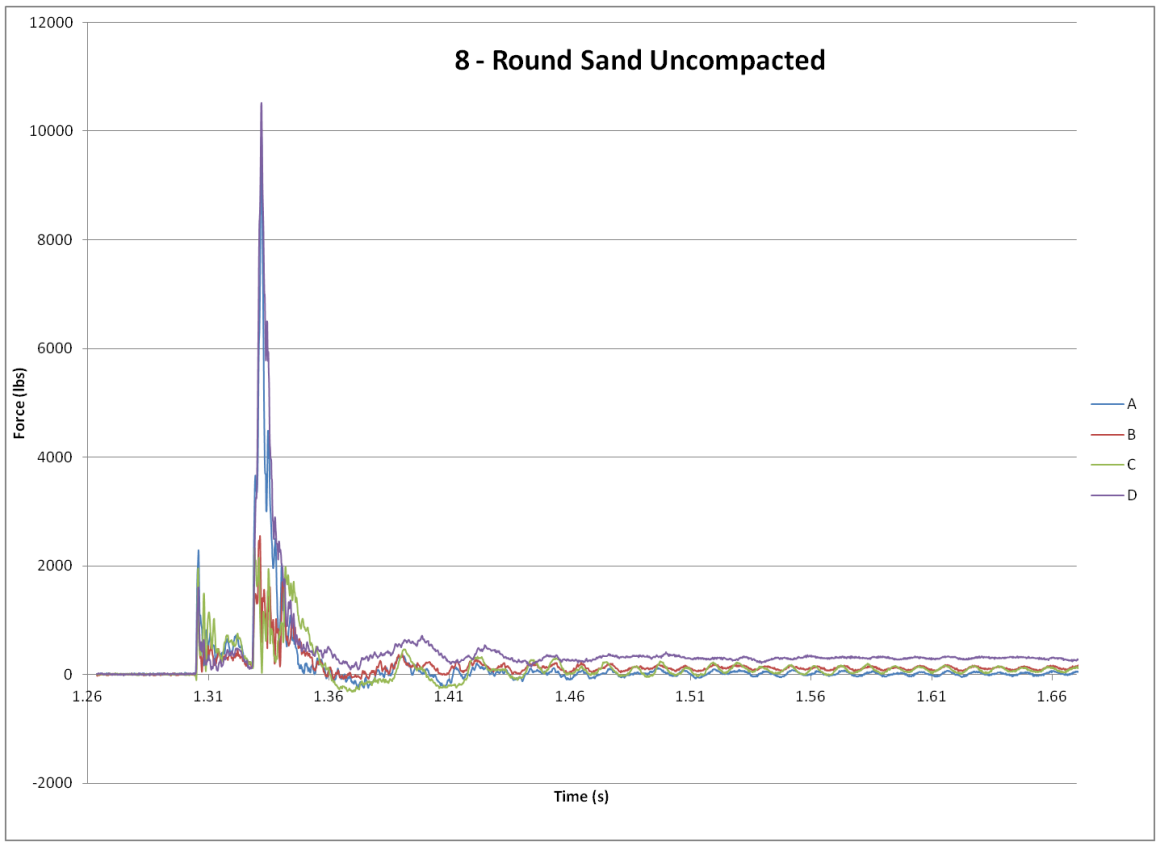

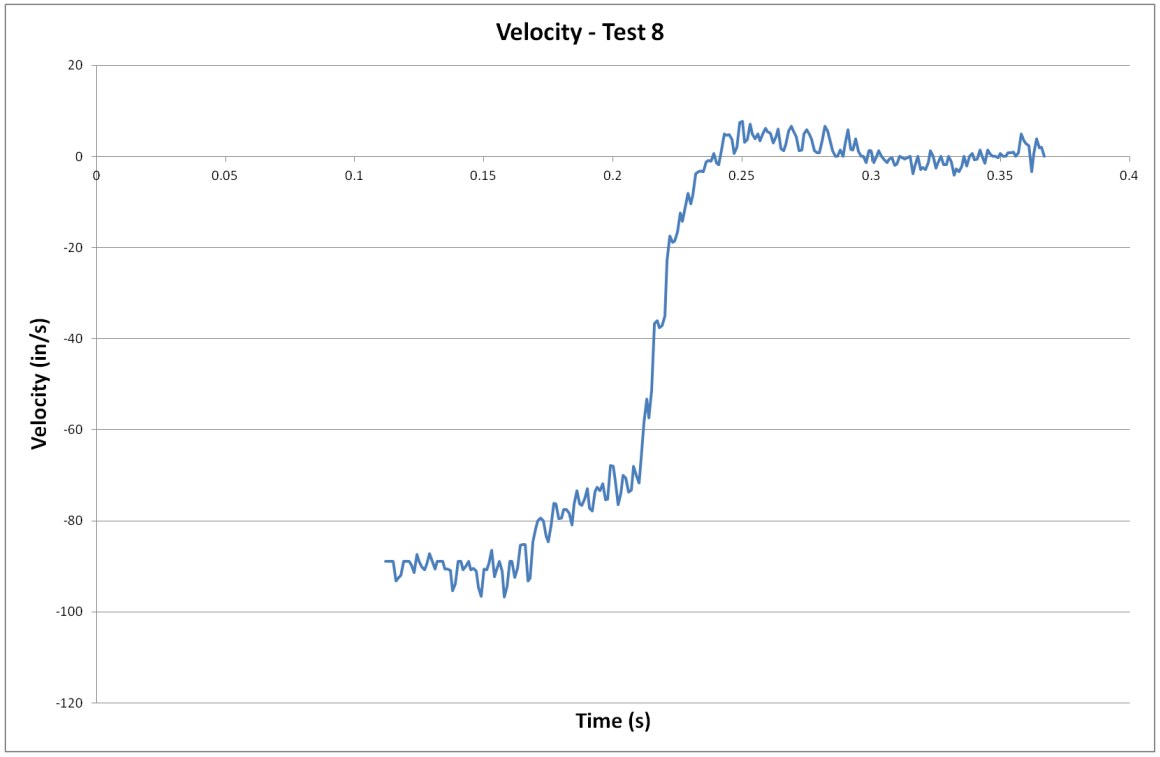
Velocity - Test 8
Velocity (in/s)
Time (s)
20
0
-20
-40
-60
-80
-100
-120
0
0.05
0.1
0.15
0.2
0.25
0.3
0.35
0.4

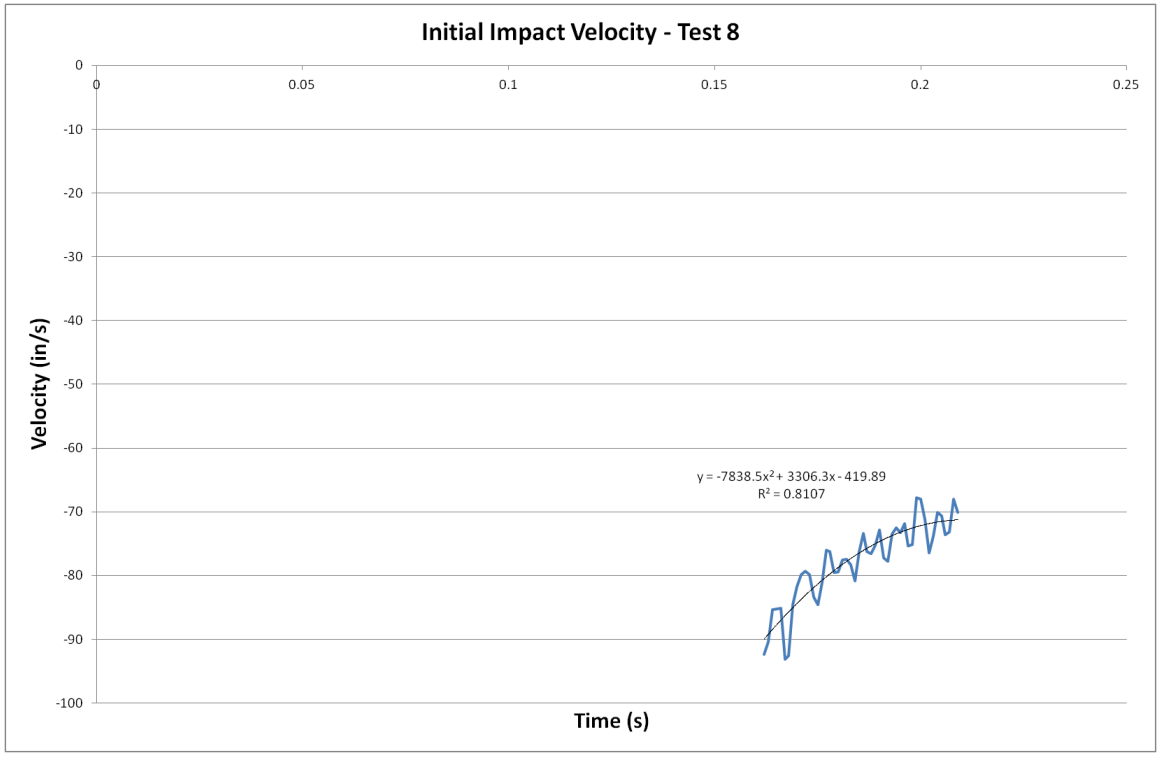
Initial Impact Velocity - Test 8
Velocity (in/s)
Time (s)
y = -7838.5x² + 3306.3x - 419.89
R² = 0.8107
0
-10
-20
-30
-40
-50
-60
-70
-80
-90
-100
0
0.05
0.1
0.15
0.2
0.25

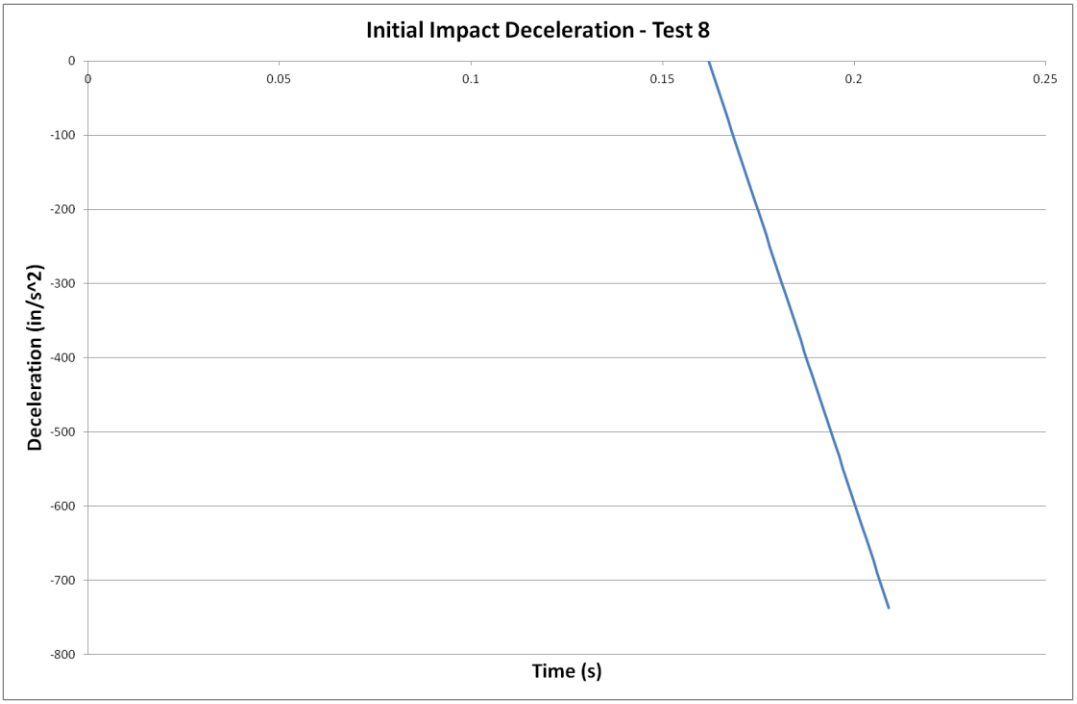
Initial Impact Deceleration - Test 8
0
-100
-200
-300
-400
-500
-600
-700
-800
Deceleration (in/s^2)
0
0.05
0.1
0.15
0.2
0.25
Time (s)

A.1.6 Round Sand Uncompacted II

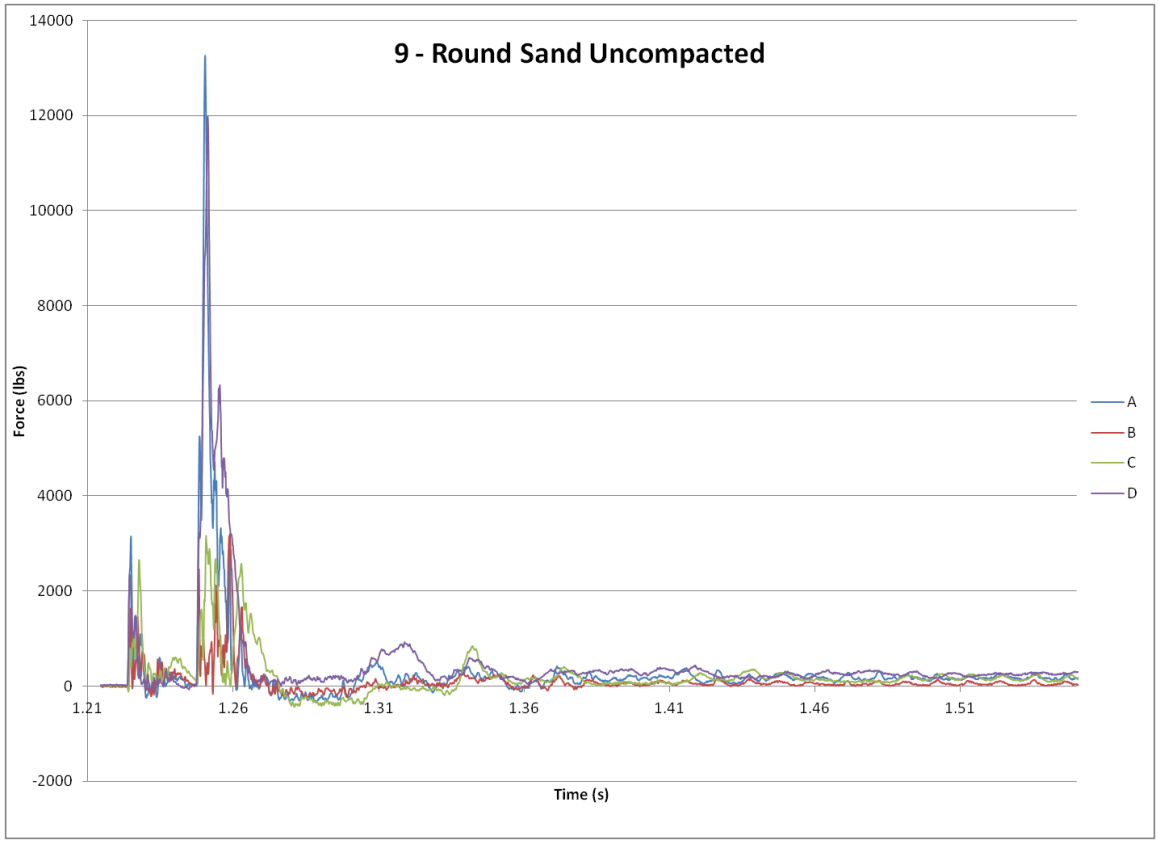

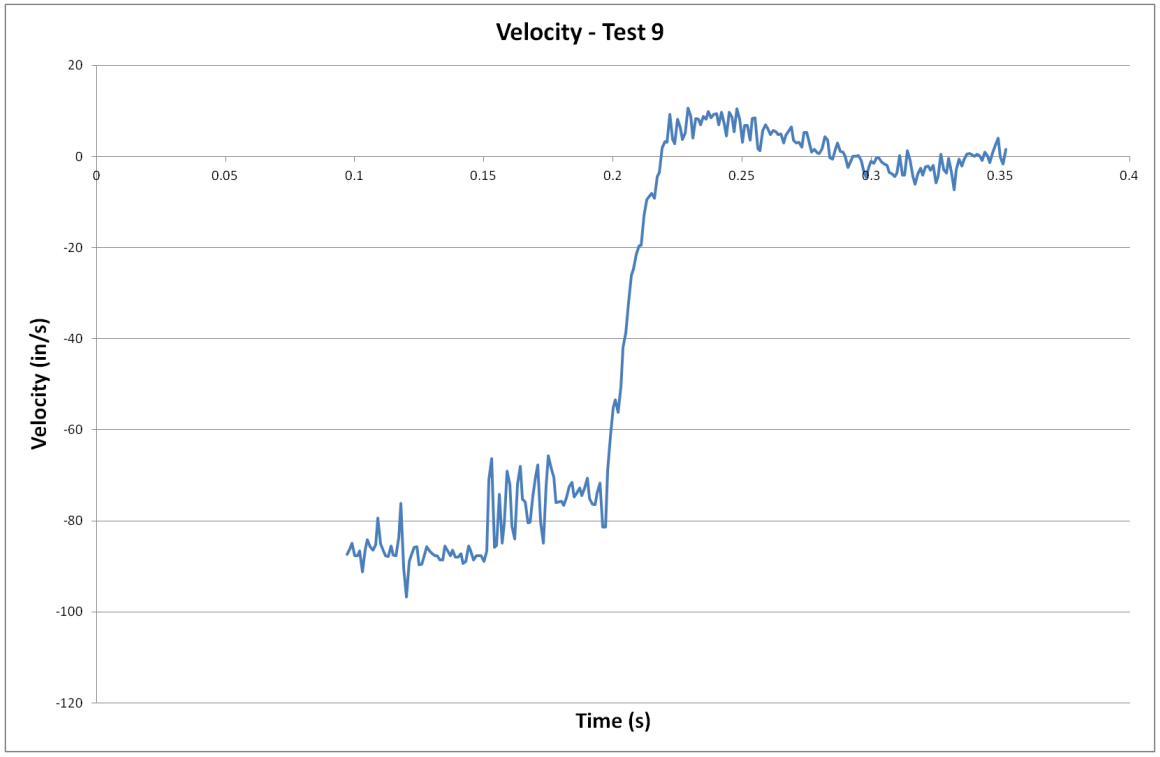
Velocity - Test 9
Velocity (in/s)
Time (s)
20
0
-20
-40
-60
-80
-100
-120
0
0.05
0.1
0.15
0.2
0.25
0.3
0.35
0.4

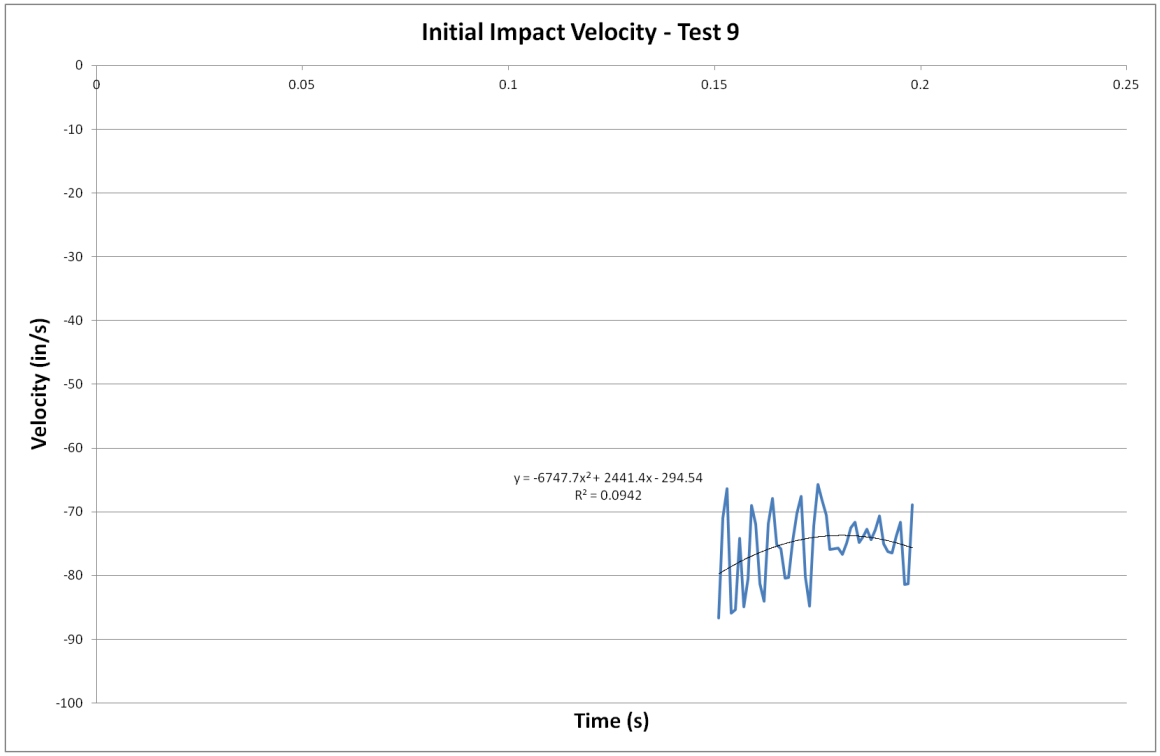
Initial Impact Velocity - Test 9
Velocity (in/s)
Time (s)
y = -6747.7x² + 2441.4x - 294.54
R² = 0.0942
0
-10
-20
-30
-40
-50
-60
-70
-80
-90
-100
0
0.05
0.1
0.15
0.2
0.25

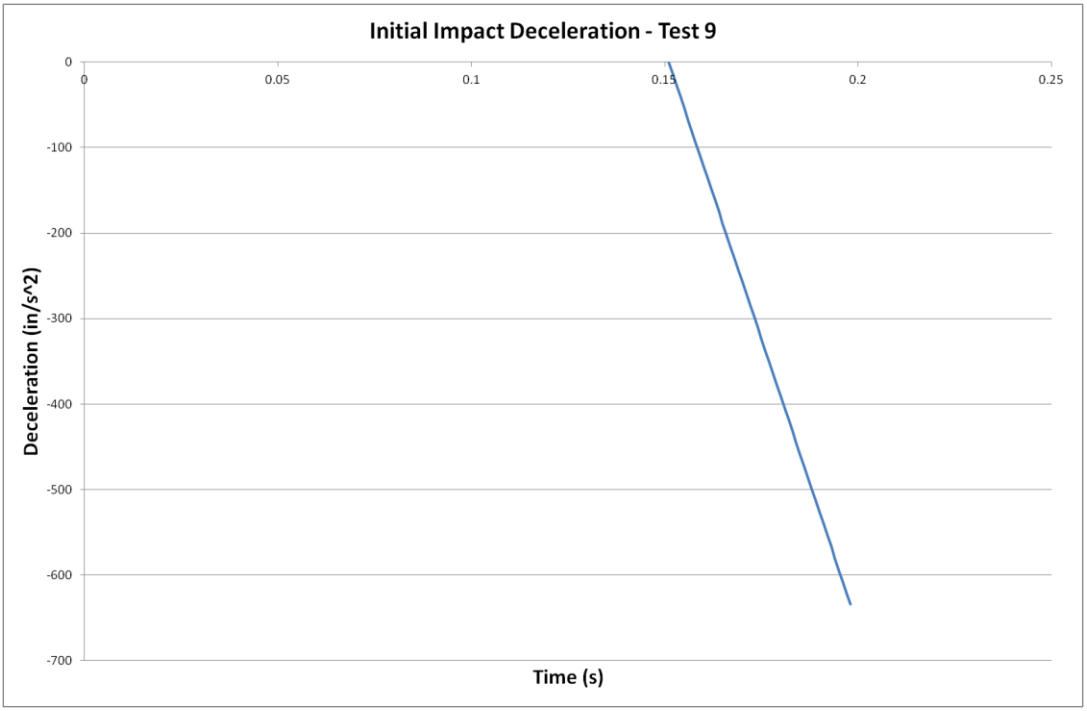
Initial Impact Deceleration - Test 9
0
-100
-200
-300
-400
-500
-600
-700
Deceleration (in/s^2)
0
0.05
0.1
0.15
0.2
0.25
Time (s)

A.1.7 Round Sand Compacted I

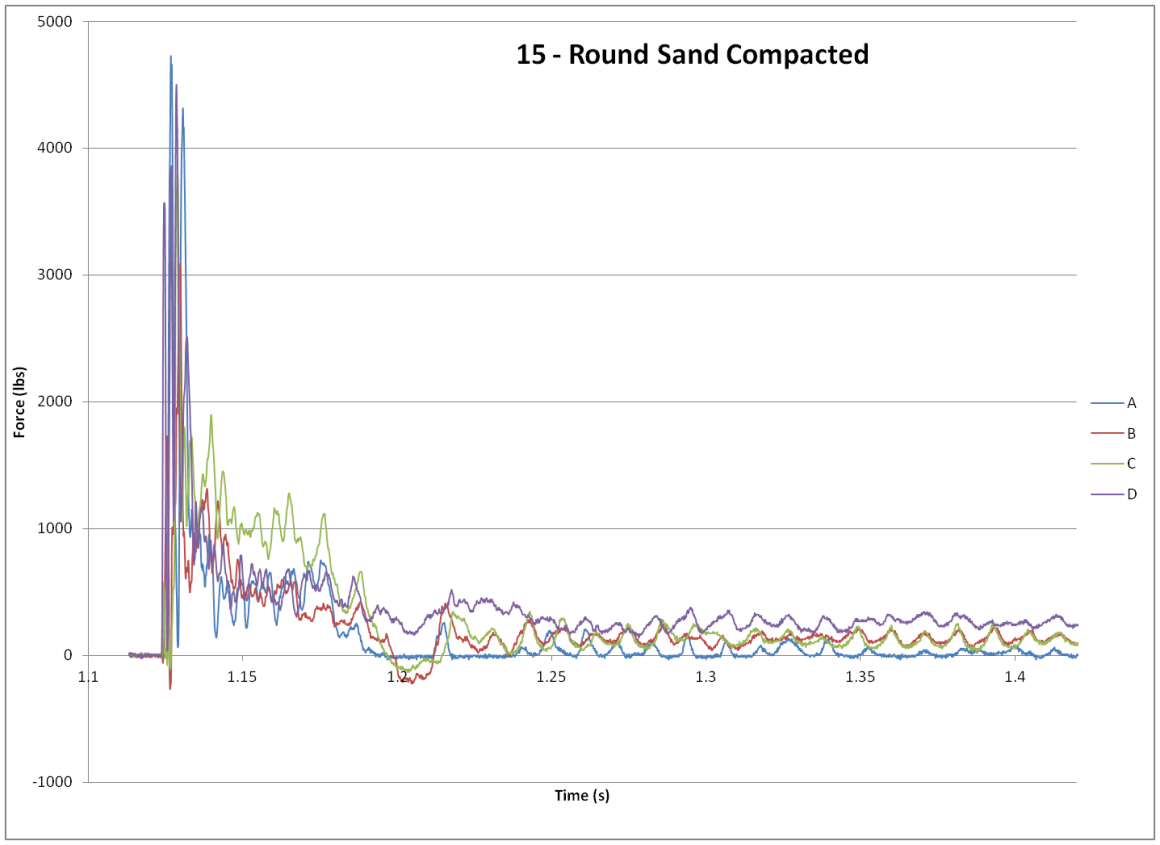

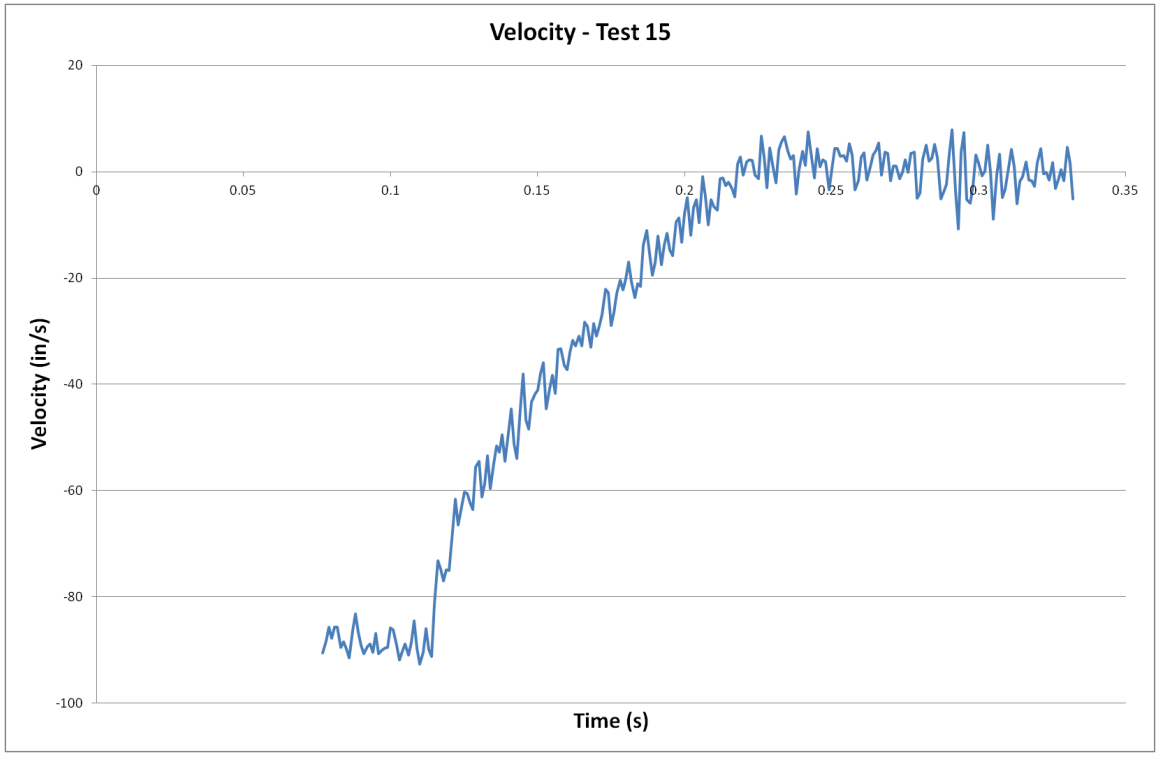
Velocity - Test 15
Velocity (in/s)
Time (s)
20
0
-20
-40
-60
-80
-100
0
0.05
0.1
0.15
0.2
0.25
0.3
0.35

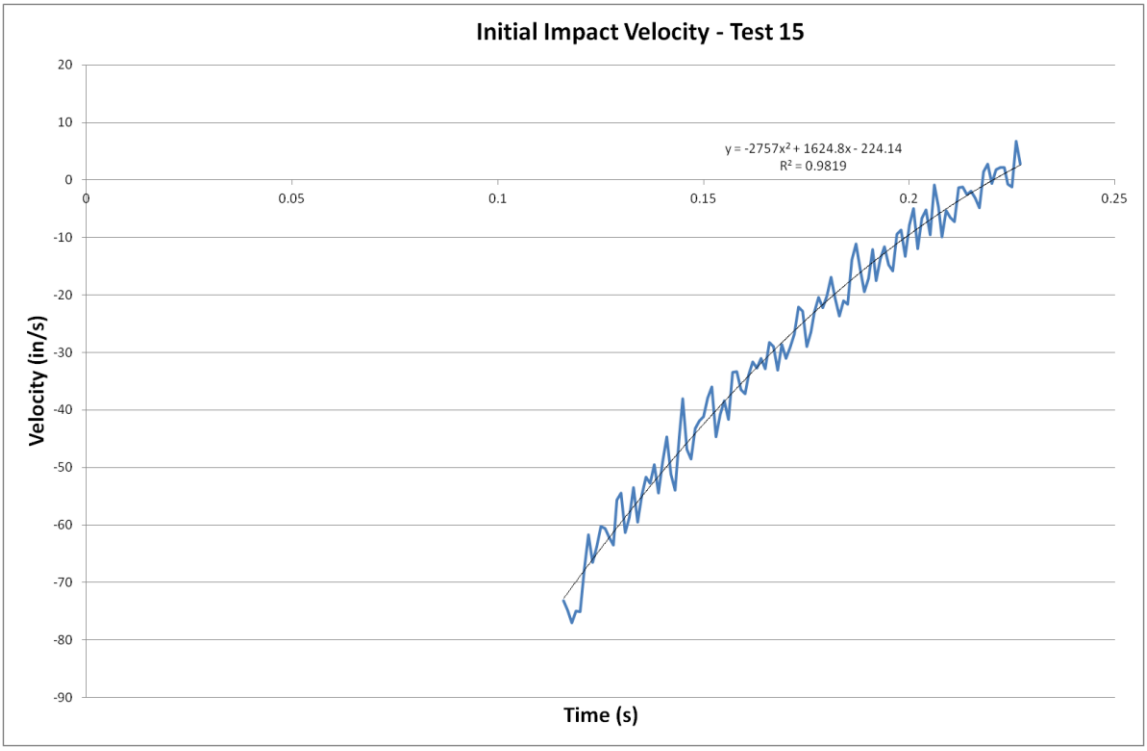
Initial Impact Velocity - Test 15
y = -2757x² + 1624.8x - 224.14
R² = 0.9819
Velocity (in/s)
Time (s)
20
10
0
-10
-20
-30
-40
-50
-60
-70
-80
-90
0
0.05
0.1
0.15
0.2
0.25

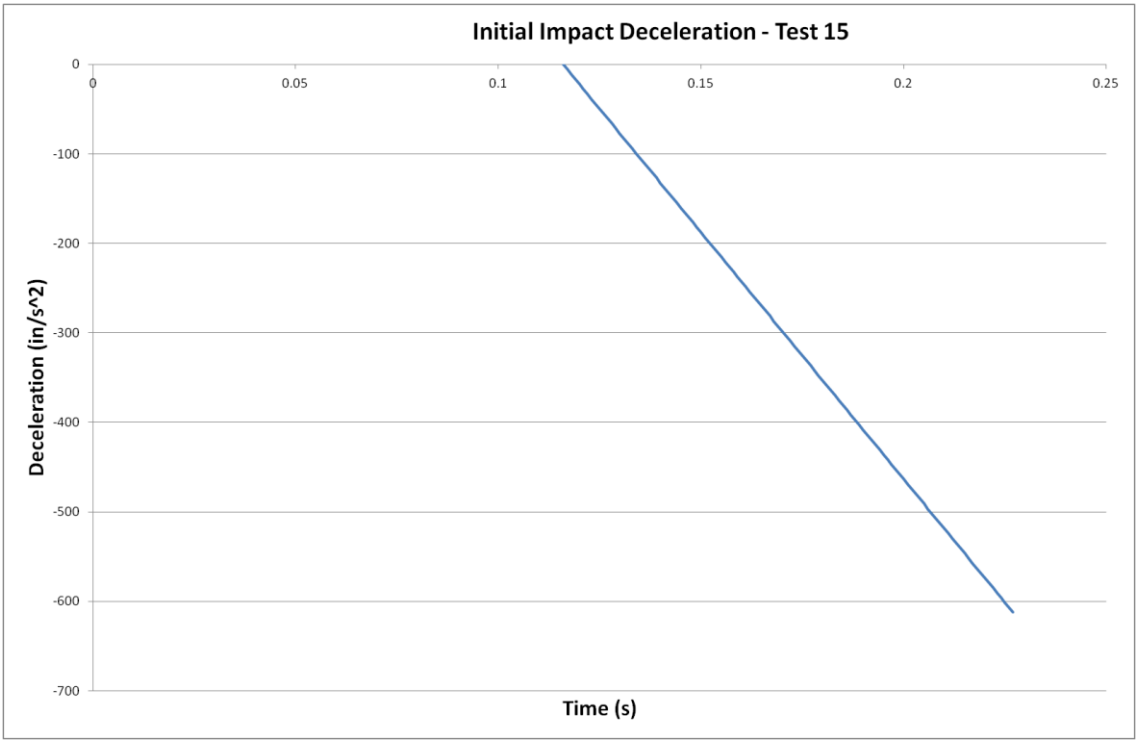
Initial Impact Deceleration - Test 15
0
-100
-200
-300
-400
-500
-600
-700
Deceleration (in/s^2)
0
0.05
0.1
0.15
0.2
0.25
Time (s)

A.1.8 Round Sand Compacted II

Load cell data for test 16 was corrupted upon transfer and is not available.

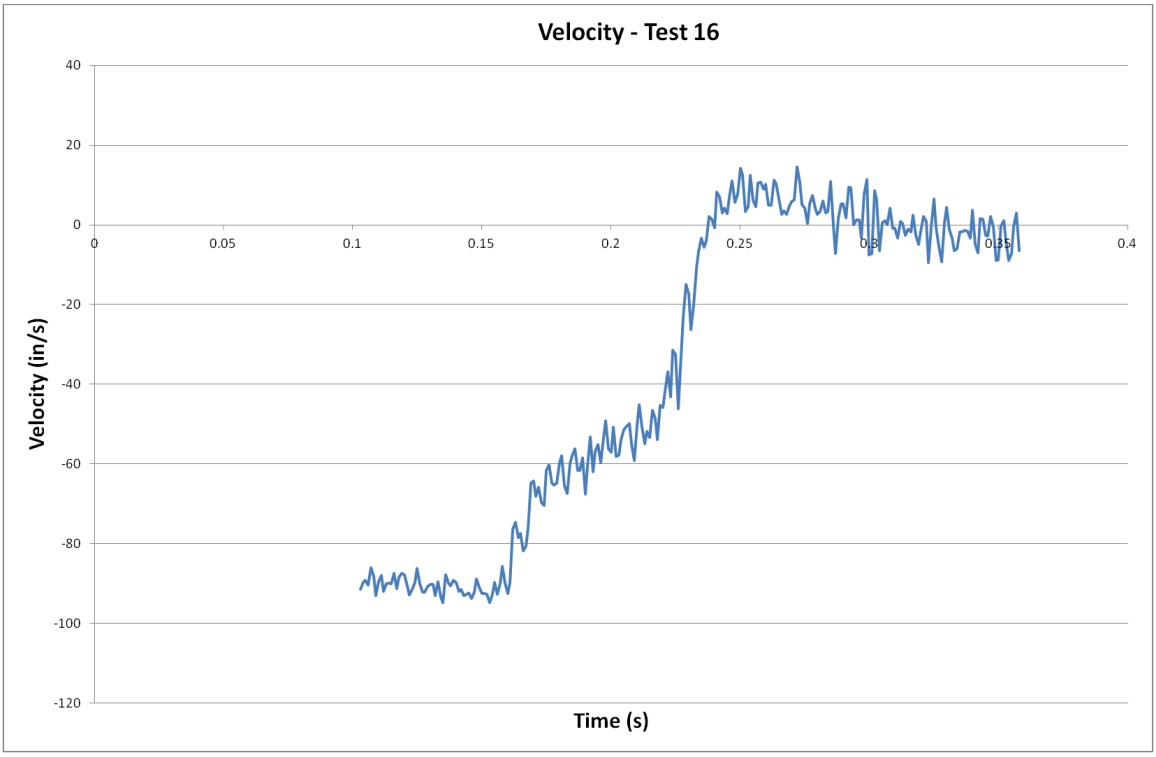

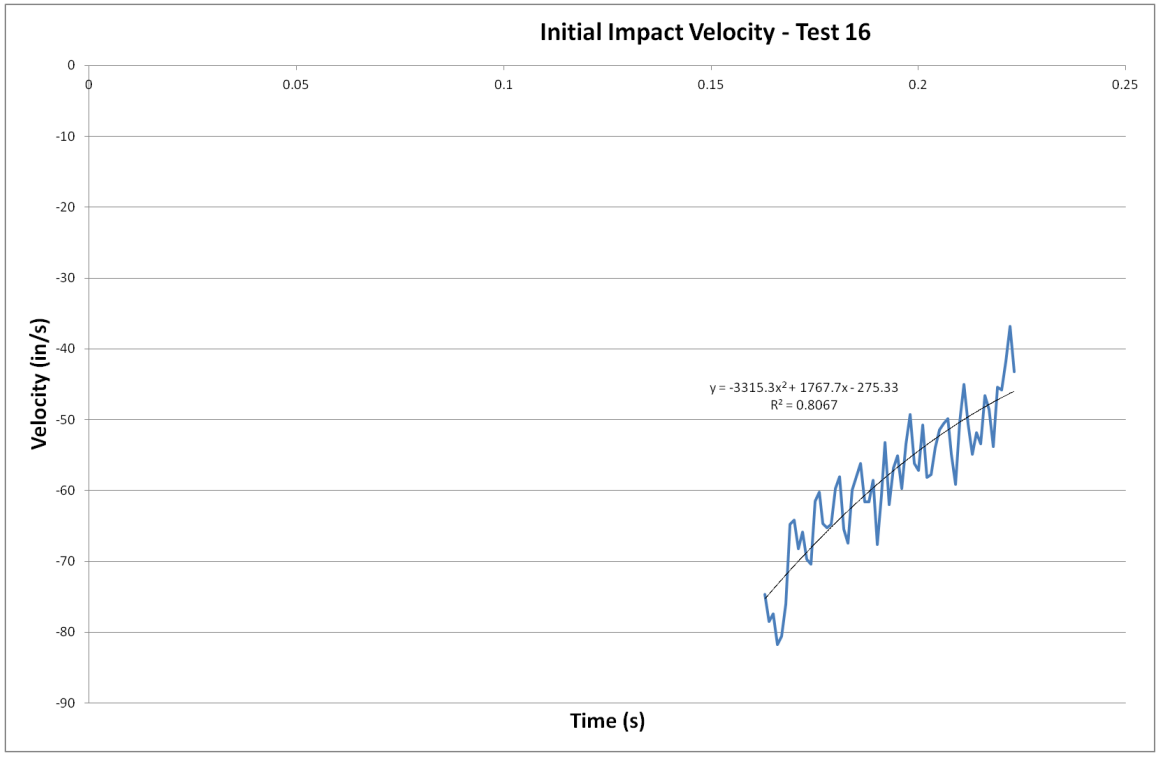
Initial Impact Velocity - Test 16
Velocity (in/s)
Time (s)
y = -3315.3x² + 1767.7x - 275.33
R² = 0.8067
0
-10
-20
-30
-40
-50
-60
-70
-80
-90
0
0.05
0.1
0.15
0.2
0.25

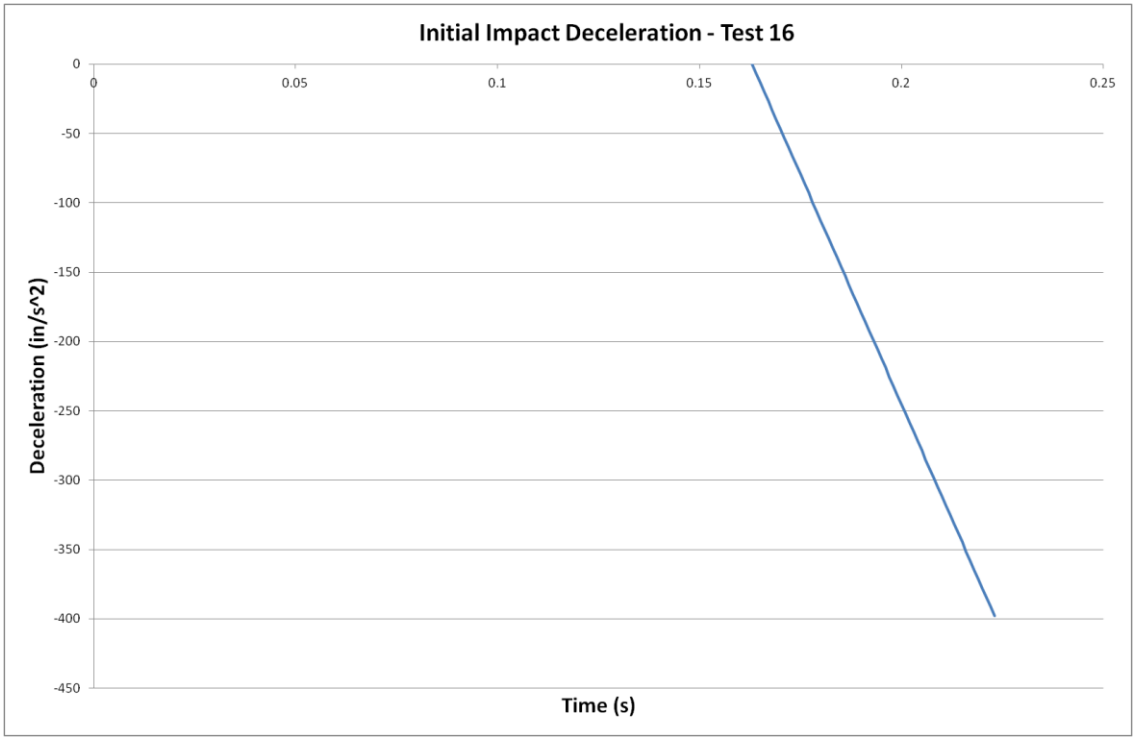
Initial Impact Deceleration - Test 16
Deceleration (in/s^2)
Time (s)
0
-50
-100
-150
-200
-250
-300
-350
-400
-450
0
0.05
0.1
0.15
0.2
0.25

A.1.9 Round Soil Uncompacted I

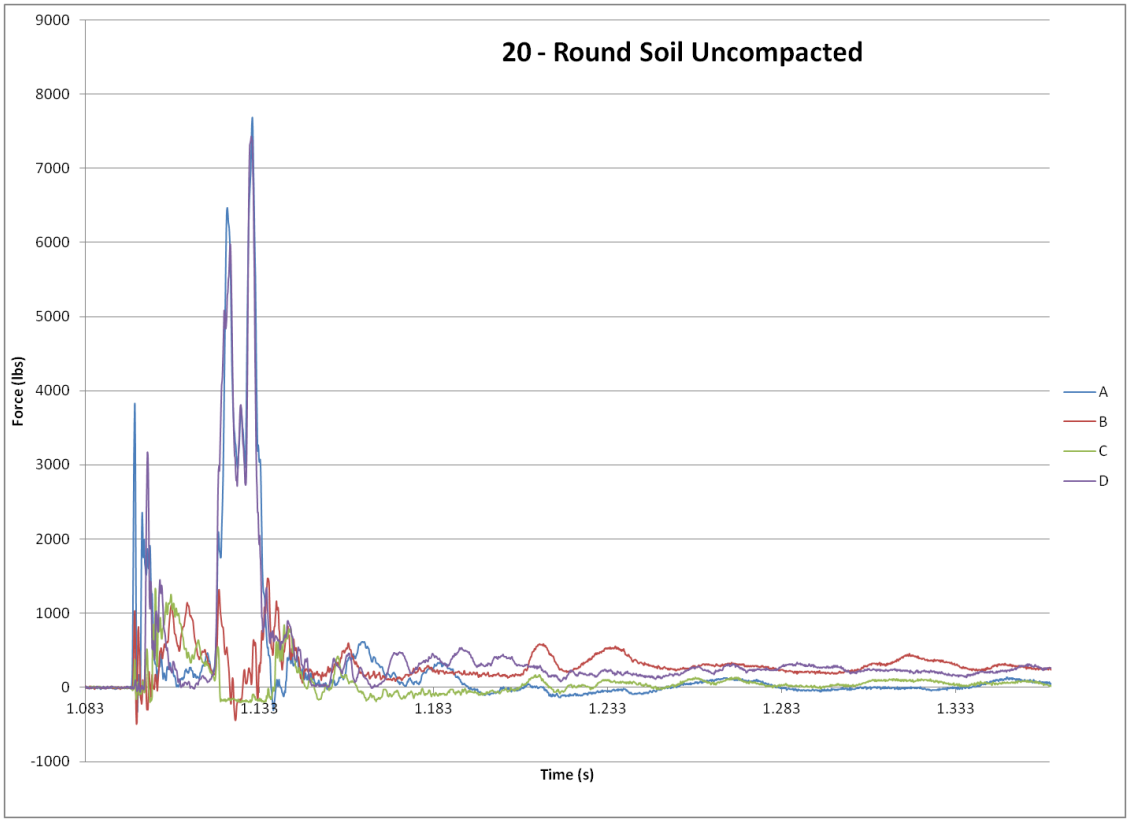

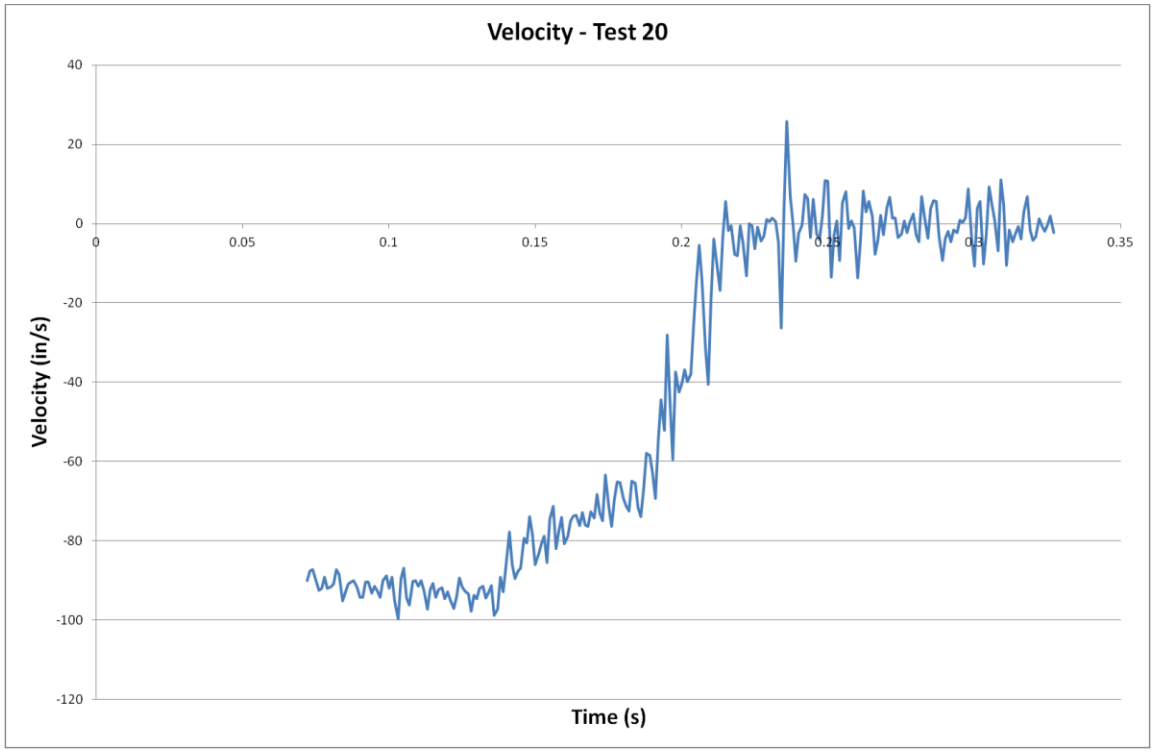
Velocity - Test 20
Velocity (in/s)
Time (s)
40
20
0
-20
-40
-60
-80
-100
-120
0
0.05
0.1
0.15
0.2
0.25
0.3
0.35

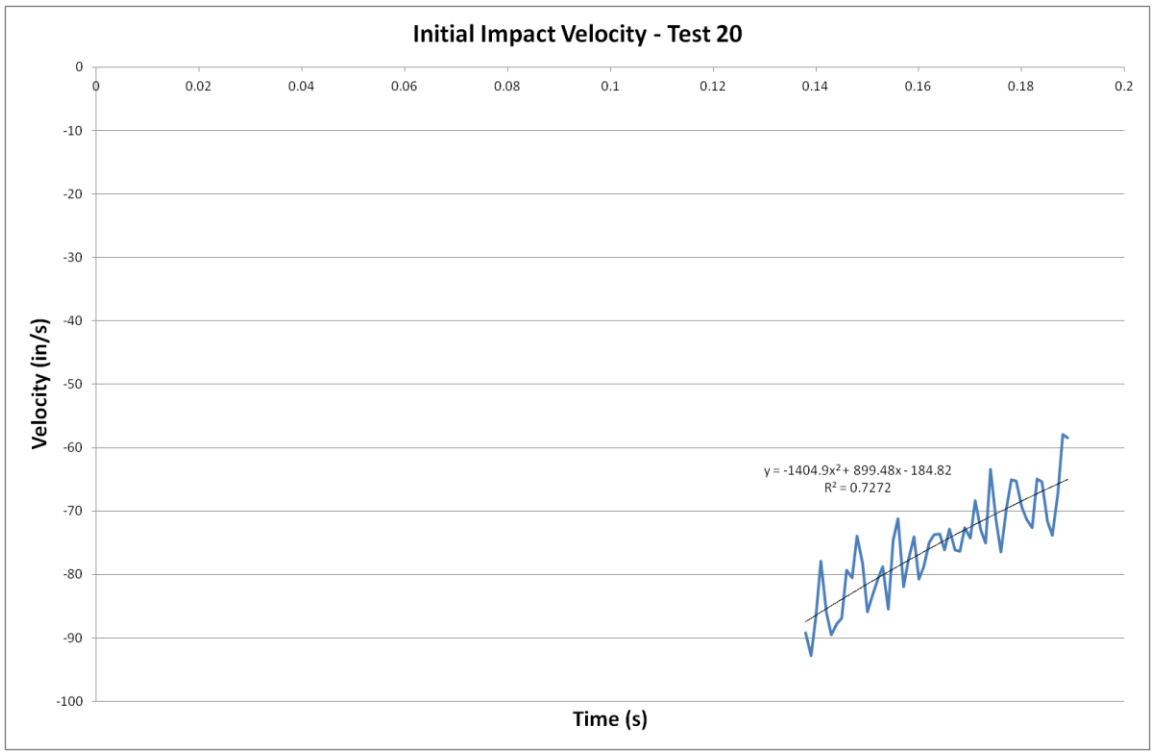
Initial Impact Velocity - Test 20
Velocity (in/s)
Time (s)
y = -1404.9x² + 899.48x - 184.82
R² = 0.7272
0
-10
-20
-30
-40
-50
-60
-70
-80
-90
-100
0
0.02
0.04
0.06
0.08
0.1
0.12
0.14
0.16
0.18
0.2

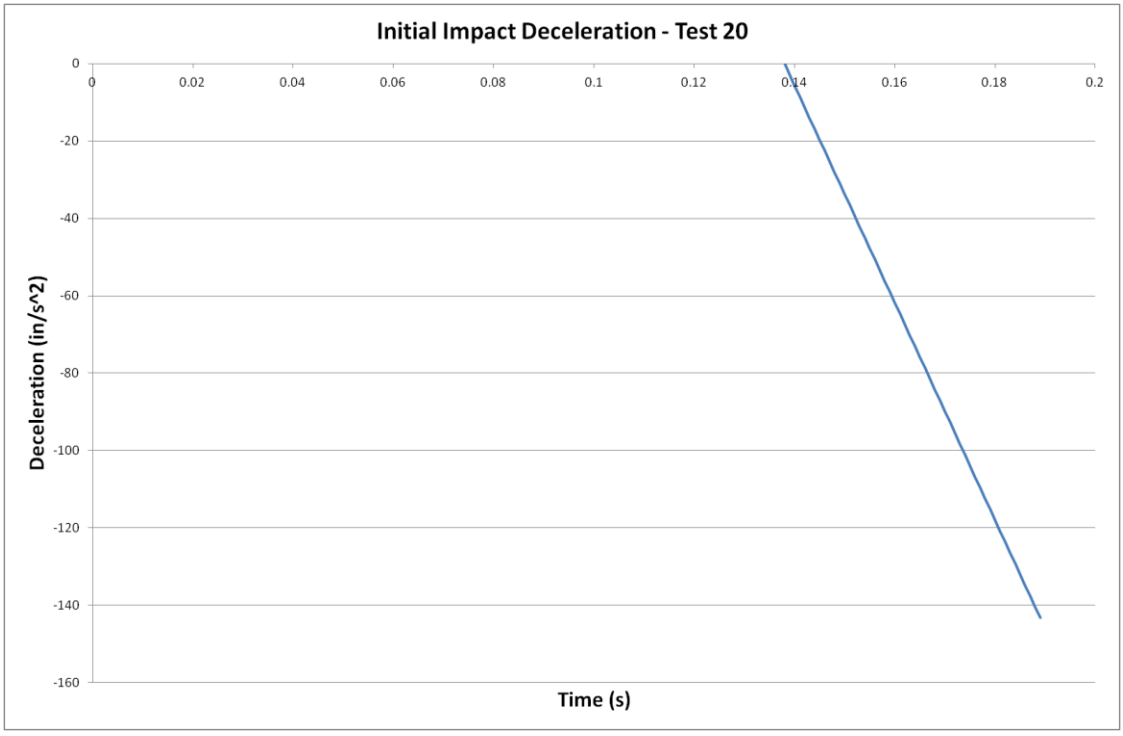
Initial Impact Deceleration - Test 20
Deceleration (in/s^2)
Time (s)
0
-20
-40
-60
-80
-100
-120
-140
-160
0
0.02
0.04
0.06
0.08
0.1
0.12
0.14
0.16
0.18
0.2

A.1.10 Round Soil Uncompacted II

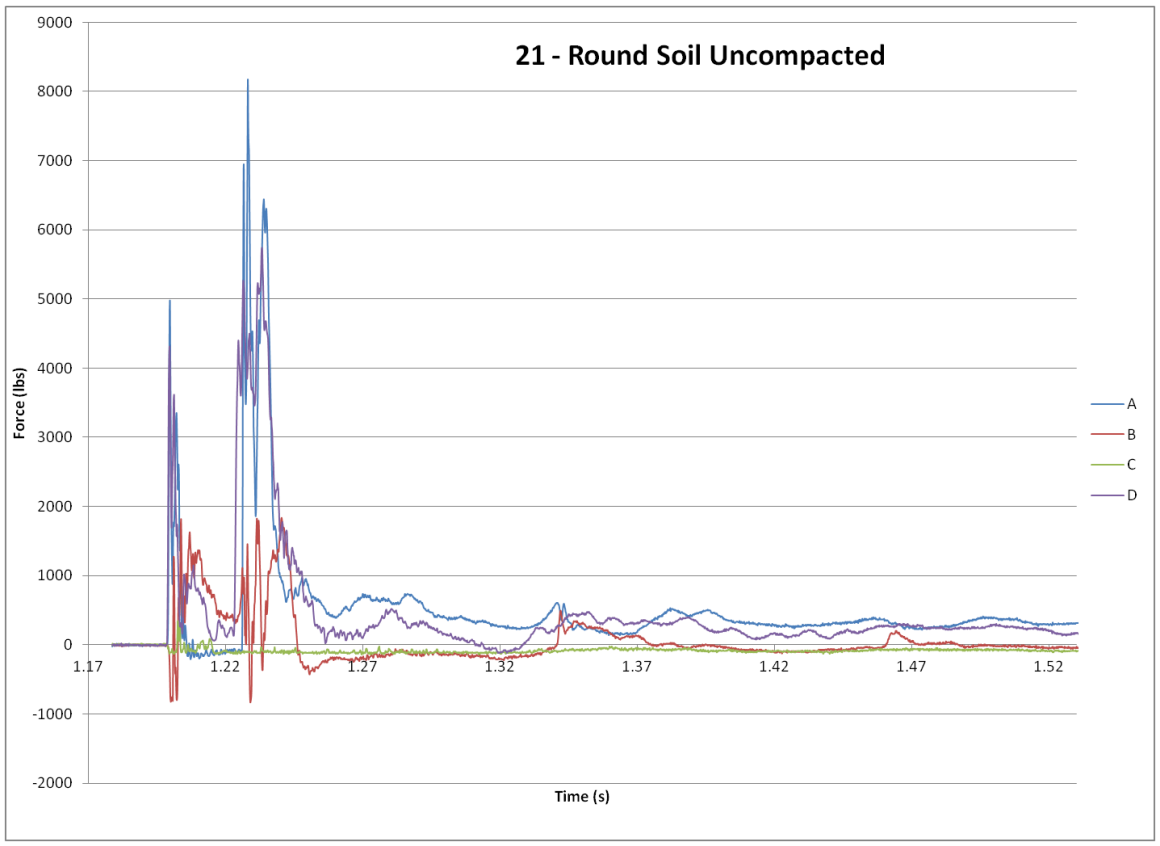

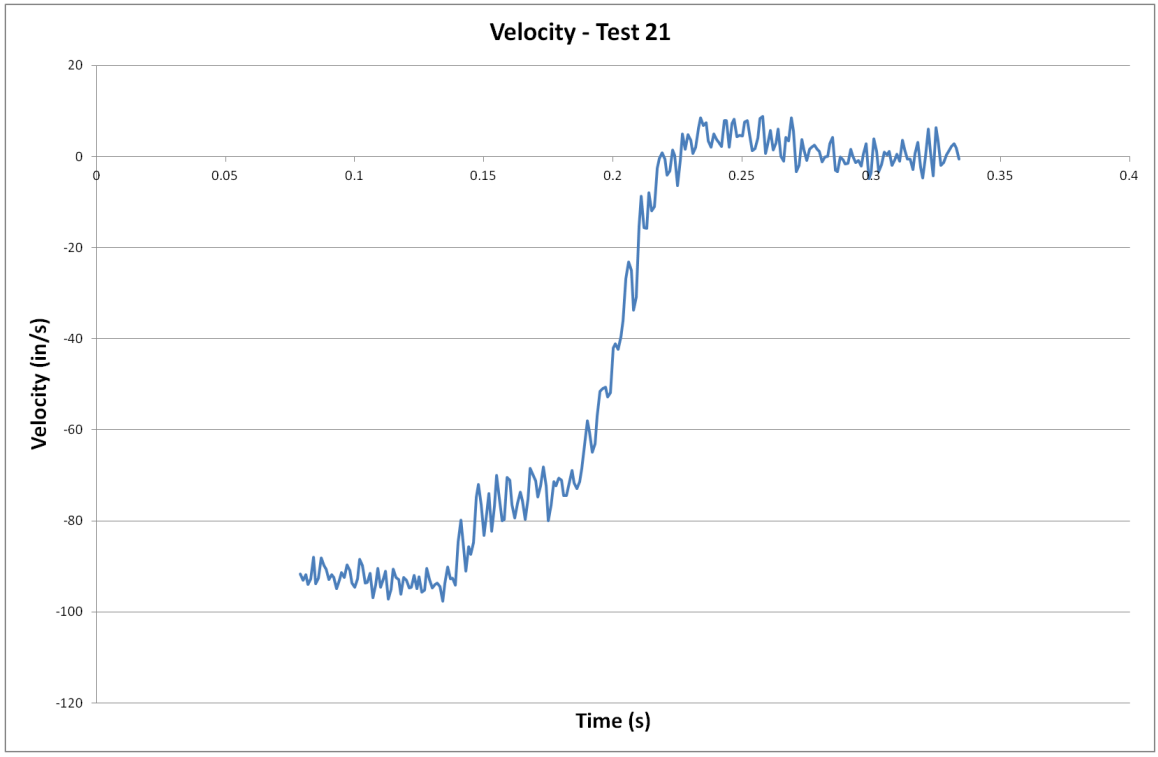
Velocity - Test 21
Velocity (in/s)
Time (s)
20
0
-20
-40
-60
-80
-100
-120
0
0.05
0.1
0.15
0.2
0.25
0.3
0.35
0.4

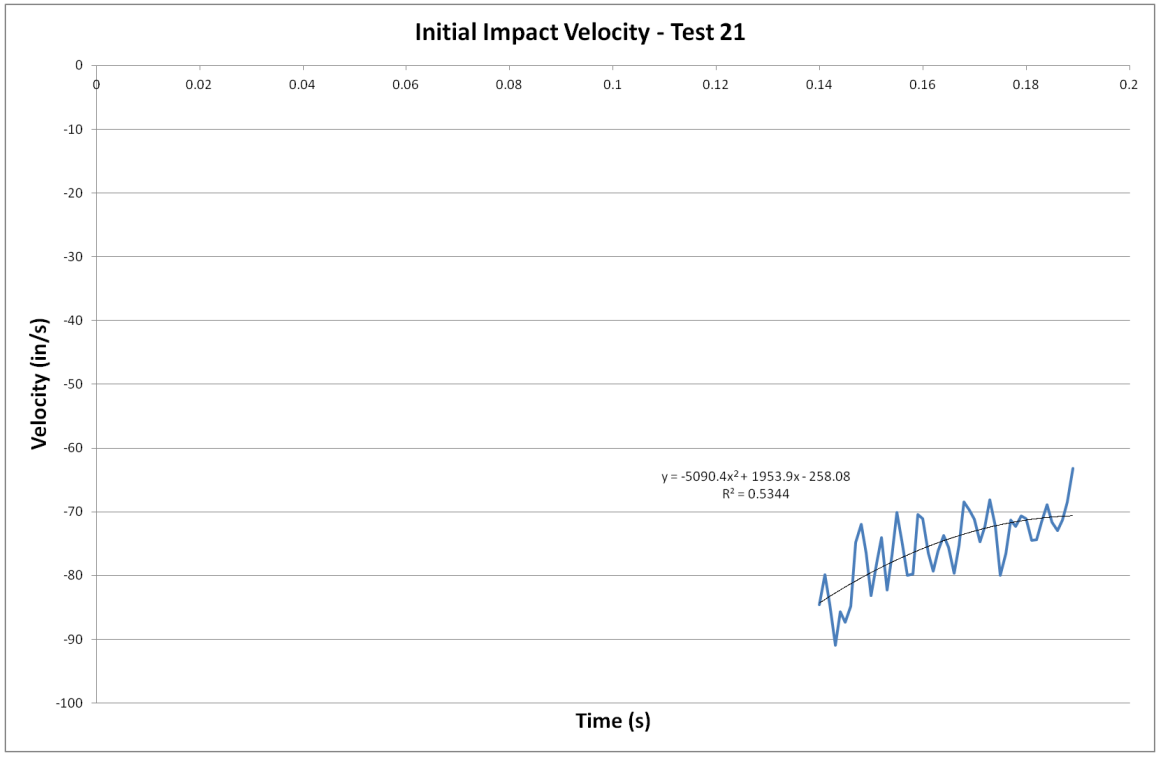
Initial Impact Velocity - Test 21
Velocity (in/s)
Time (s)
y = -5090.4x² + 1953.9x - 258.08
R² = 0.5344
0
-10
-20
-30
-40
-50
-60
-70
-80
-90
-100
0
0.02
0.04
0.06
0.08
0.1
0.12
0.14
0.16
0.18
0.2

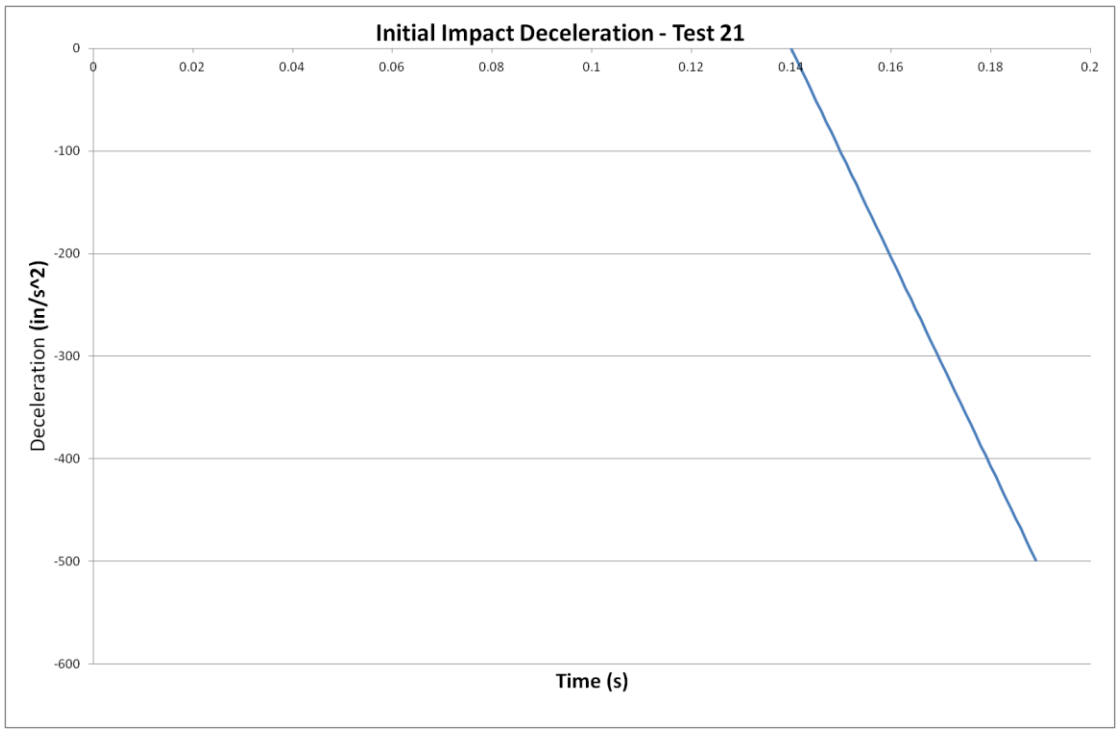
Initial Impact Deceleration - Test 21
0
-100
-200
-300
-400
-500
-600
0
0.02
0.04
0.06
0.08
0.1
0.12
0.14
0.16
0.18
0.2
Deceleration (in/s^2)
Time (s)

A.1.11 Round Soil Compacted I

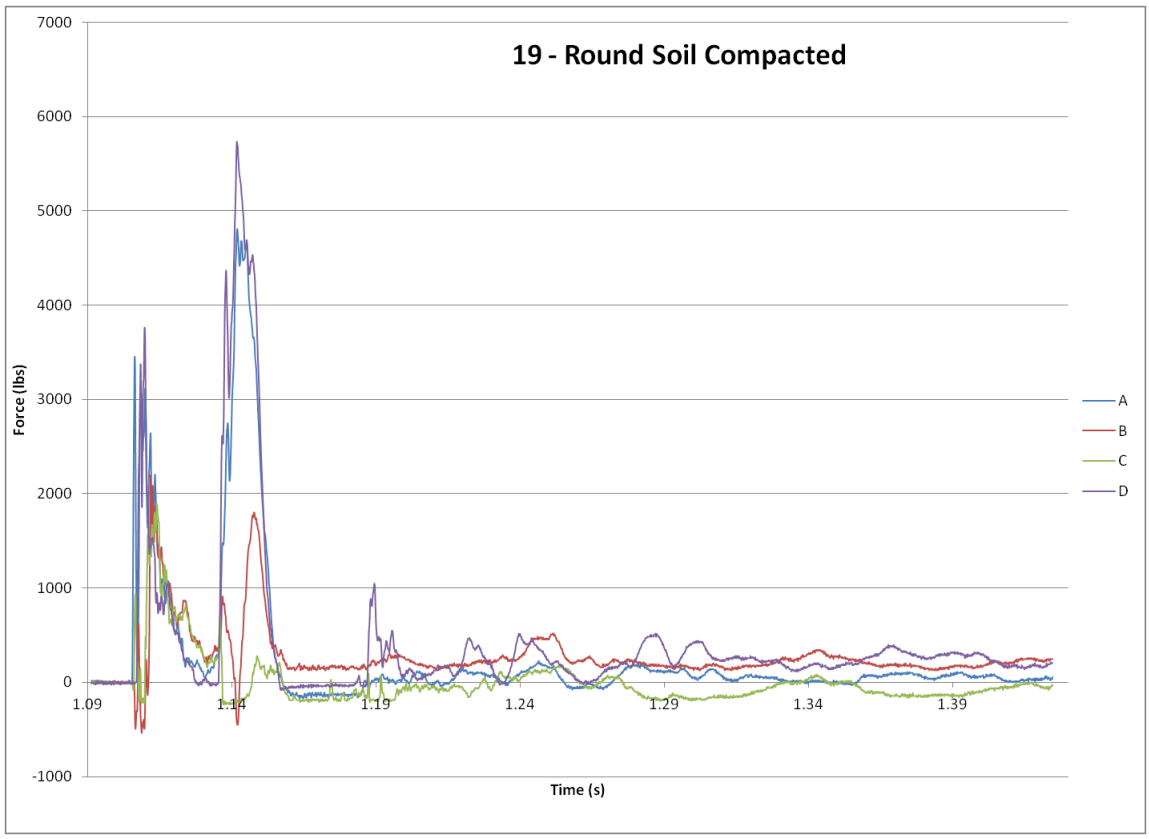

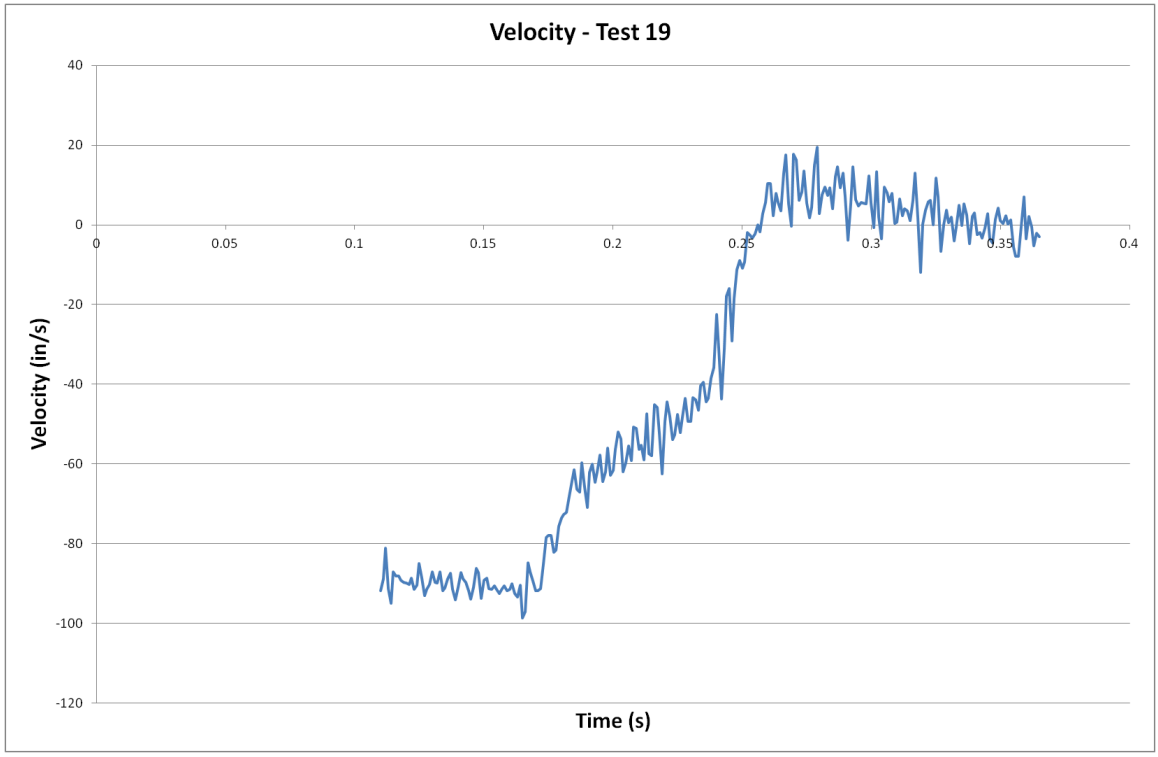
Velocity - Test 19
Velocity (in/s)
Time (s)
40
20
0
-20
-40
-60
-80
-100
-120
0
0.05
0.1
0.15
0.2
0.25
0.3
0.35
0.4

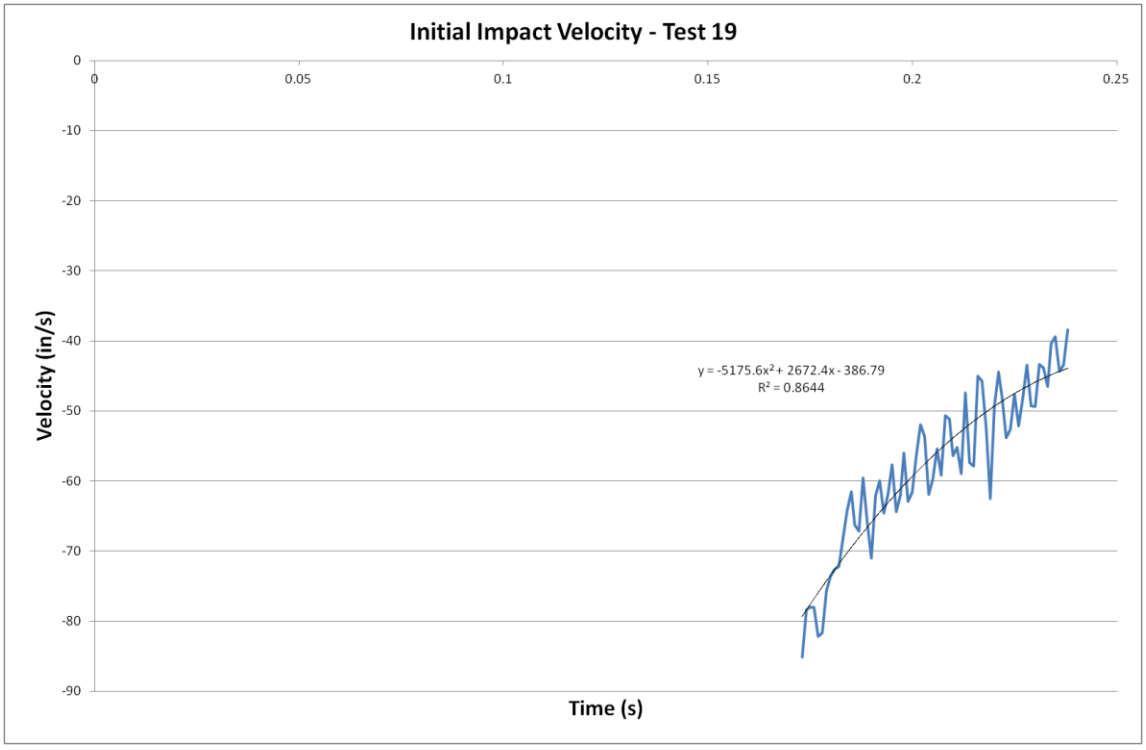
Initial Impact Velocity - Test 19
Velocity (in/s)
Time (s)
y = -5175.6x² + 2672.4x - 386.79
R² = 0.8644
0
-10
-20
-30
-40
-50
-60
-70
-80
-90
0
0.05
0.1
0.15
0.2
0.25

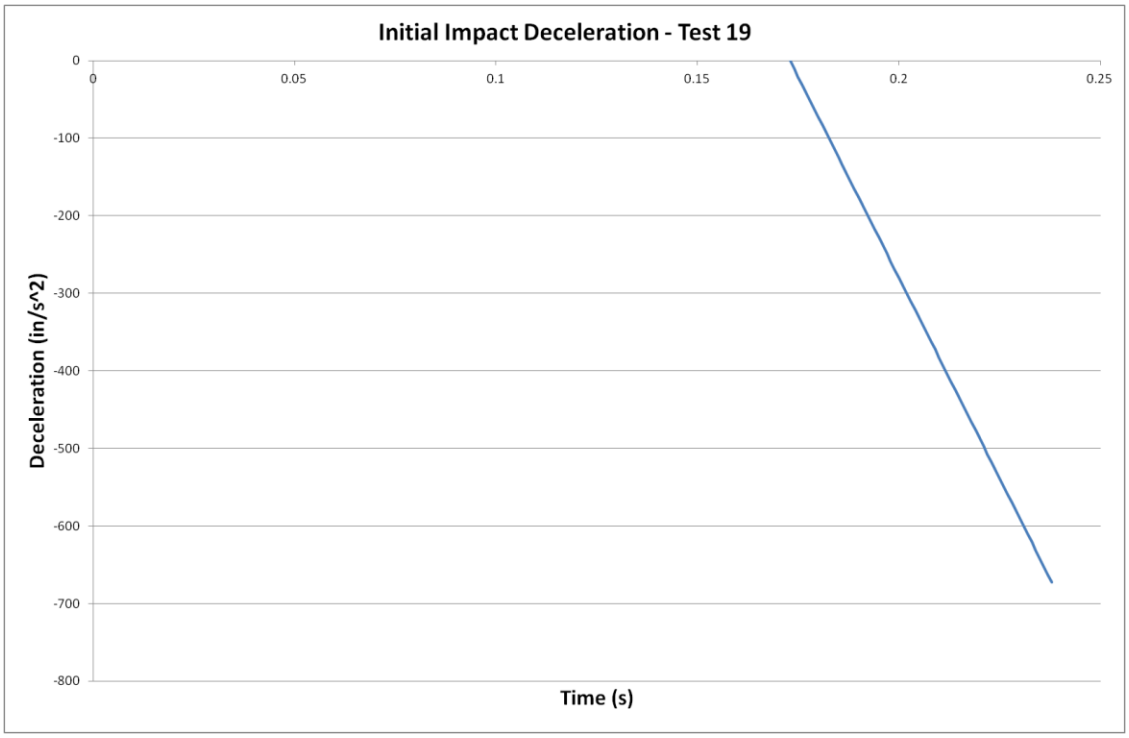
Initial Impact Deceleration - Test 19
0
-100
-200
-300
-400
-500
-600
-700
-800
Deceleration (in/s^2)
0
0.05
0.1
0.15
0.2
0.25
Time (s)

A.1.12 Round Soil Compacted II

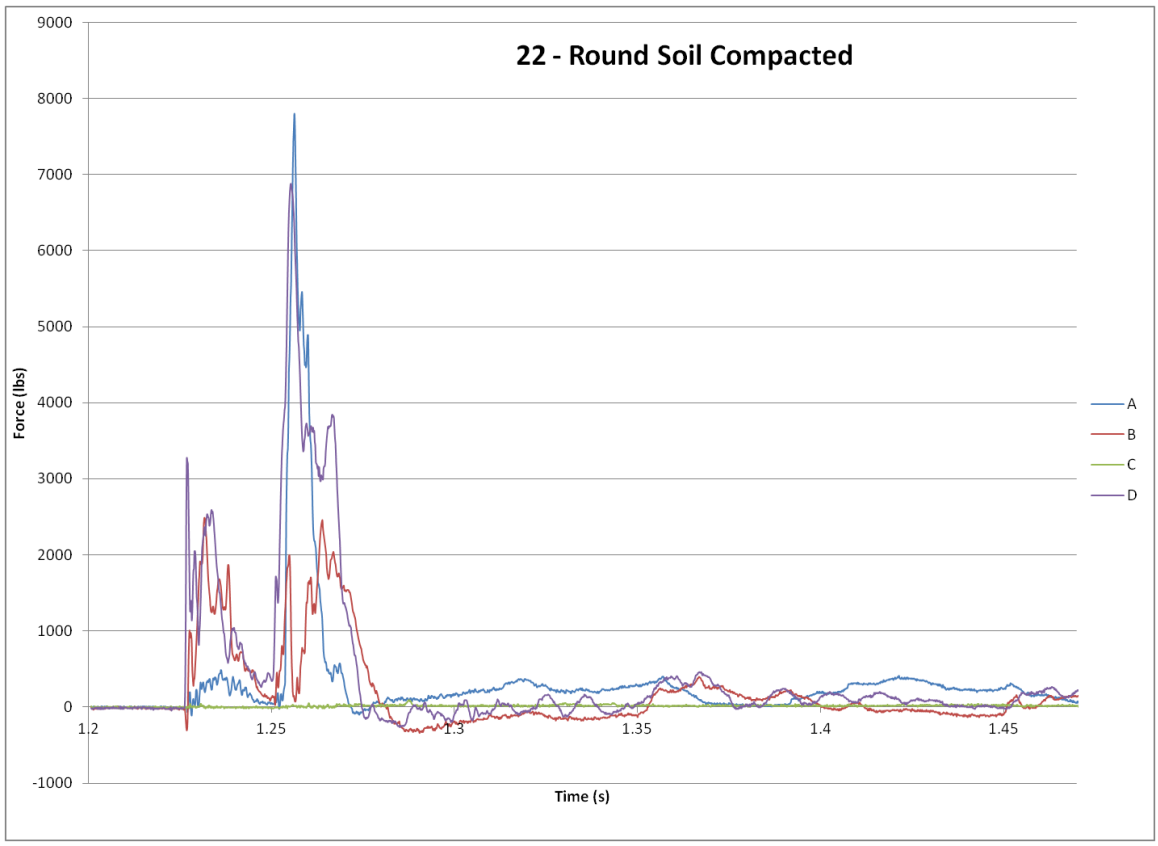

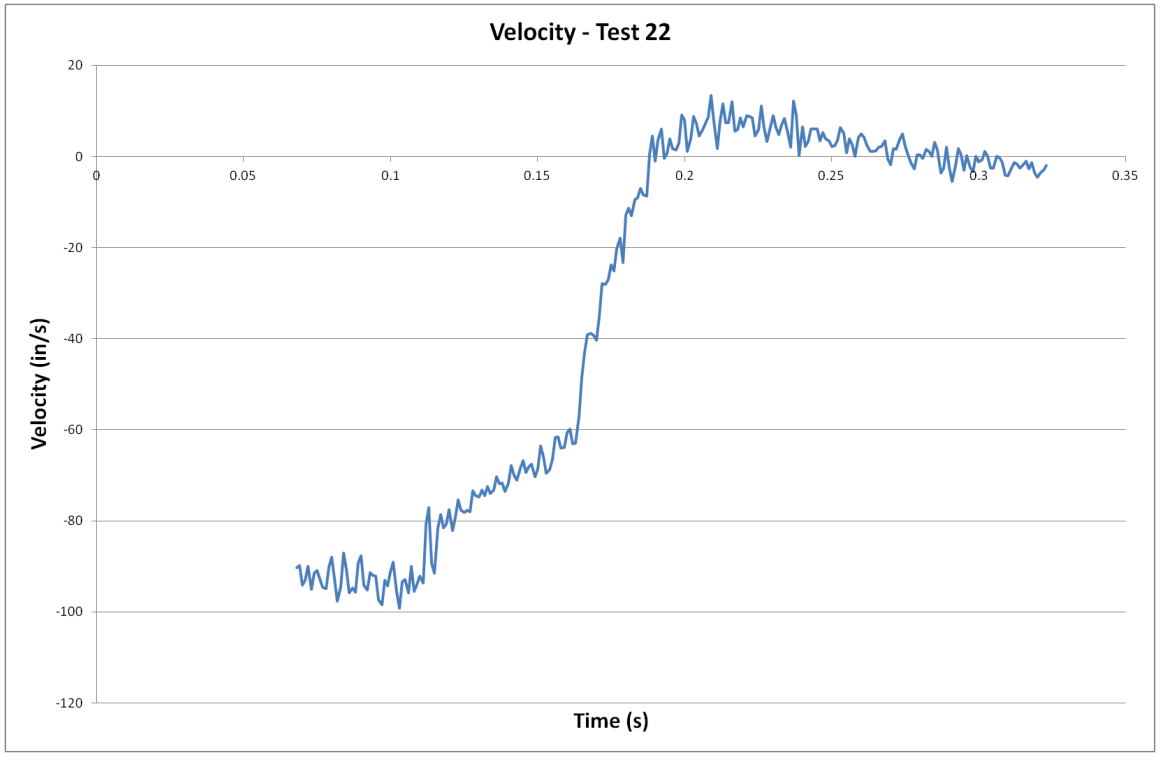
Velocity - Test 22
Velocity (in/s)
Time (s)
20
0
-20
-40
-60
-80
-100
-120
0
0.05
0.1
0.15
0.2
0.25
0.3
0.35

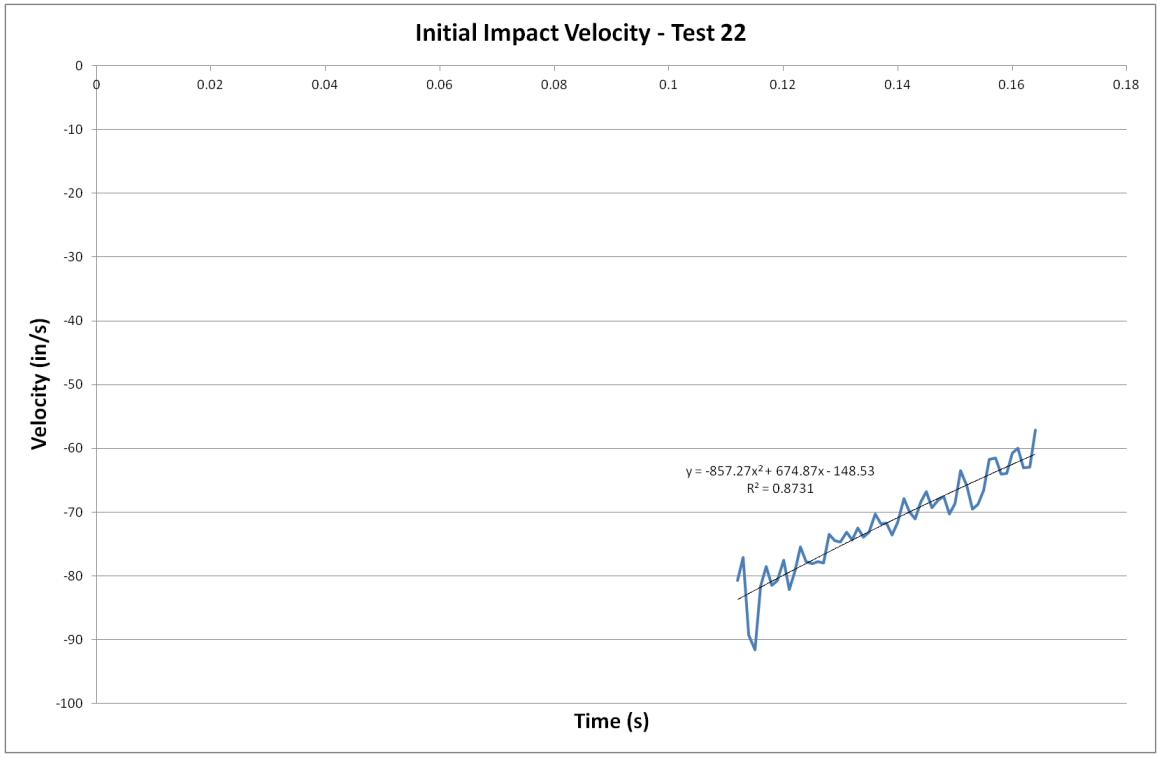
Initial Impact Velocity - Test 22
Velocity (in/s)
Time (s)
y = -857.27x² + 674.87x - 148.53
R² = 0.8731
0
-10
-20
-30
-40
-50
-60
-70
-80
-90
-100
0
0.02
0.04
0.06
0.08
0.1
0.12
0.14
0.16
0.18

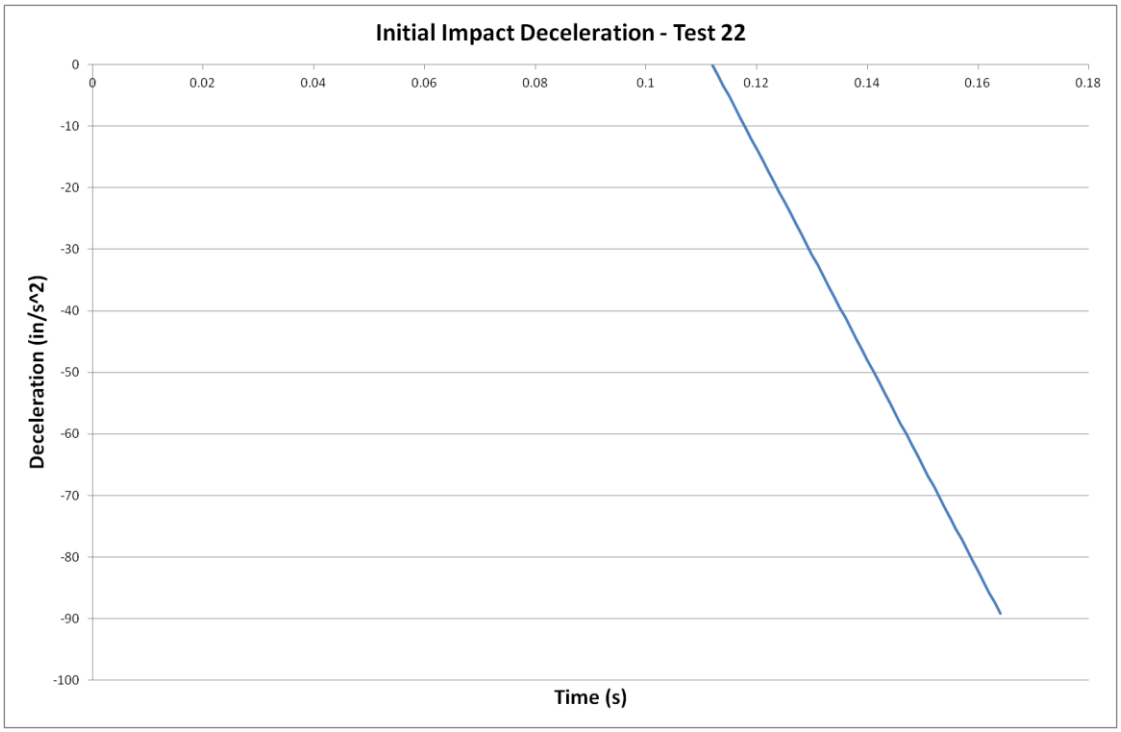
Initial Impact Deceleration - Test 22
Deceleration (in/s^2)
Time (s)
0
-10
-20
-30
-40
-50
-60
-70
-80
-90
-100
0
0.02
0.04
0.06
0.08
0.1
0.12
0.14
0.16
0.18

A.1.13 Round River Gravel I

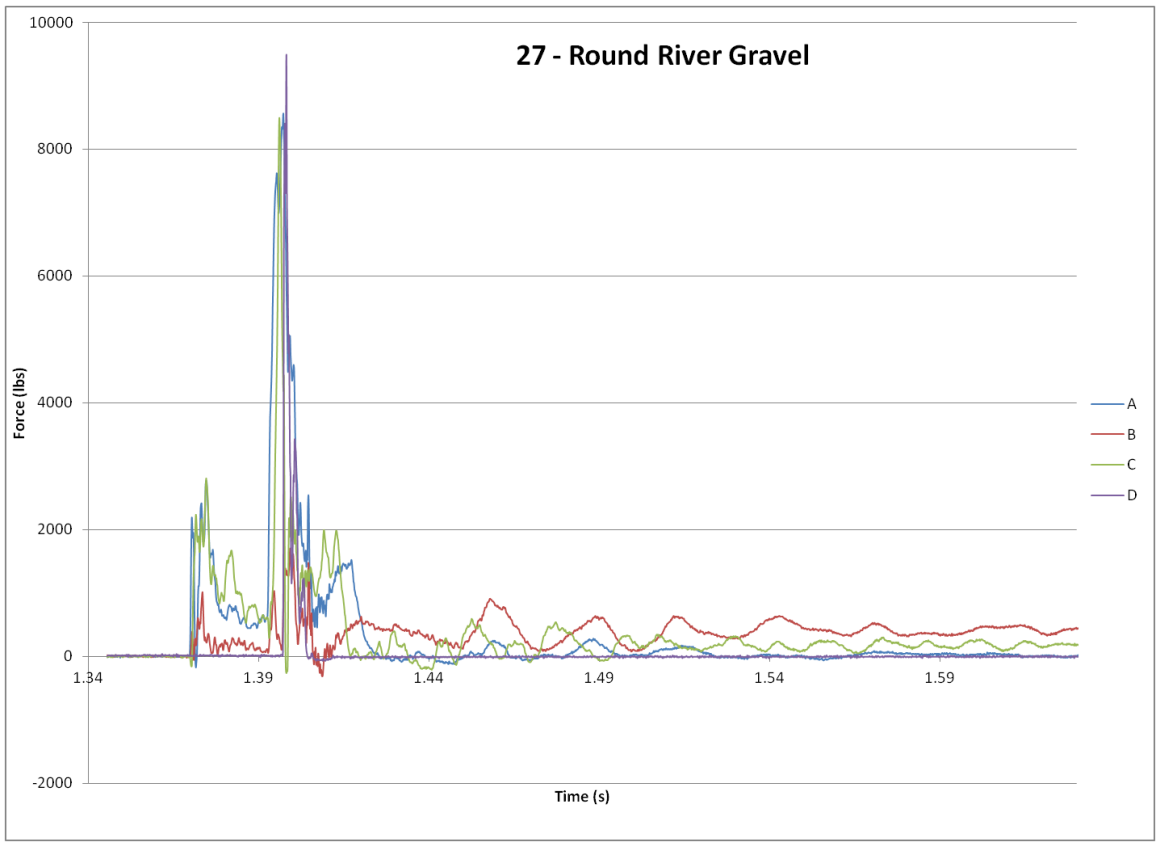

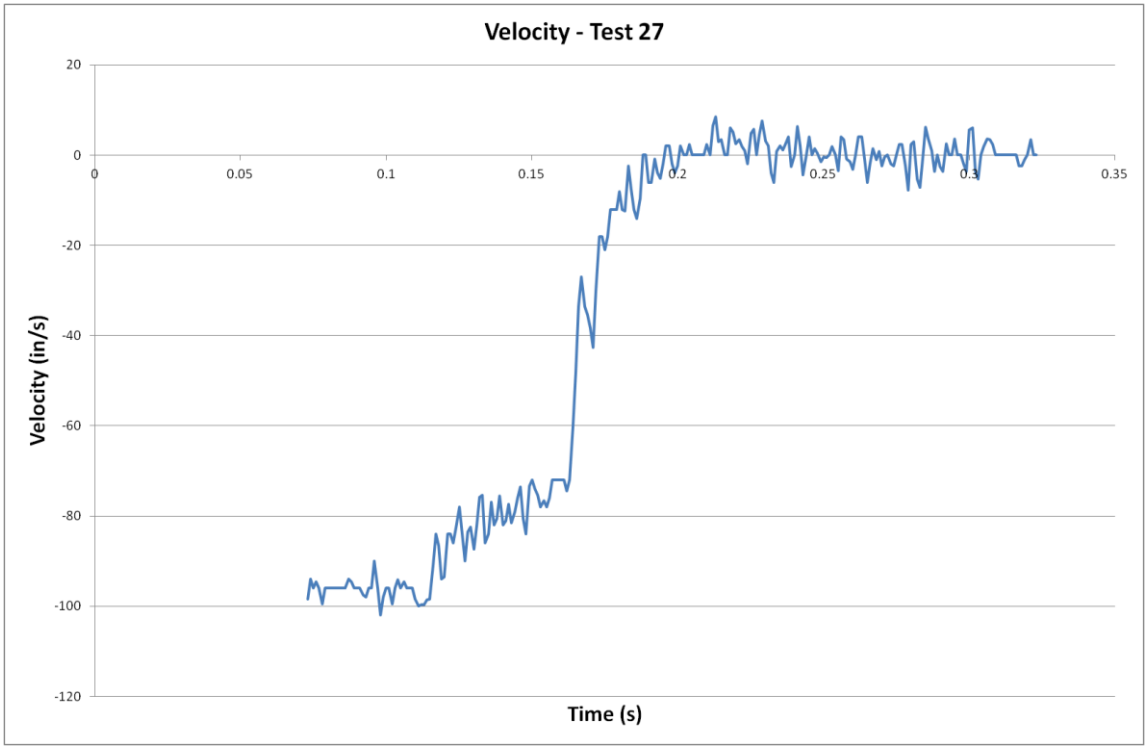
Velocity - Test 27
20
0
-20
-40
-60
-80
-100
-120
0
0.05
0.1
0.15
0.2
0.25
0.3
0.35
Velocity (in/s)
Time (s)

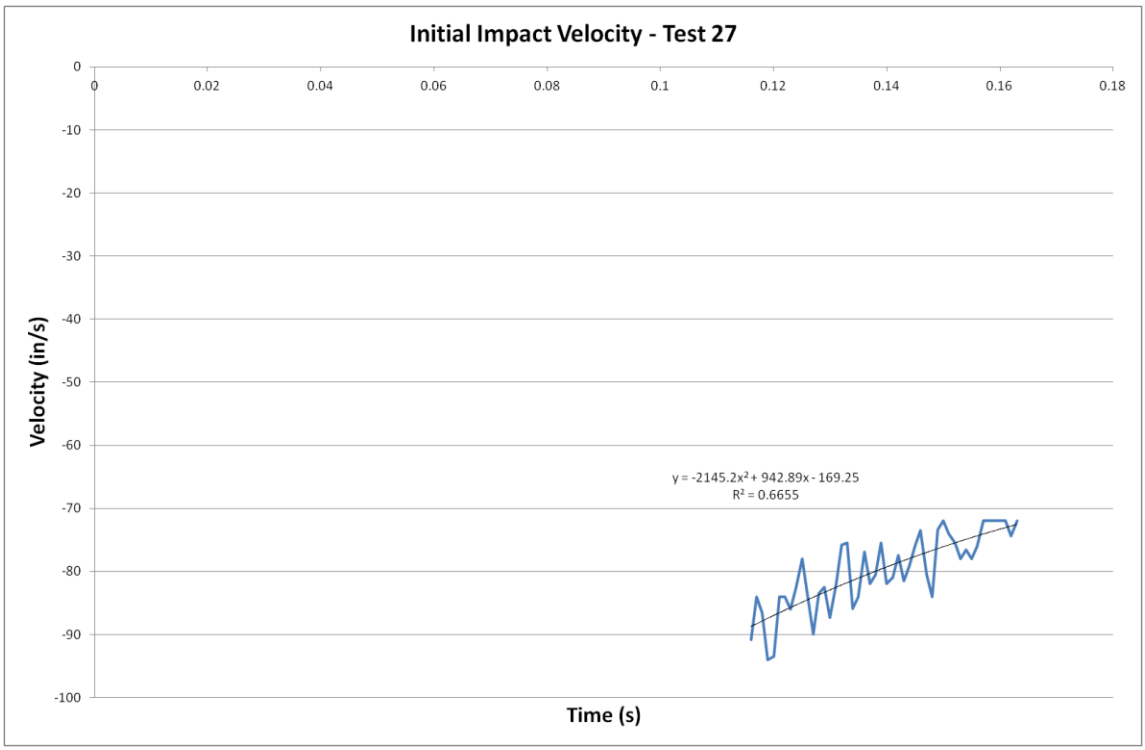
Initial Impact Velocity - Test 27
0
-10
-20
-30
-40
-50
-60
-70
-80
-90
-100
0
0.02
0.04
0.06
0.08
0.1
0.12
0.14
0.16
0.18
y = -2145.2x² + 942.89x - 169.25
R² = 0.6655
Velocity (in/s)
Time (s)

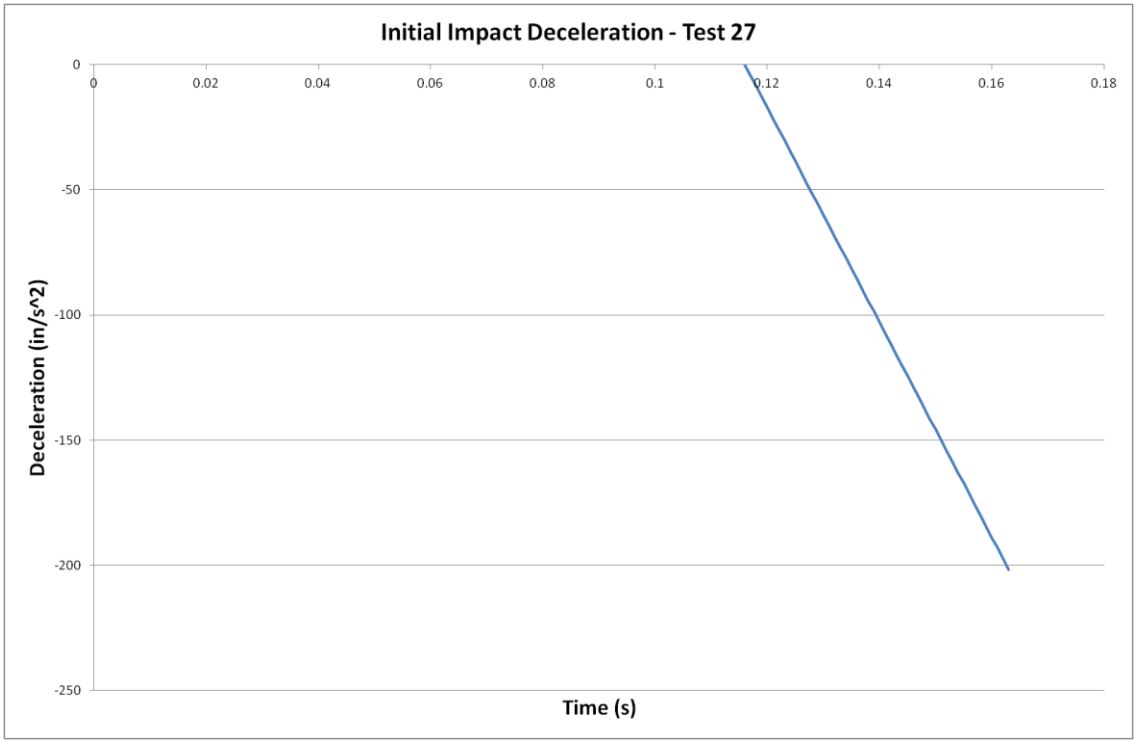
Initial Impact Deceleration - Test 27
Deceleration (in/s^2)
Time (s)
0
-50
-100
-150
-200
-250
0
0.02
0.04
0.06
0.08
0.1
0.12
0.14
0.16
0.18

A.1.14 Round River Gravel II

Load cell data was lost for test 28 and is therefore not included.

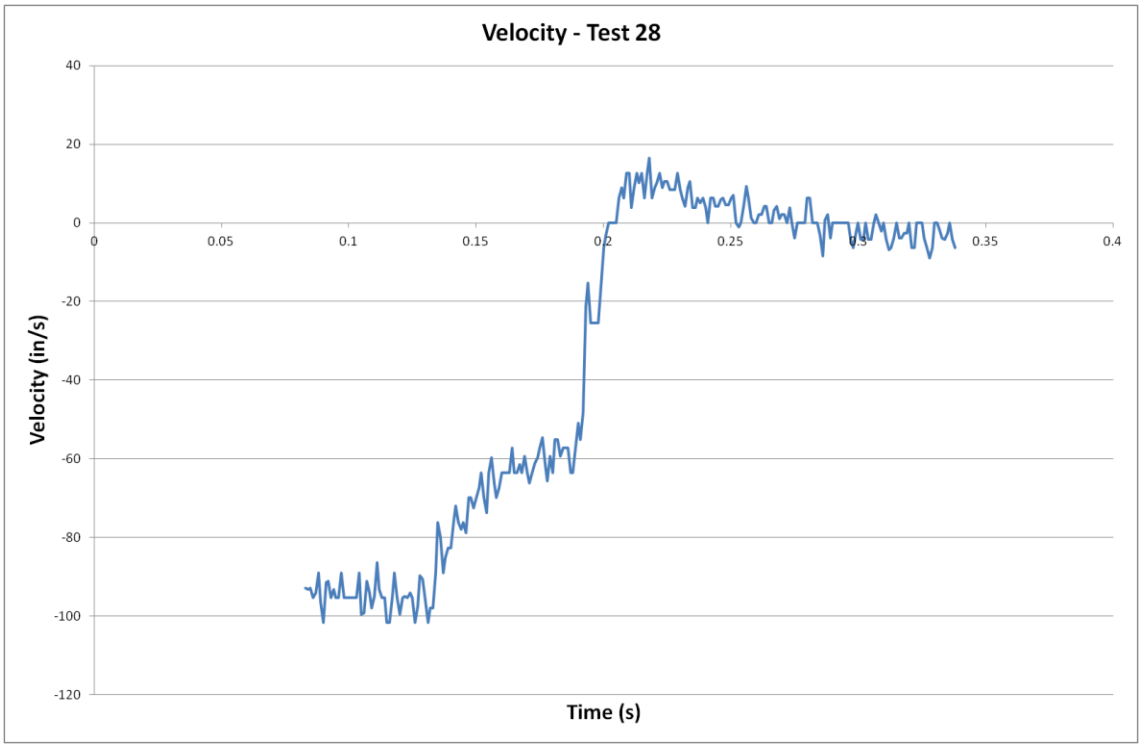

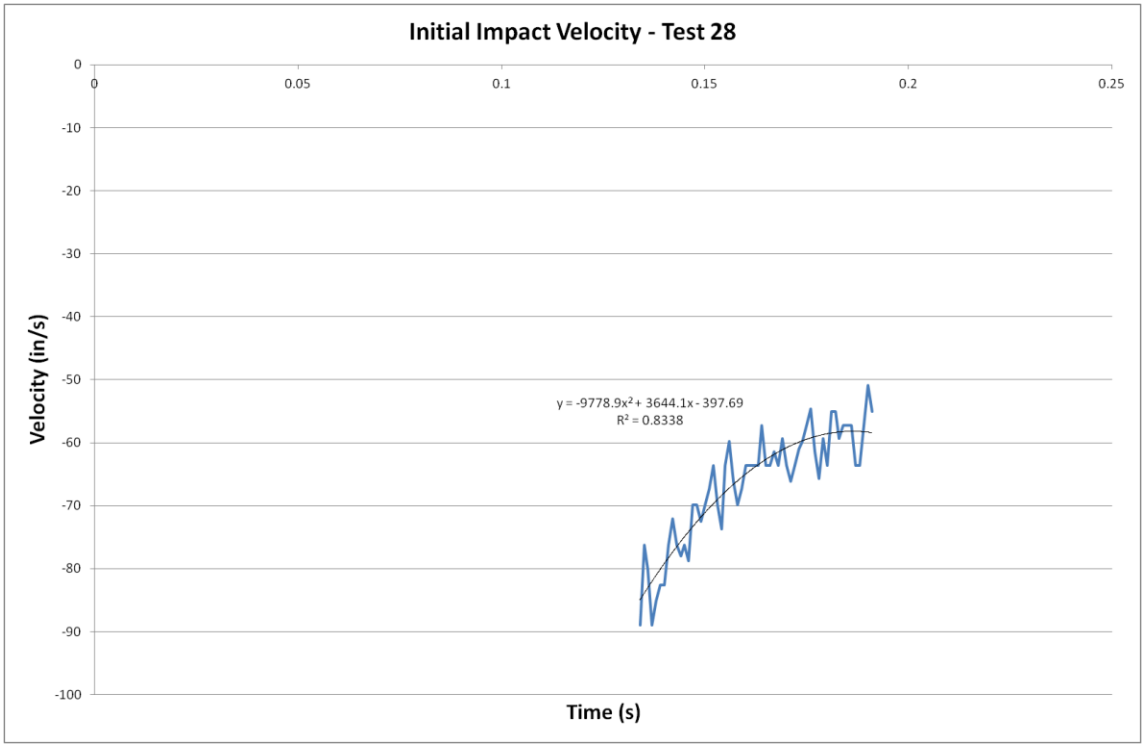
Initial Impact Velocity - Test 28
Velocity (in/s)
Time (s)
y = -9778.9x² + 3644.1x - 397.69
R² = 0.8338
0
-10
-20
-30
-40
-50
-60
-70
-80
-90
-100
0
0.05
0.1
0.15
0.2
0.25

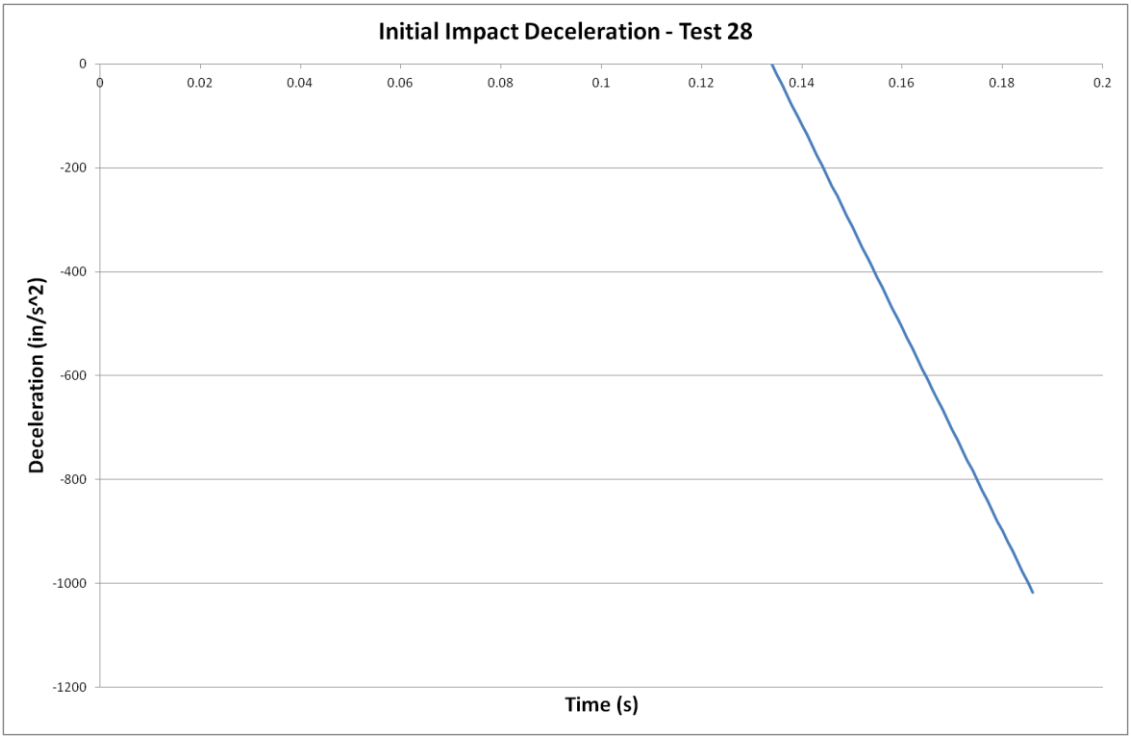
Initial Impact Deceleration - Test 28
Deceleration (in/s^2)
Time (s)
0
-200
-400
-600
-800
-1000
-1200
0
0.02
0.04
0.06
0.08
0.1
0.12
0.14
0.16
0.18
0.2

A.2 Plate Impacting Head

A.2.1 Plate Control I

All plate control load cell data was either lost or non-usable.

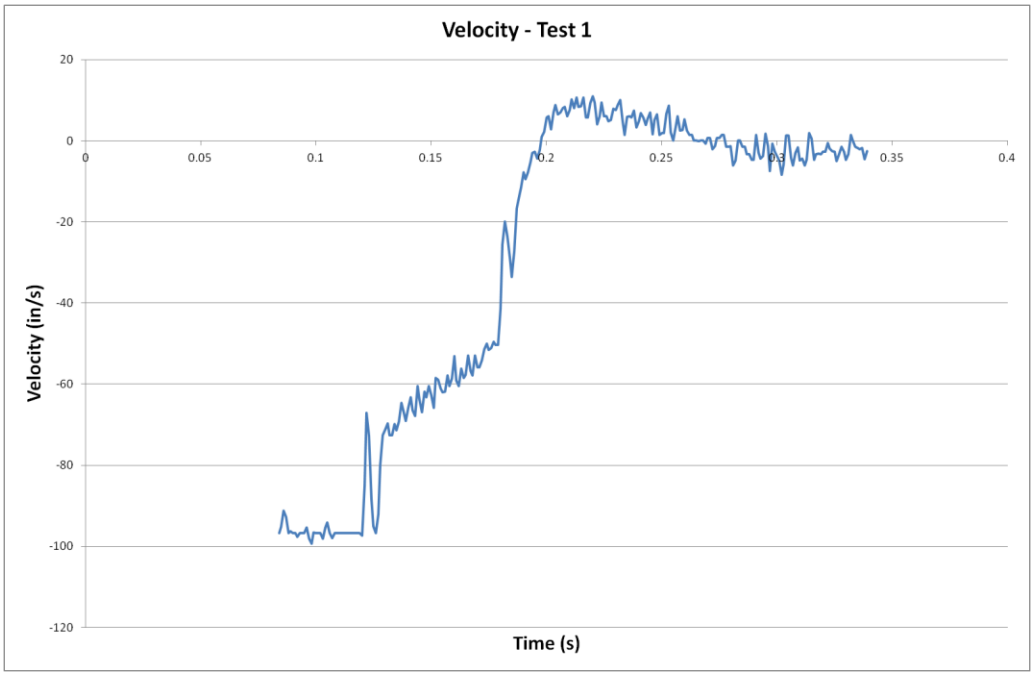

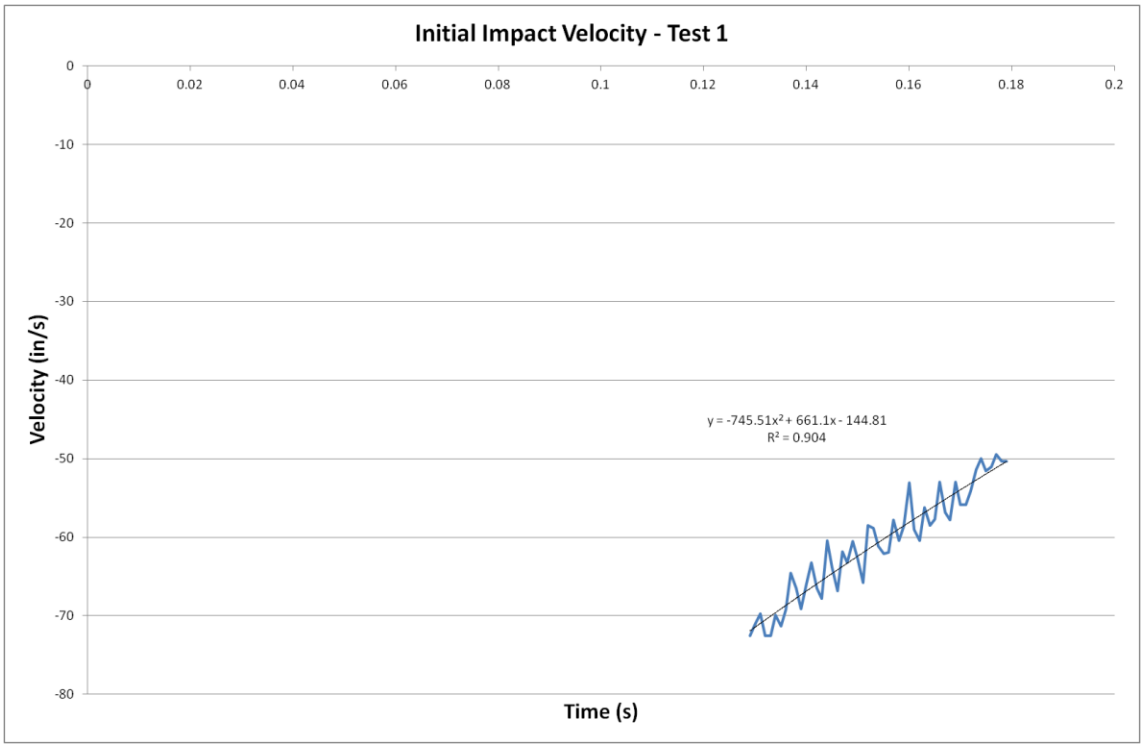
Initial Impact Velocity - Test 1
Velocity (in/s)
Time (s)
y = -745.51x² + 661.1x - 144.81
R² = 0.904
0
-10
-20
-30
-40
-50
-60
-70
-80
0
0.02
0.04
0.06
0.08
0.1
0.12
0.14
0.16
0.18
0.2

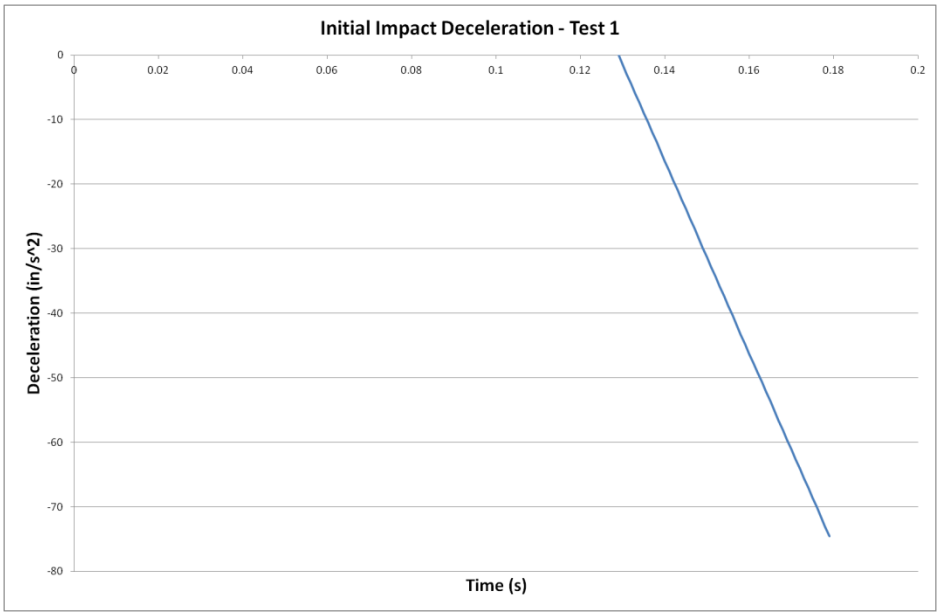
Initial Impact Deceleration - Test 1
Deceleration (in/s^2)
Time (s)
0
-10
-20
-30
-40
-50
-60
-70
-80
0
0.02
0.04
0.06
0.08
0.1
0.12
0.14
0.16
0.18
0.2

A.2.2 Plate Control II

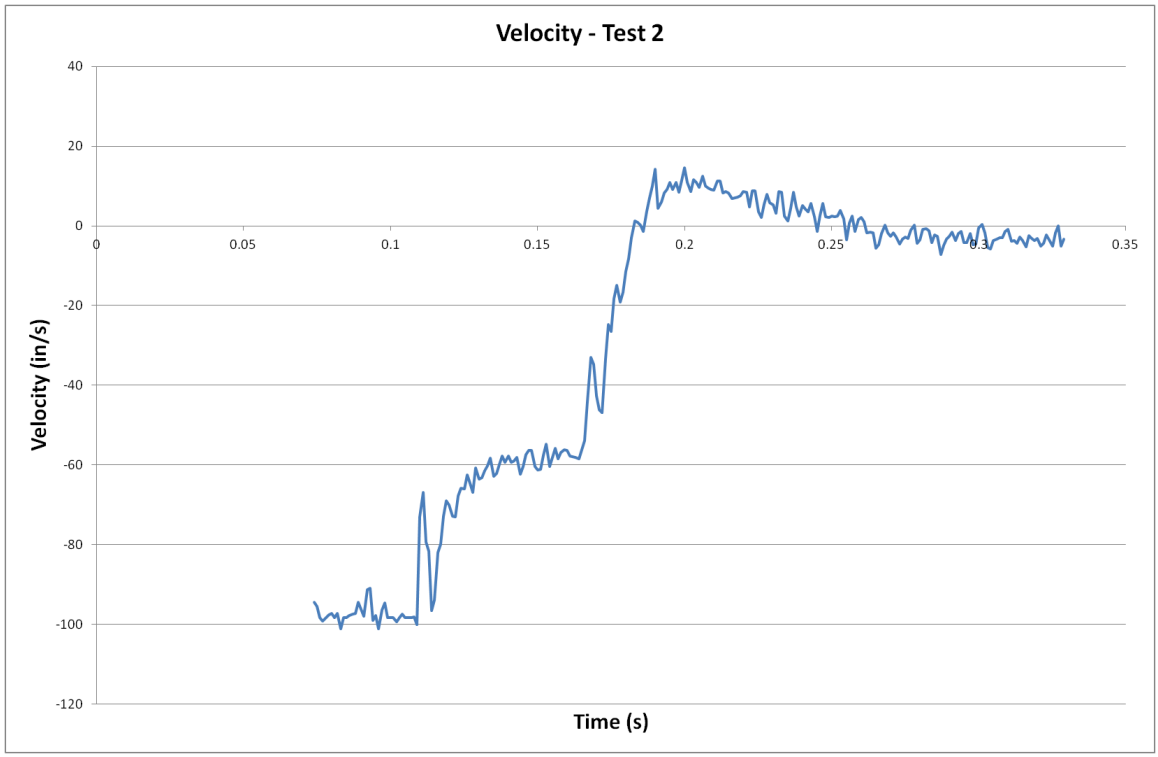

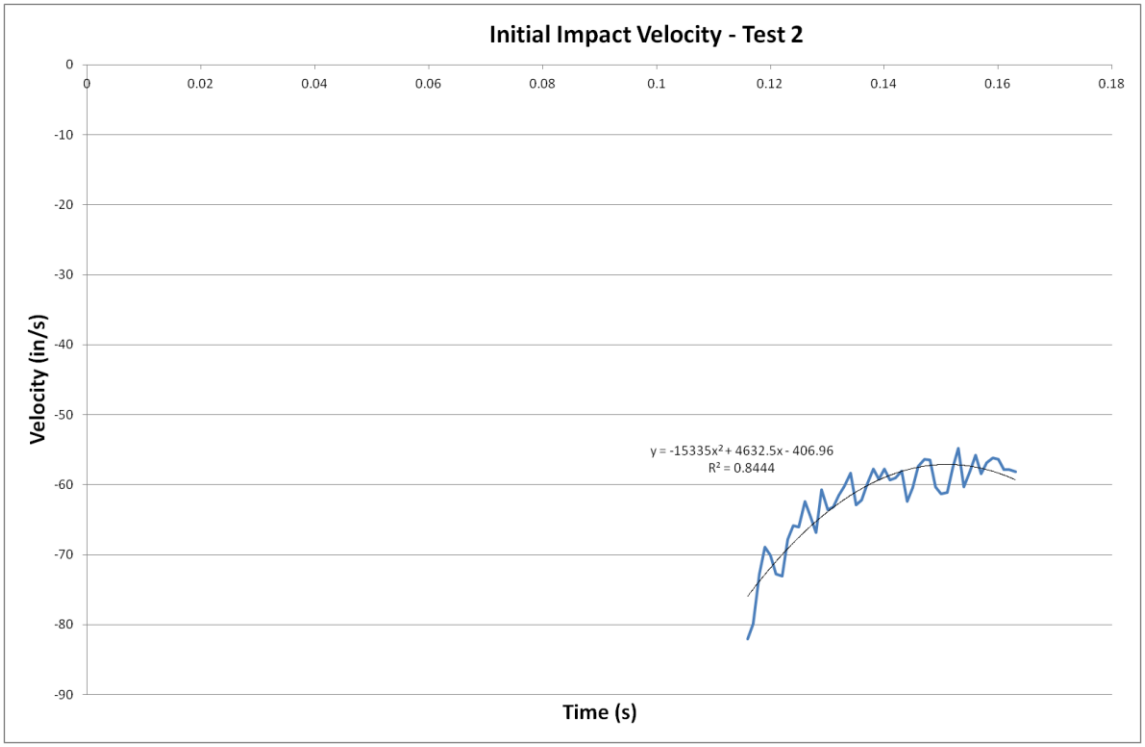

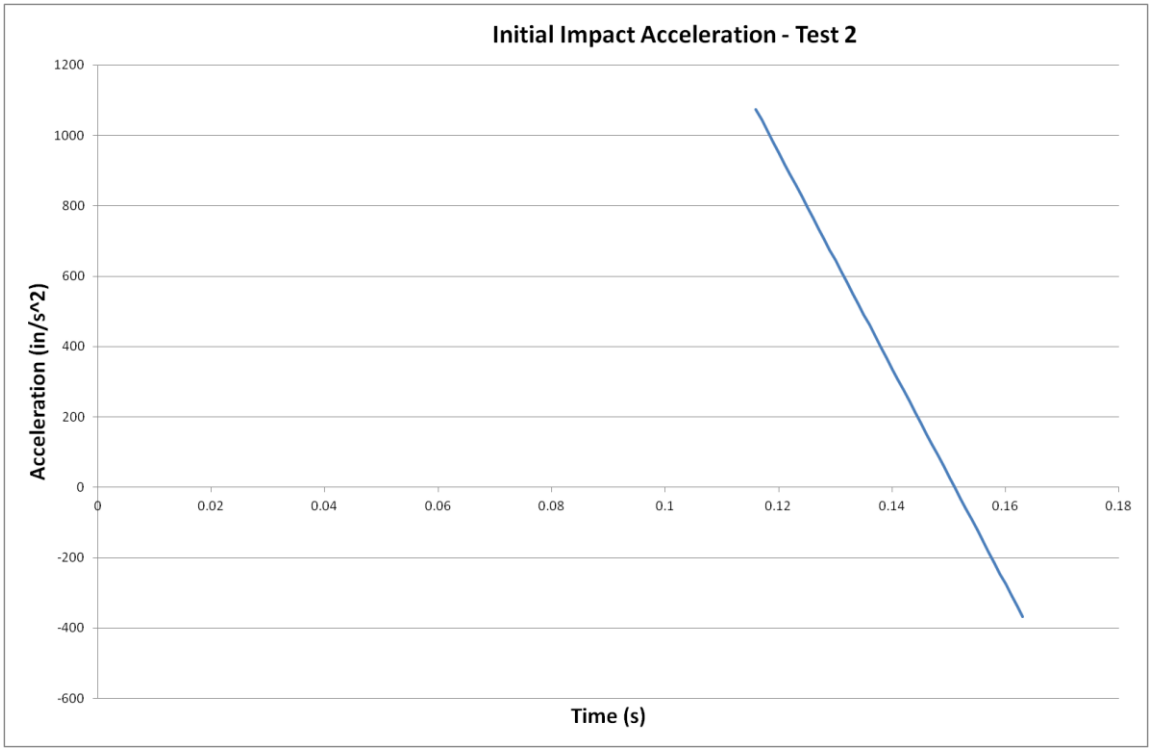

A.2.3 Plate Control III

A.2.4 Plate Control IV

Velocity and acceleration data for tests 29 and 30, both additional plate control tests, were inconclusive due to debris flying in front of the tracking dot. This caused the tracking software to misread the test and is impossible to counteract.

A.2.5 Plate Coarse Aggregate I

No load cell data is available for test #3. The data was taken on the wrong load scale.

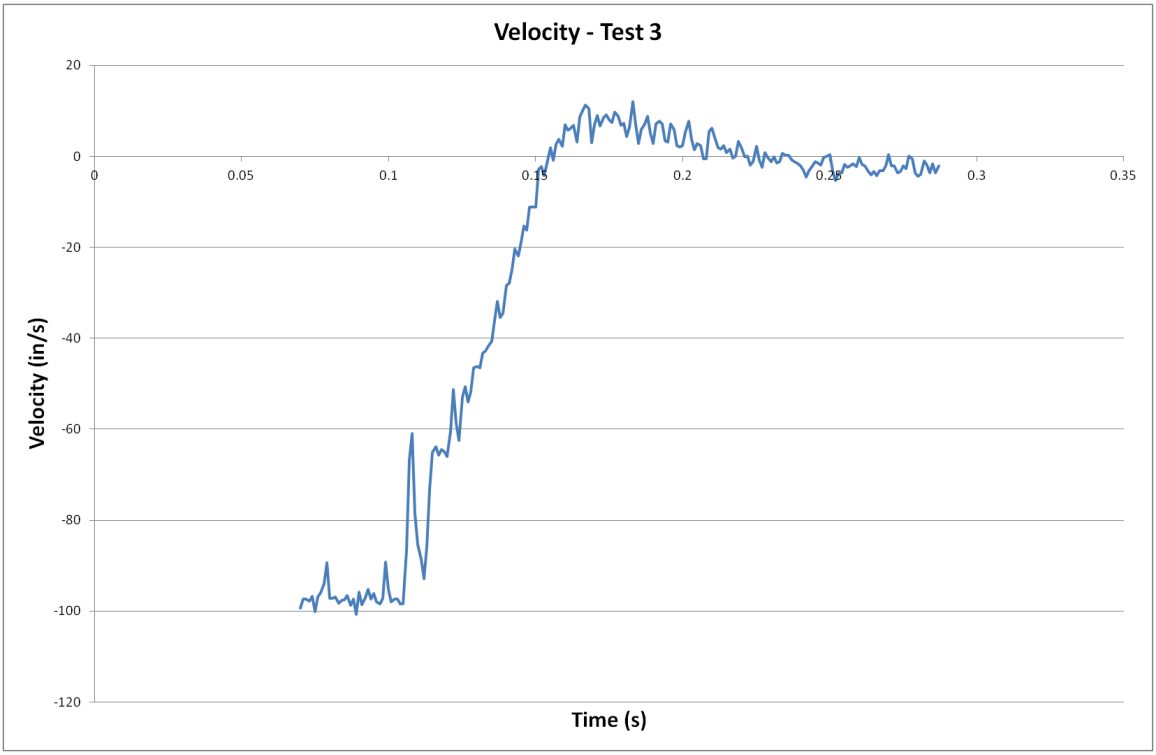

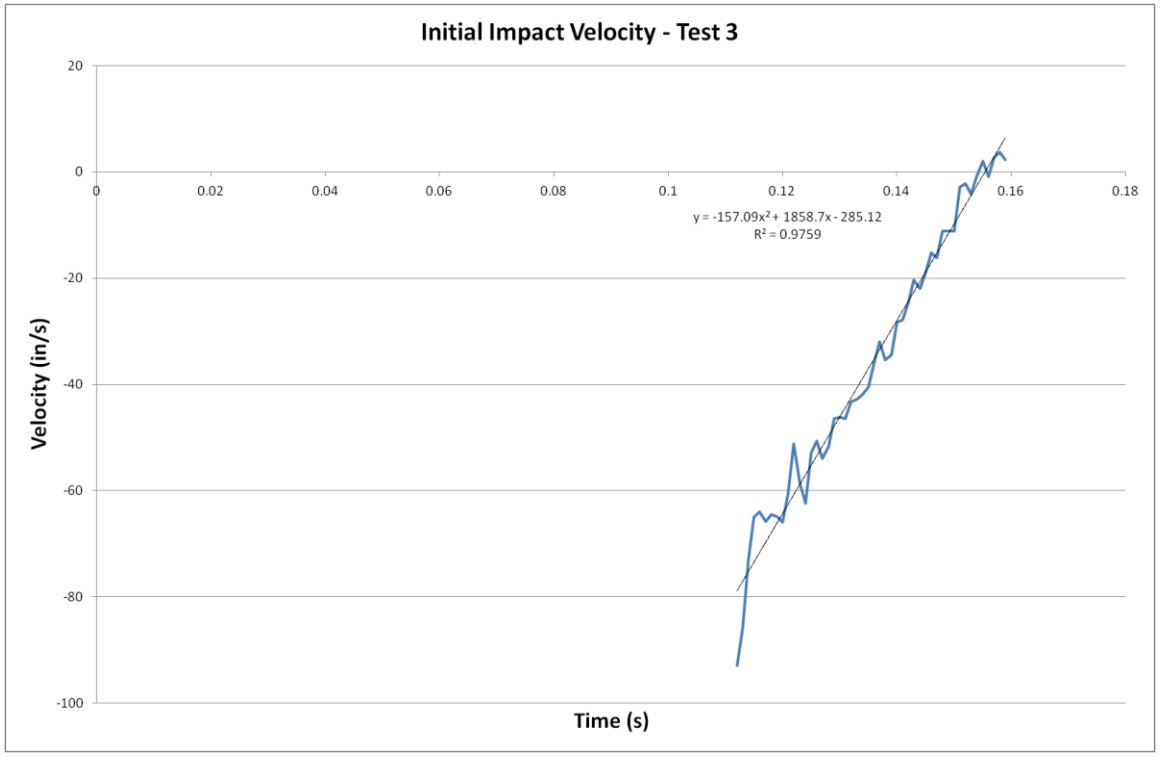
Initial Impact Velocity - Test 3
20
0
-20
-40
-60
-80
-100
0
0.02
0.04
0.06
0.08
0.1
0.12
0.14
0.16
0.18
y = -157.09x² + 1858.7x - 285.12
R² = 0.9759
Velocity (in/s)
Time (s)

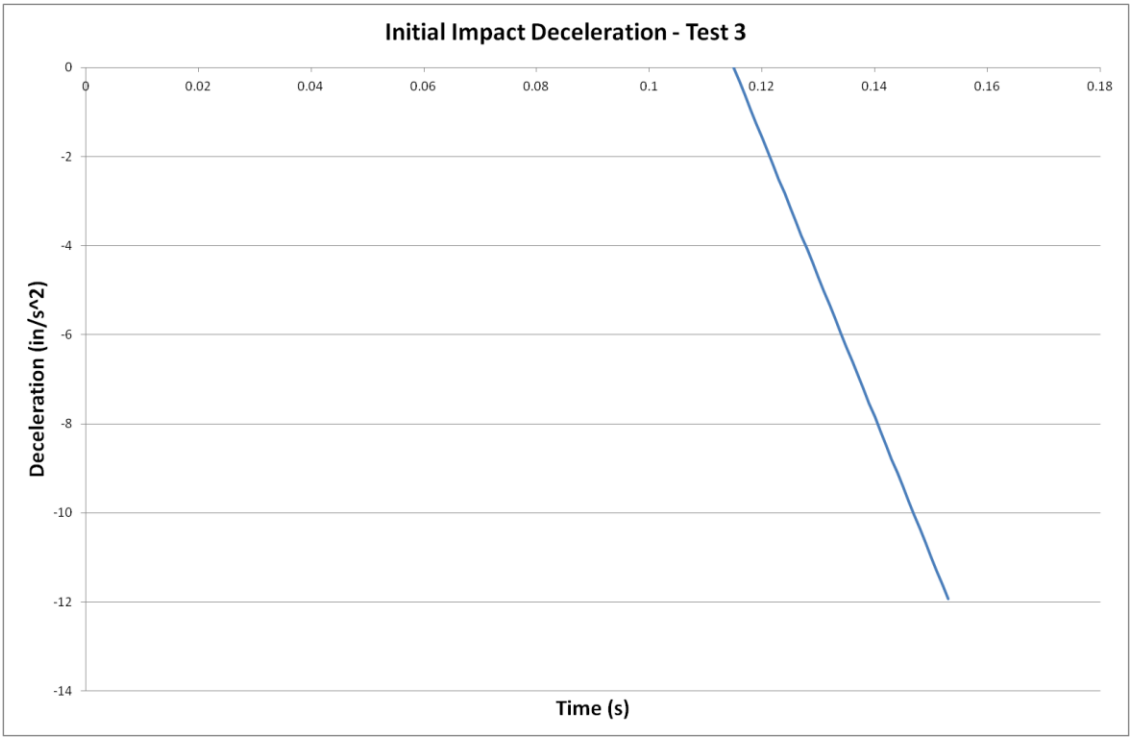
Initial Impact Deceleration - Test 3
0
-2
-4
-6
-8
-10
-12
-14
0
0.02
0.04
0.06
0.08
0.1
0.12
0.14
0.16
0.18
Deceleration (in/s^2)
Time (s)

A.2.6 Plate Coarse Aggregate II

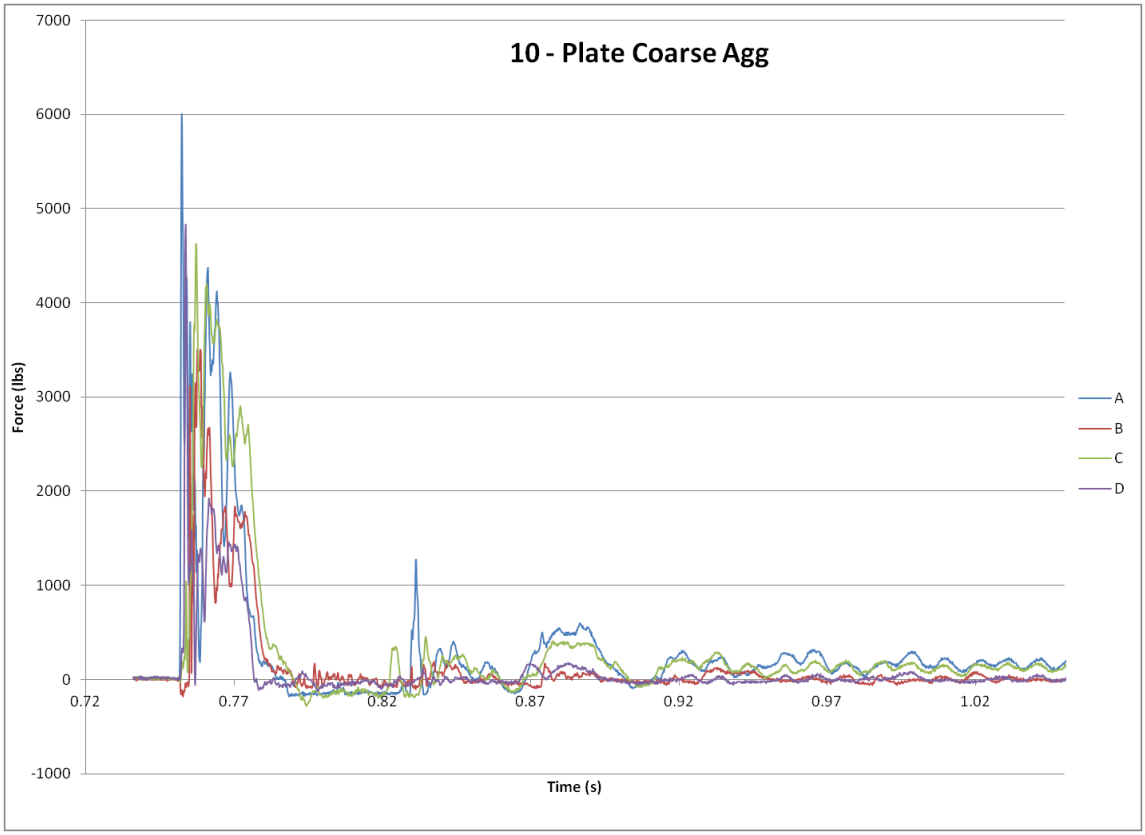

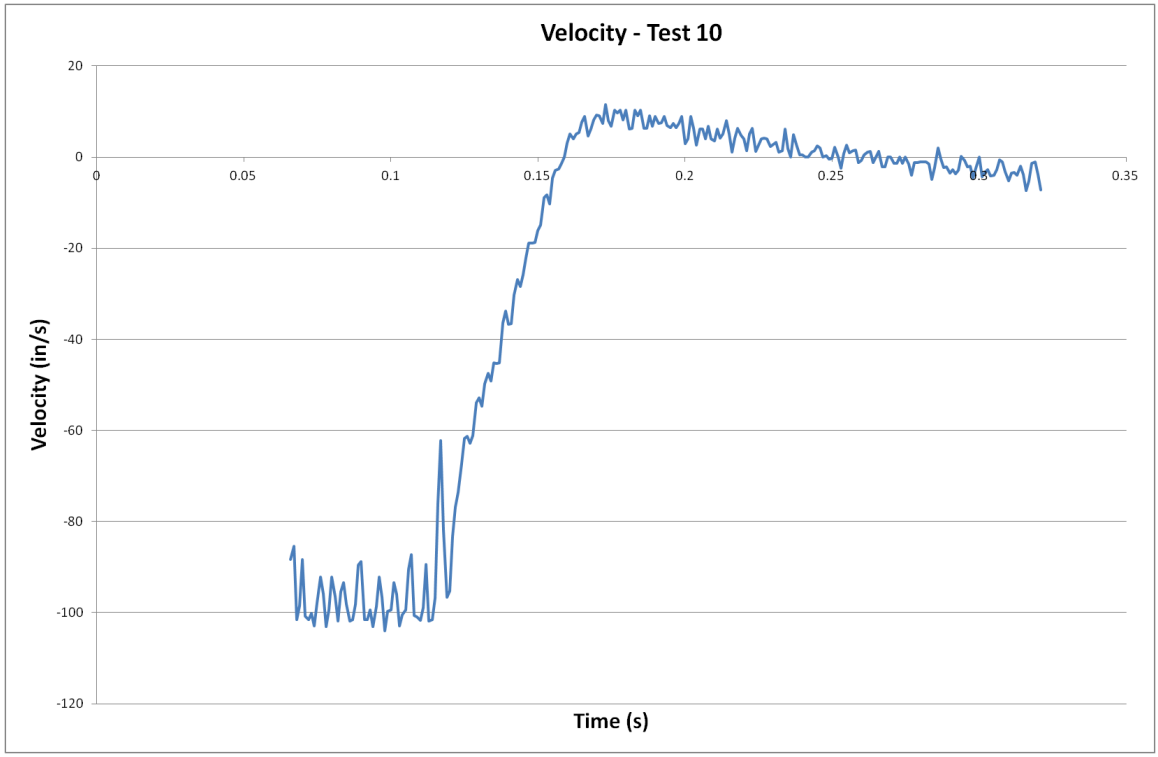
Velocity - Test 10
Velocity (in/s)
Time (s)
20
0
-20
-40
-60
-80
-100
-120
0
0.05
0.1
0.15
0.2
0.25
0.35

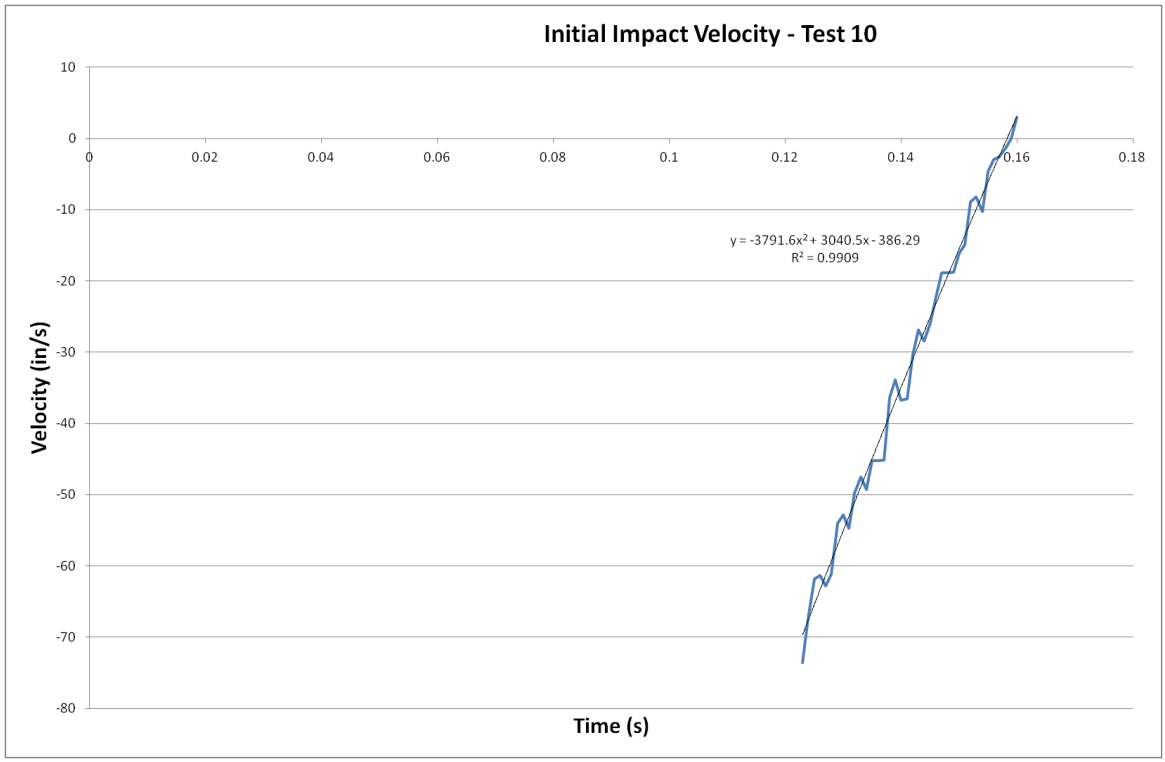
Initial Impact Velocity - Test 10
Velocity (in/s)
Time (s)
y = -3791.6x² + 3040.5x - 386.29
R² = 0.9909
10
0
-10
-20
-30
-40
-50
-60
-70
-80
0
0.02
0.04
0.06
0.08
0.1
0.12
0.14
0.16
0.18

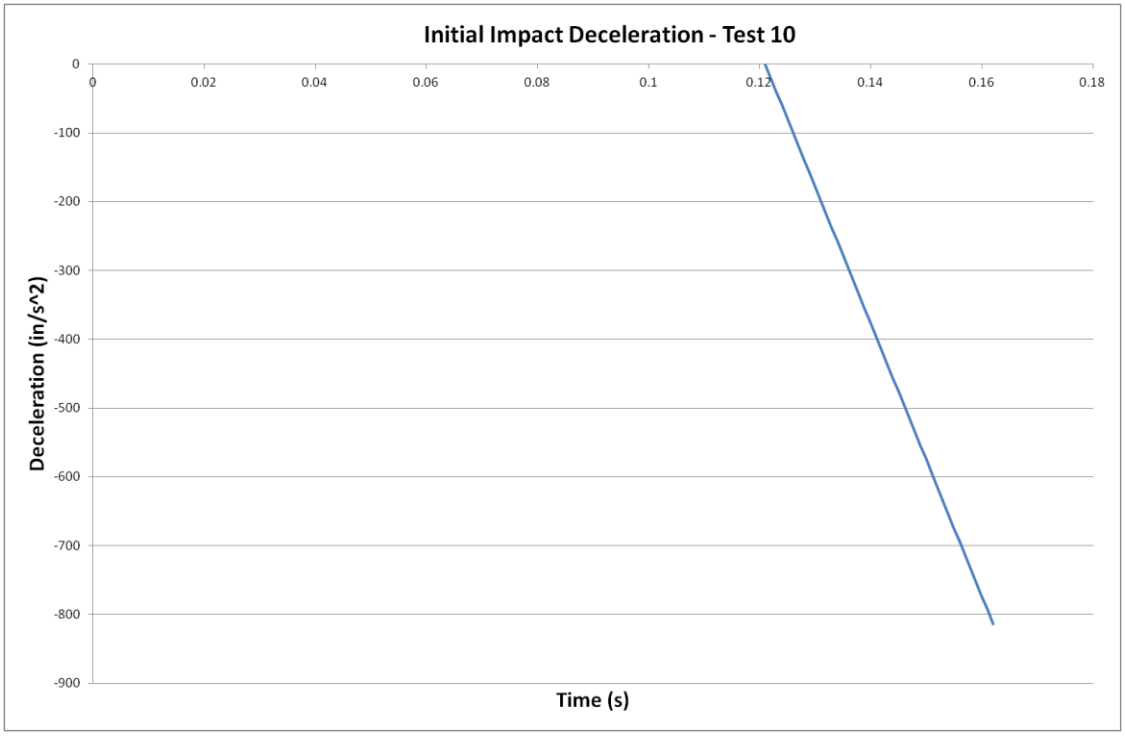
Initial Impact Deceleration - Test 10
Deceleration (in/s^2)
Time (s)
0
-100
-200
-300
-400
-500
-600
-700
-800
-900
0
0.02
0.04
0.06
0.08
0.1
0.12
0.14
0.16
0.18

A.2.7 Plate Sand Compacted I

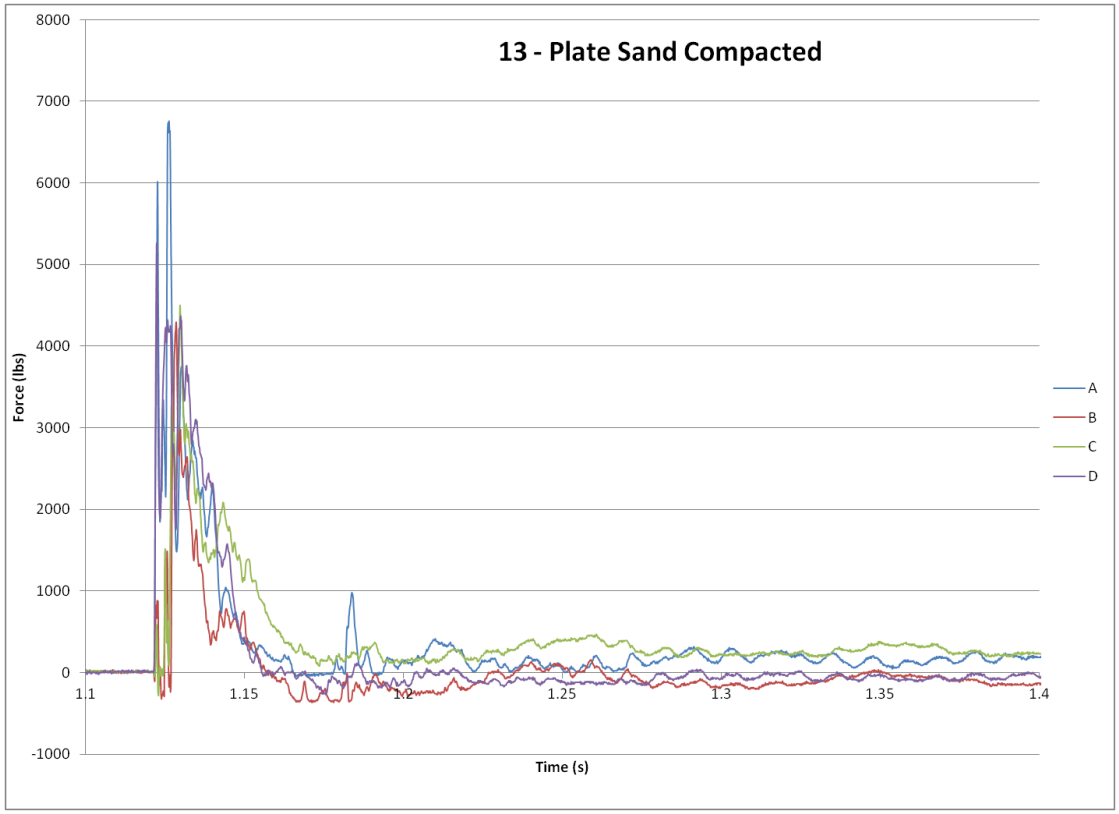

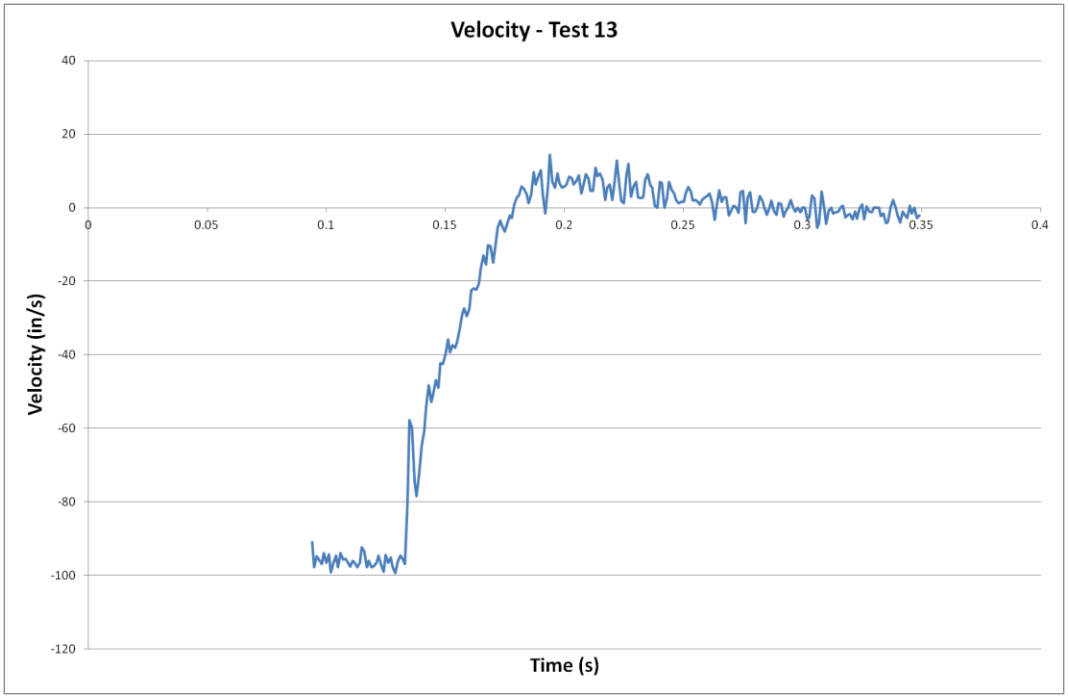
Velocity - Test 13
Velocity (in/s)
Time (s)
40
20
0
-20
-40
-60
-80
-100
-120
0
0.05
0.1
0.15
0.2
0.25
0.3
0.35
0.4

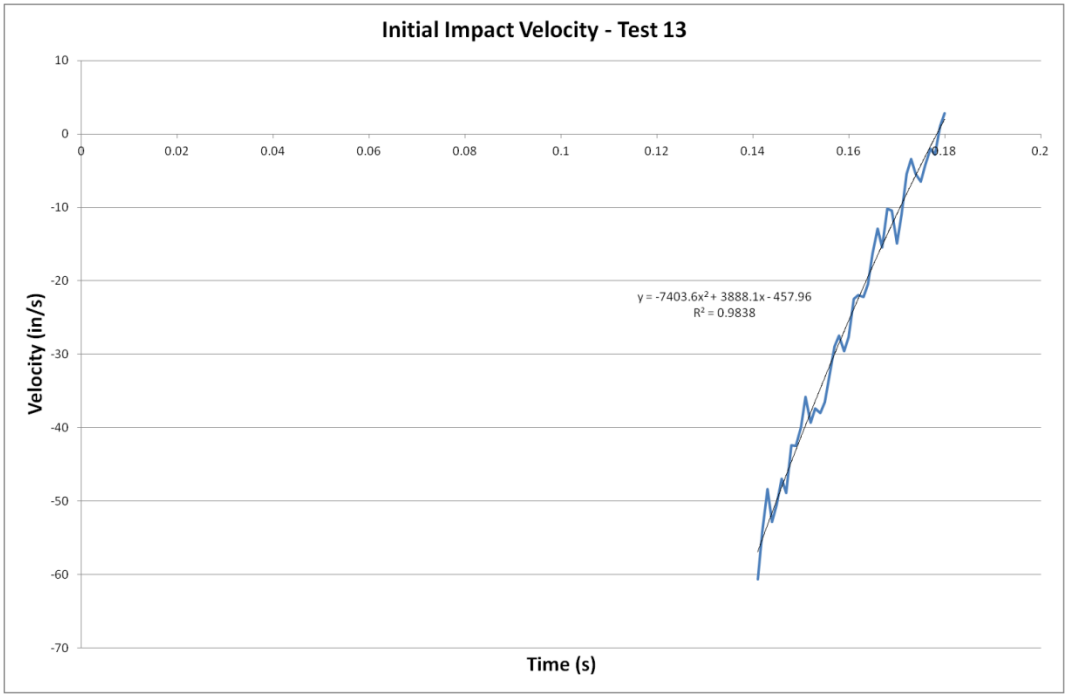
Initial Impact Velocity - Test 13
Velocity (in/s)
Time (s)
y = -7403.6x² + 3888.1x - 457.96
R² = 0.9838
10
0
-10
-20
-30
-40
-50
-60
-70
0
0.02
0.04
0.06
0.08
0.1
0.12
0.14
0.16
0.18
0.2

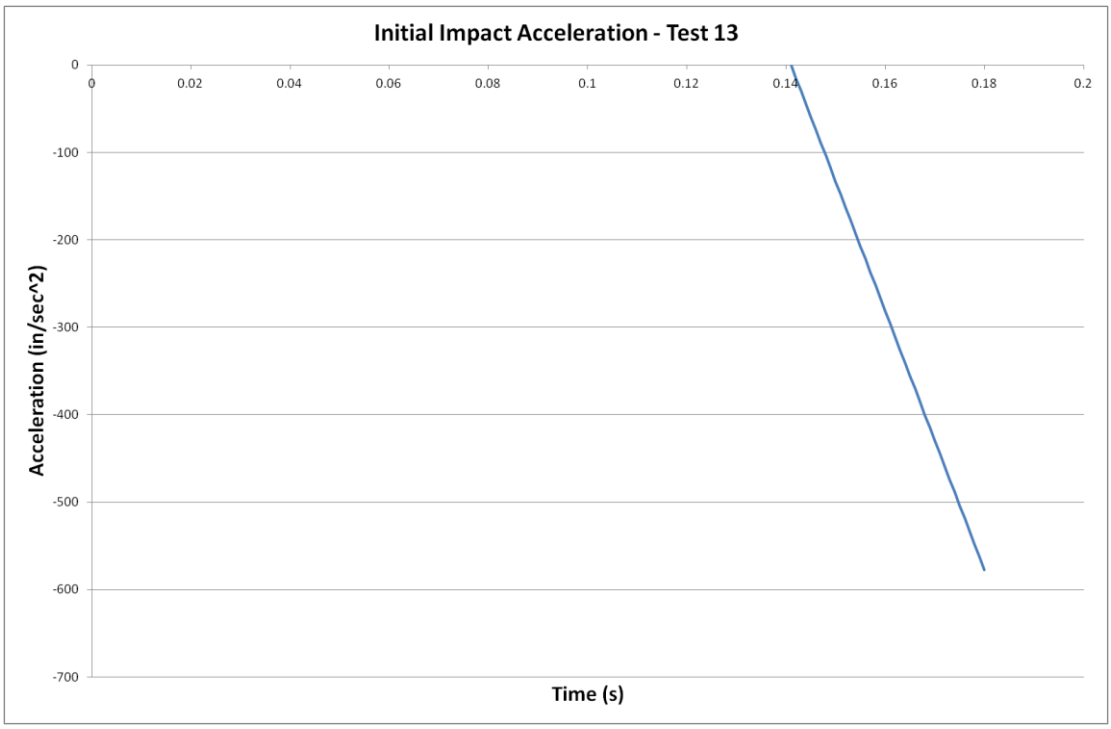
Initial Impact Acceleration - Test 13
Acceleration (in/sec^2)
0
-100
-200
-300
-400
-500
-600
-700
0
0.02
0.04
0.06
0.08
0.1
0.12
0.14
0.16
0.18
0.2
Time (s)

A.2.8 Plate Sand Compacted II

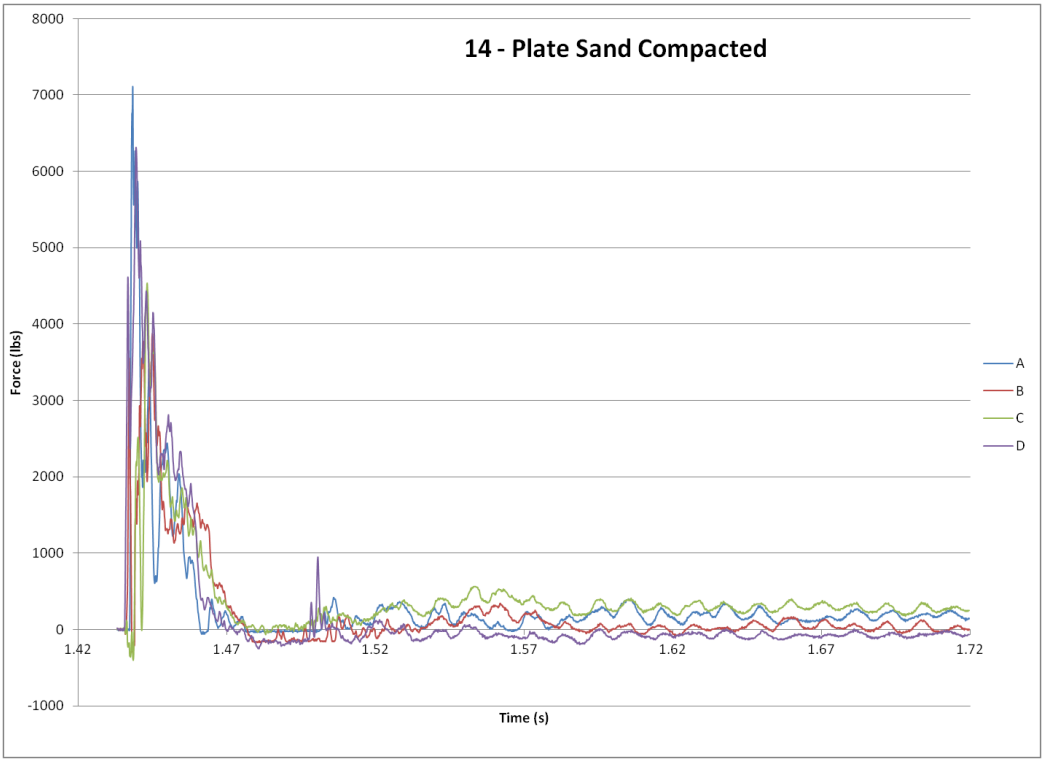

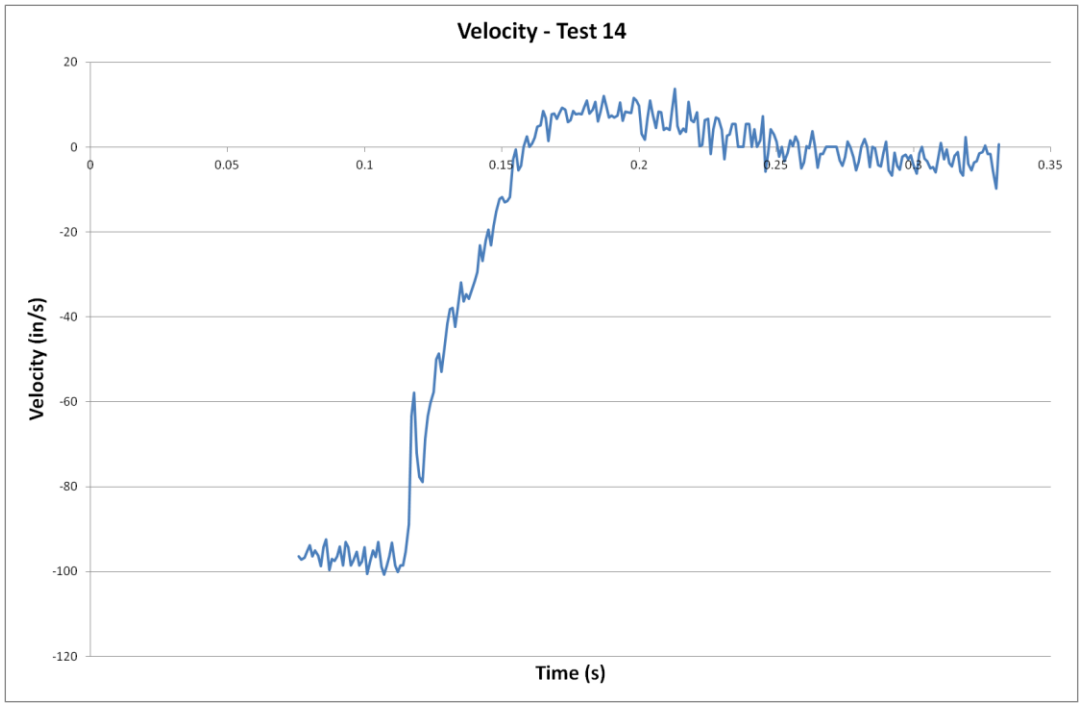
Velocity - Test 14
Velocity (in/s)
Time (s)
20
0
-20
-40
-60
-80
-100
-120
0
0.05
0.1
0.15
0.2
0.25
0.35

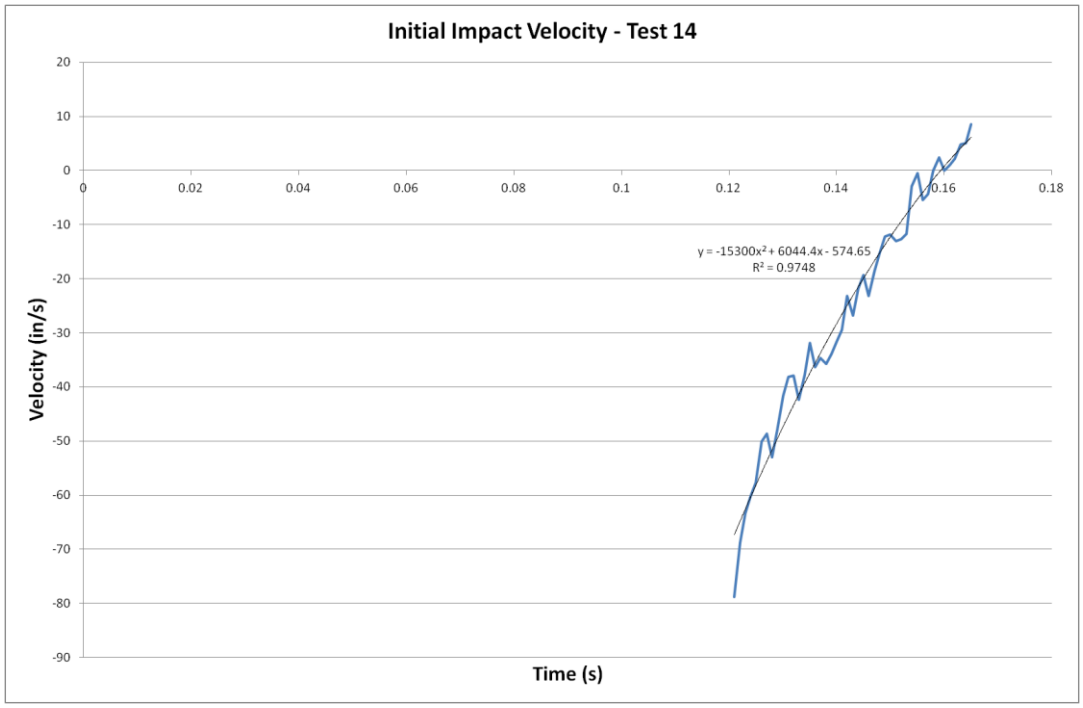
Initial Impact Velocity - Test 14
Velocity (in/s)
Time (s)
y = -15300x² + 6044.4x - 574.65
R² = 0.9748
20
10
0
-10
-20
-30
-40
-50
-60
-70
-80
-90
0
0.02
0.04
0.06
0.08
0.1
0.12
0.14
0.16
0.18

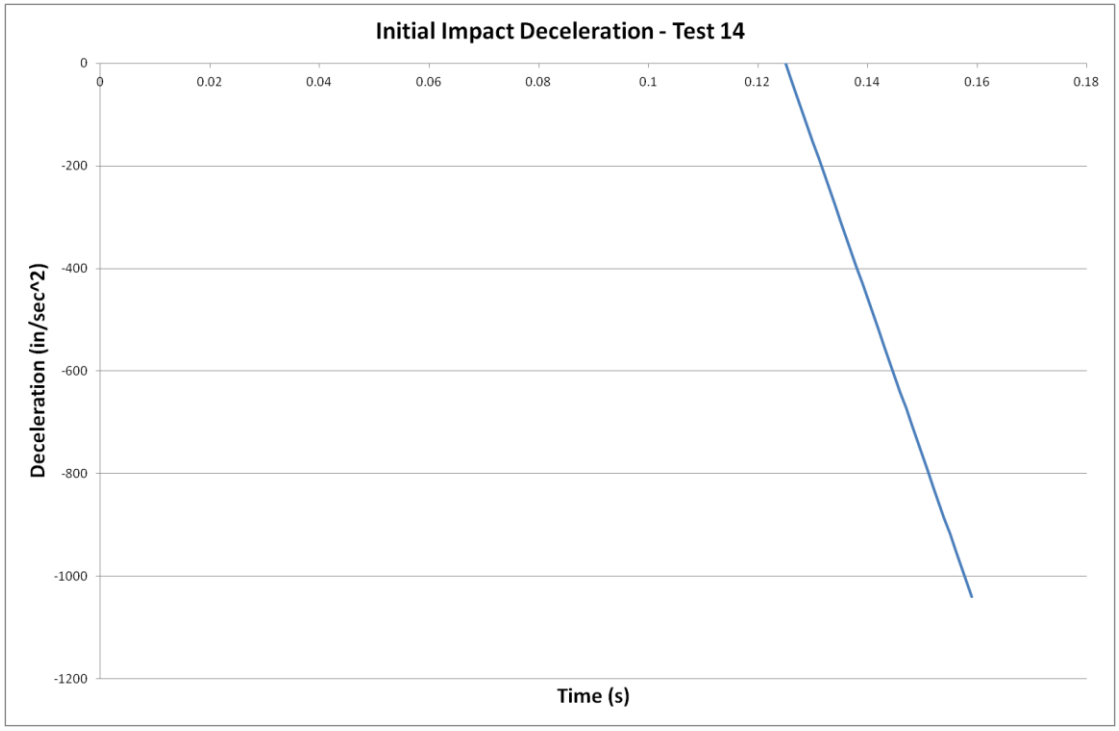
Initial Impact Deceleration - Test 14
Deceleration (in/sec^2)
Time (s)
0
-200
-400
-600
-800
-1000
-1200
0
0.02
0.04
0.06
0.08
0.1
0.12
0.14
0.16
0.18

A.2.9 Plate Uncompacted Sand I

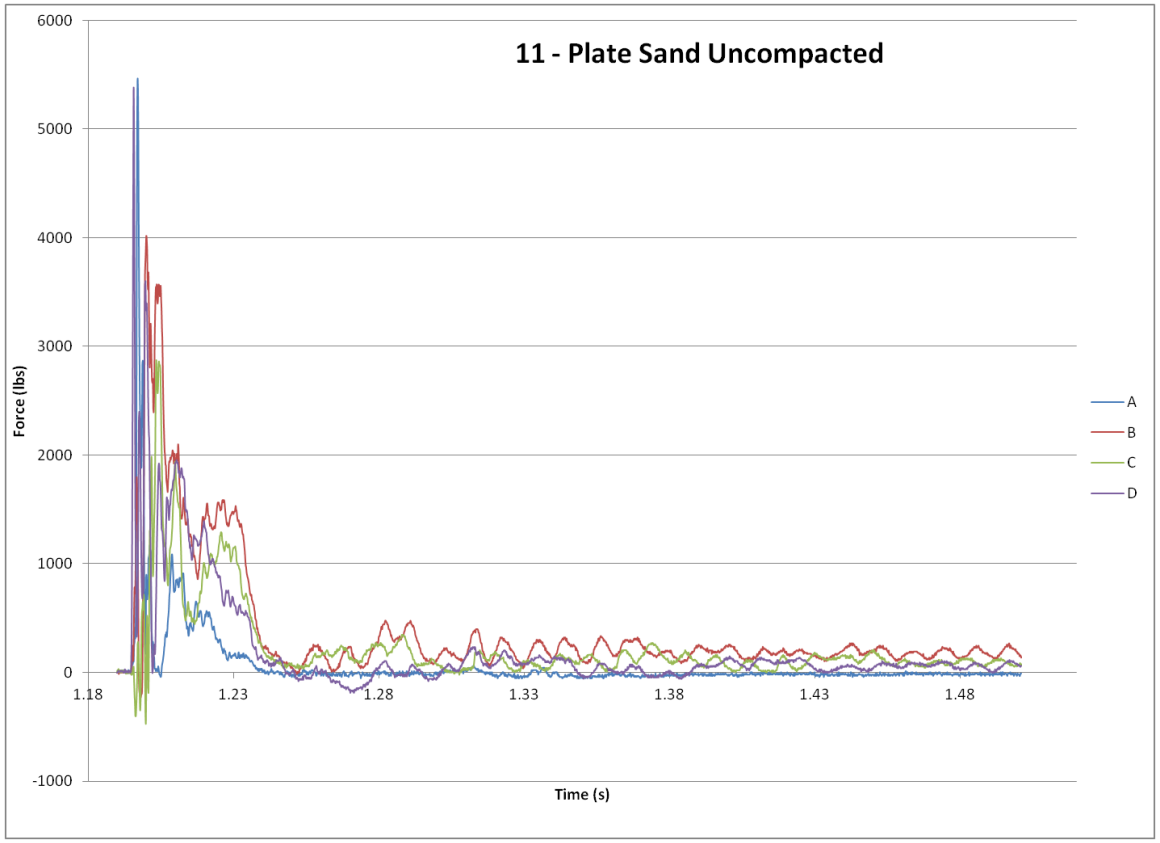

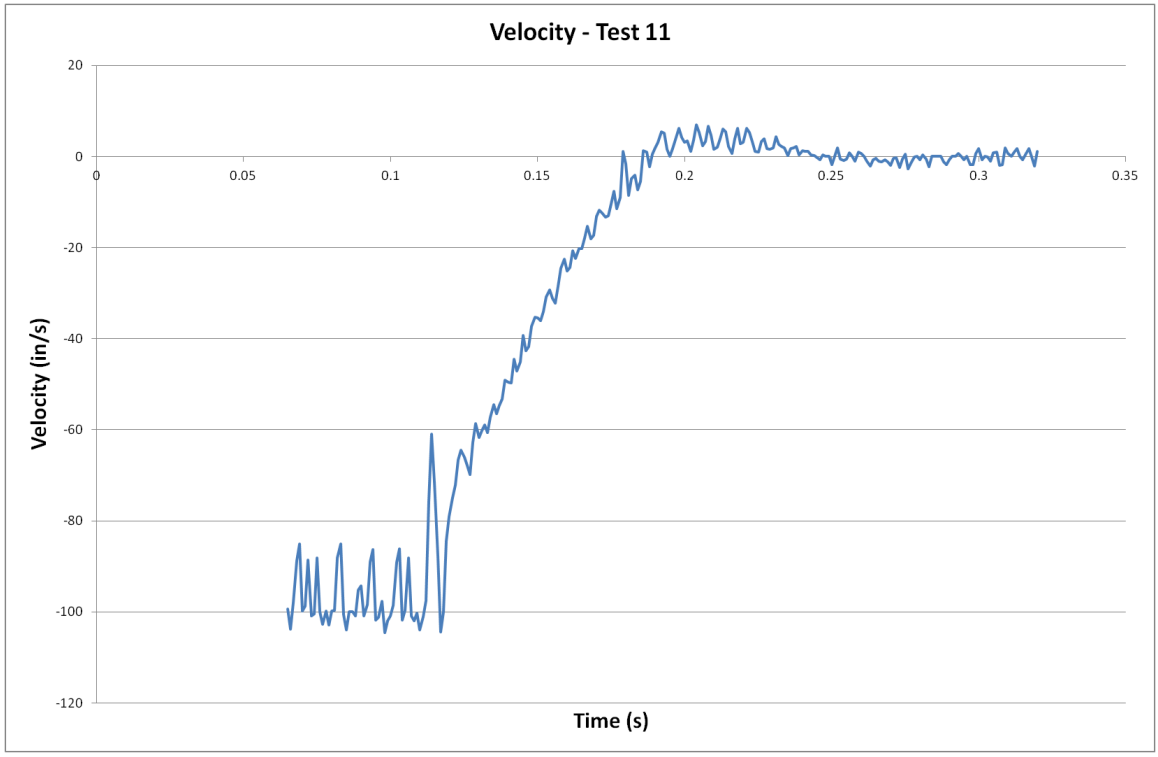
Velocity - Test 11
20
0
-20
-40
-60
-80
-100
-120
0
0.05
0.1
0.15
0.2
0.25
0.3
0.35
Velocity (in/s)
Time (s)

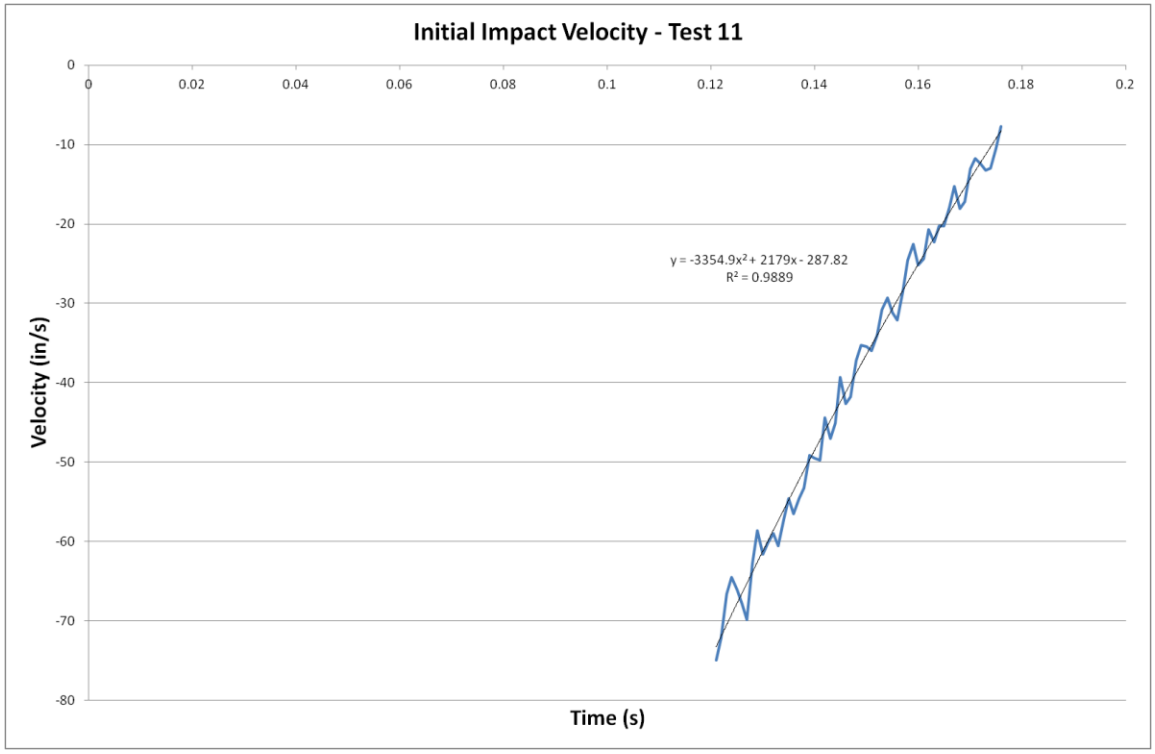
Initial Impact Velocity - Test 11
0
-10
-20
-30
-40
-50
-60
-70
-80
0
0.02
0.04
0.06
0.08
0.1
0.12
0.14
0.16
0.18
0.2
y = -3354.9x² + 2179x - 287.82
R² = 0.9889
Velocity (in/s)
Time (s)

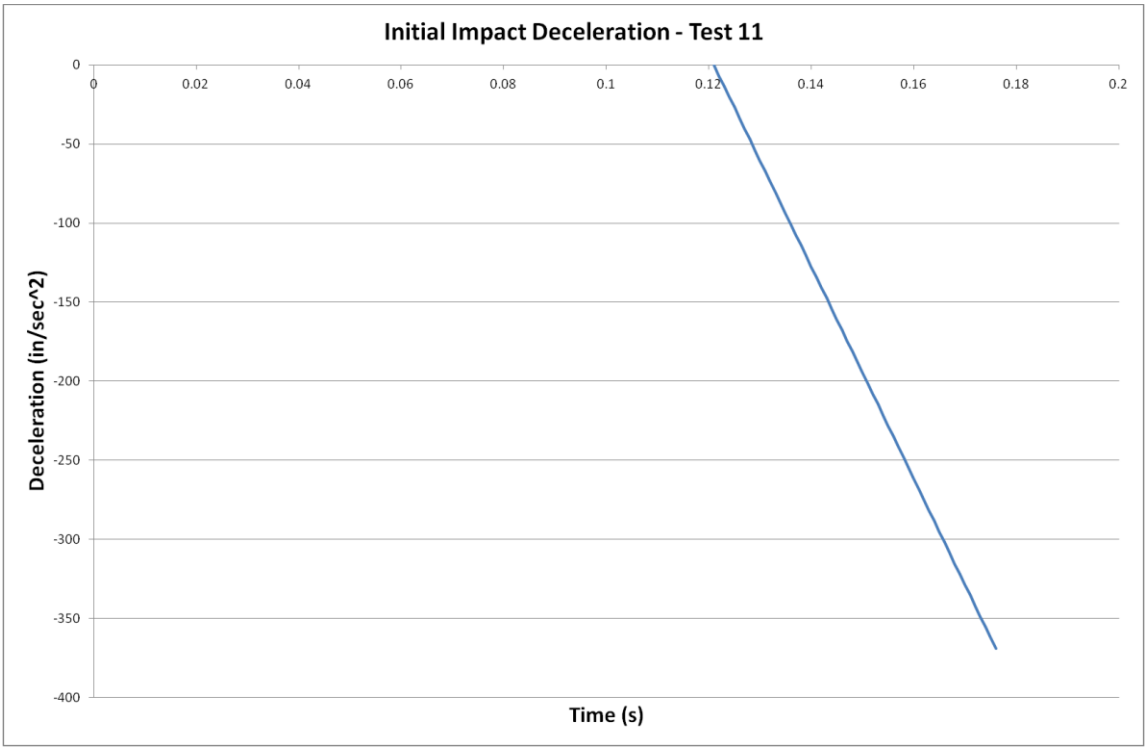
Initial Impact Deceleration - Test 11
Deceleration (in/sec^2)
Time (s)
0
-50
-100
-150
-200
-250
-300
-350
-400
0
0.02
0.04
0.06
0.08
0.1
0.12
0.14
0.16
0.18
0.2

A.2.10 Plate Uncompacted Sand II

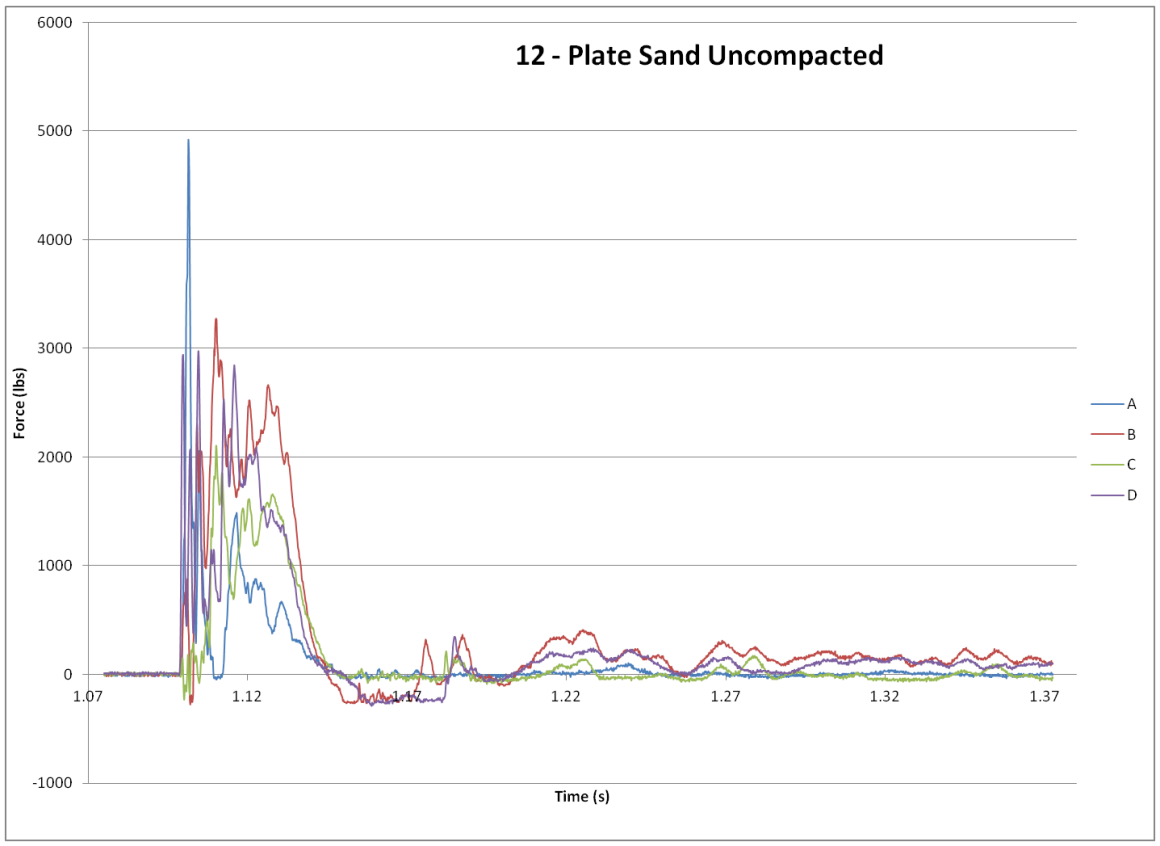

No velocity or acceleration data is available for tests #12. Particles of concrete flew in front of the tracking dot causing unusable results

A.2.11 Plate Soil Uncompacted I

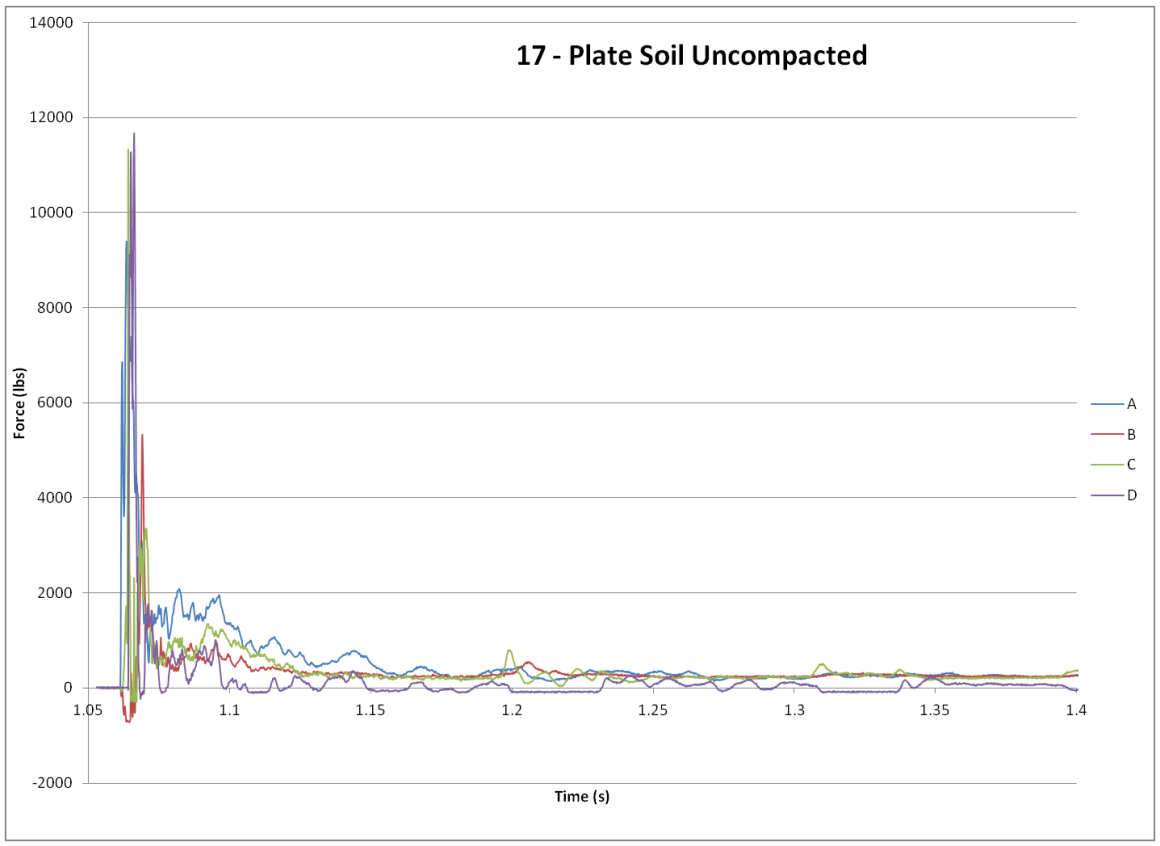

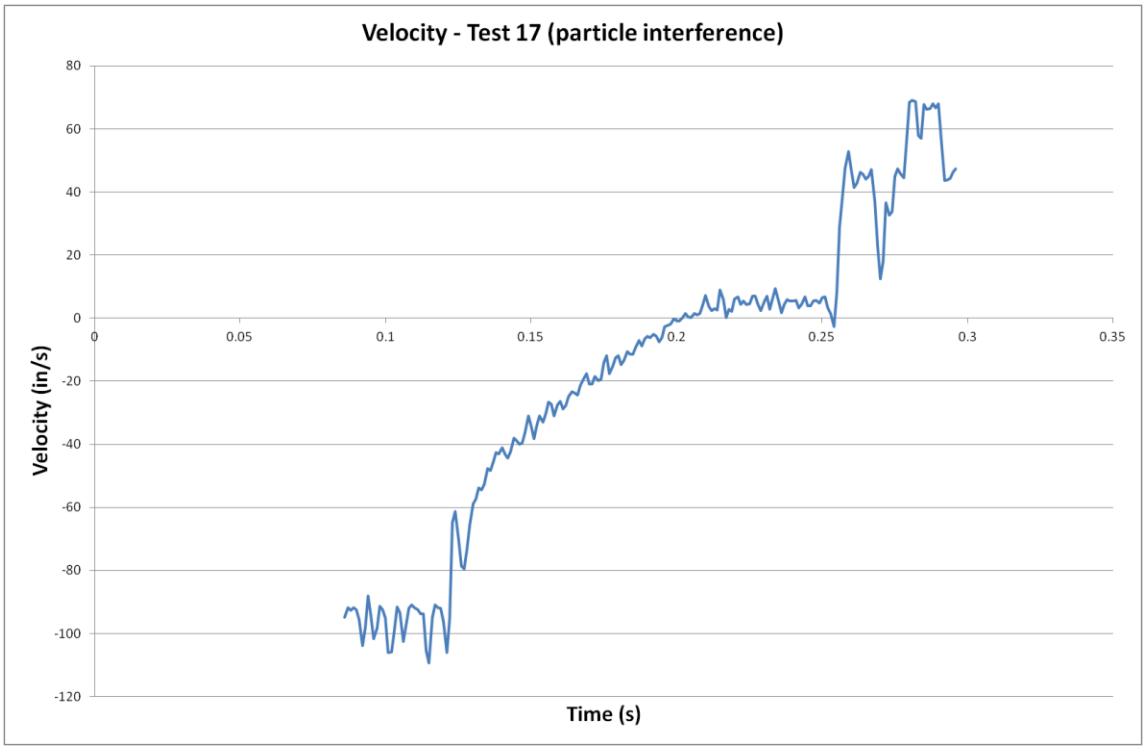
Velocity - Test 17 (particle interference)
Velocity (in/s)
Time (s)
80
60
40
20
0
-20
-40
-60
-80
-100
-120
0
0.05
0.1
0.15
0.2
0.25
0.3
0.35

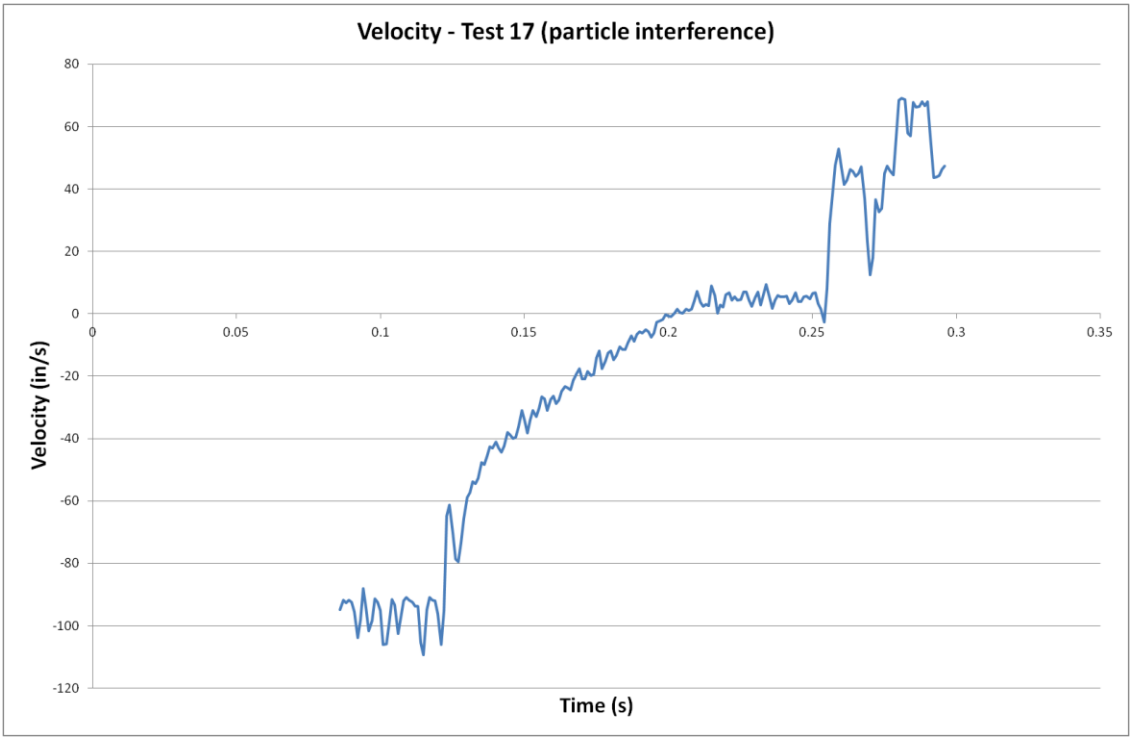
Velocity - Test 17 (particle interference)
Velocity (in/s)
Time (s)
80
60
40
20
0
-20
-40
-60
-80
-100
-120
0
0.05
0.1
0.15
0.2
0.25
0.3
0.35

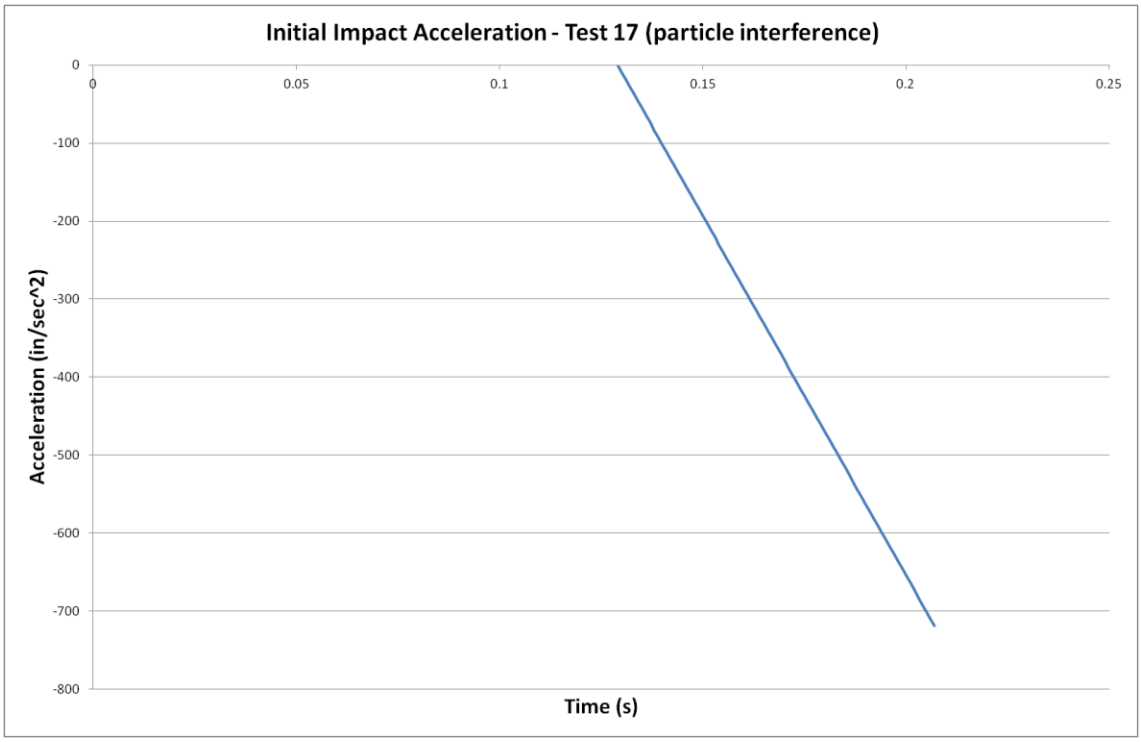
Initial Impact Acceleration - Test 17 (particle interference)
Acceleration (in/sec^2)
0
-100
-200
-300
-400
-500
-600
-700
-800
0
0.05
0.1
0.15
0.2
0.25
Time (s)

A.2.12 Plate Soil Uncompacted II

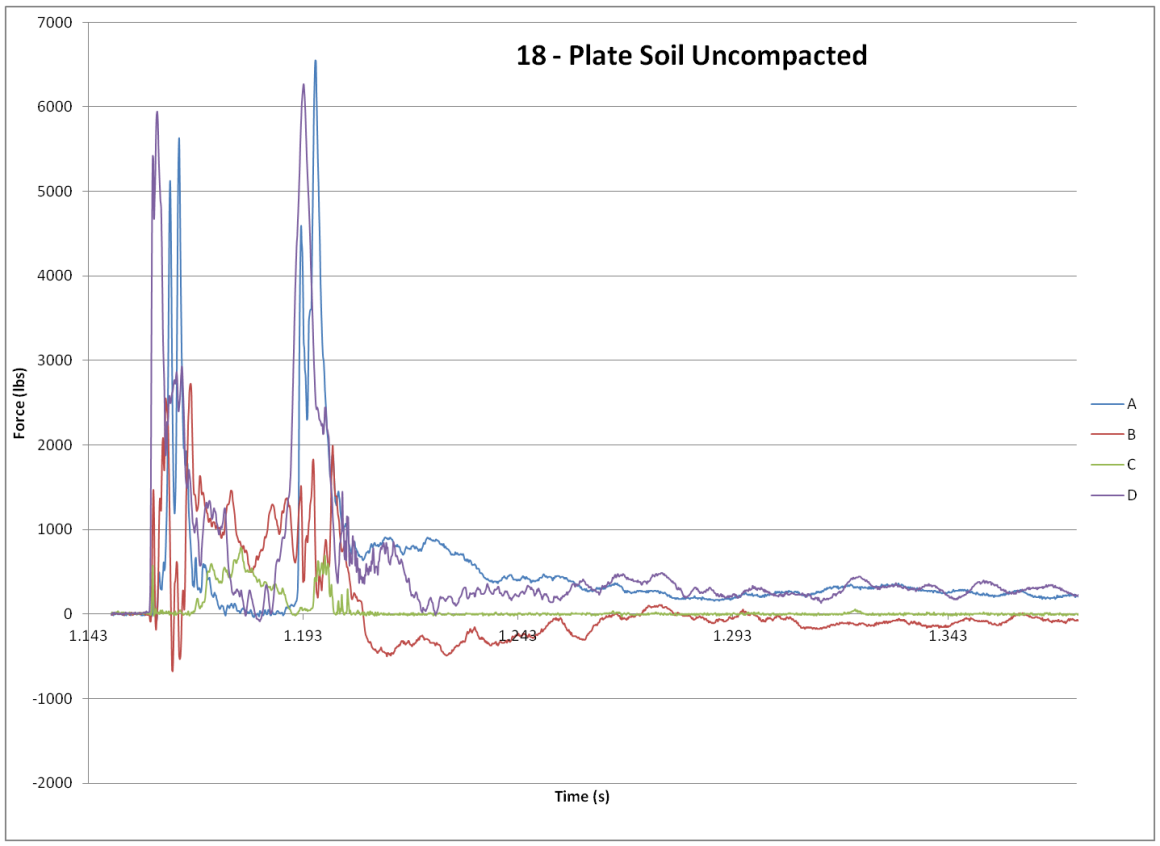

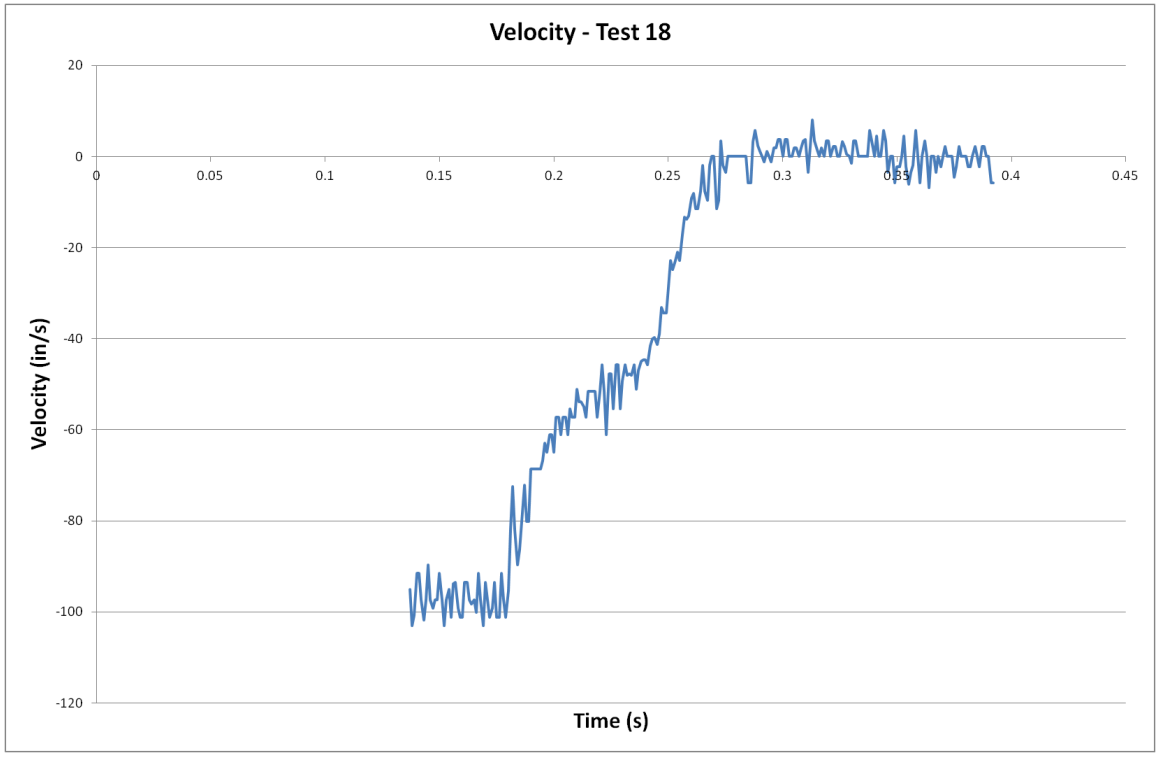
Velocity - Test 18
20
0
-20
-40
-60
-80
-100
-120
0
0.05
0.1
0.15
0.2
0.25
0.3
0.35
0.4
0.45
Velocity (in/s)
Time (s)

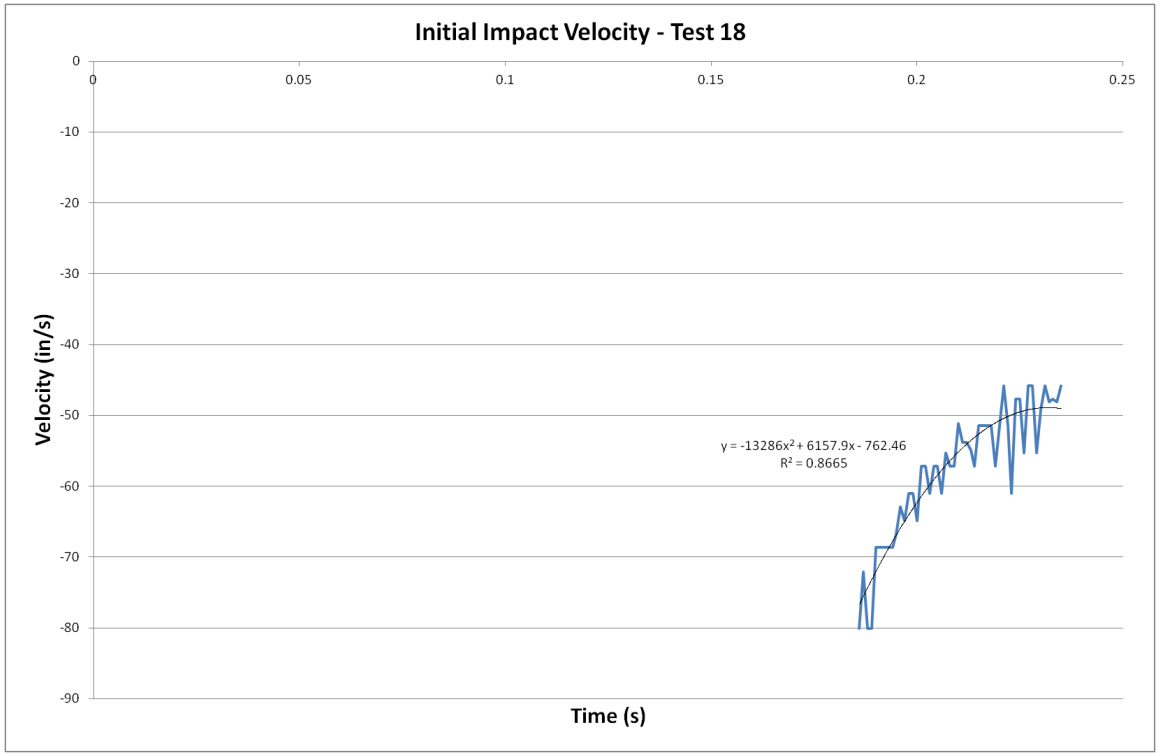
Initial Impact Velocity - Test 18
0
-10
-20
-30
-40
-50
-60
-70
-80
-90
0
0.05
0.1
0.15
0.2
0.25
y = -13286x² + 6157.9x - 762.46
R² = 0.8665
Velocity (in/s)
Time (s)

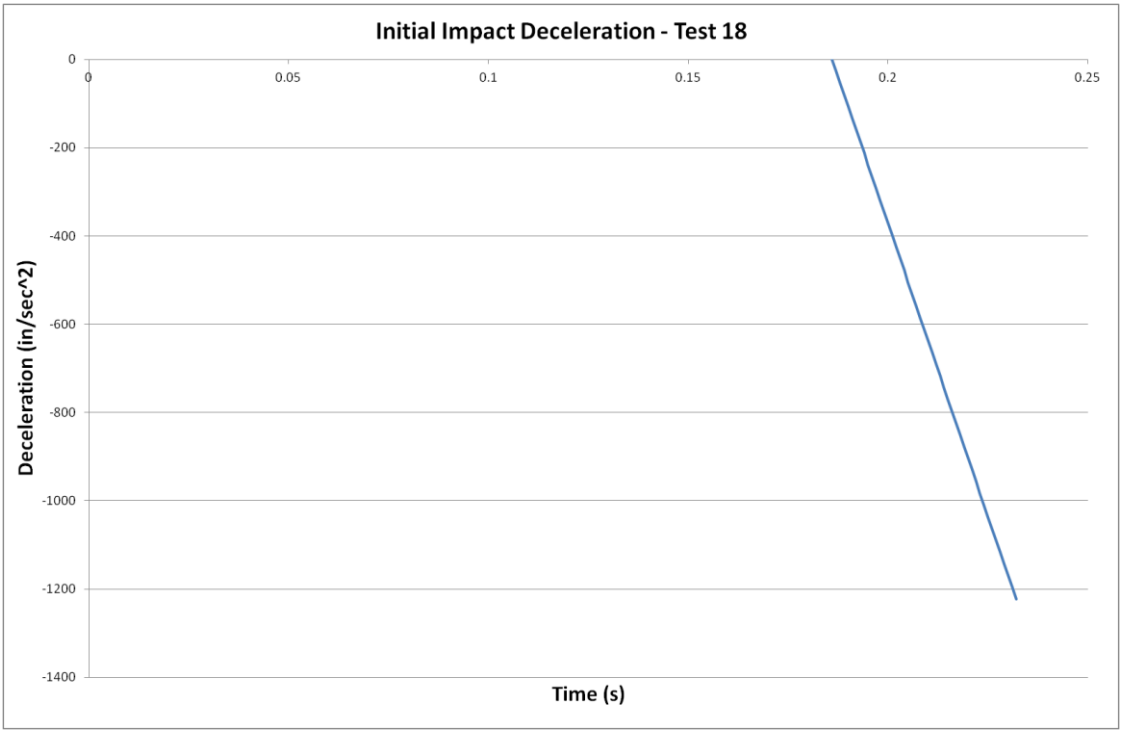
Initial Impact Deceleration - Test 18
Deceleration (in/sec^2)
Time (s)
0
-200
-400
-600
-800
-1000
-1200
-1400
0
0.05
0.1
0.15
0.2
0.25

A.2.13 Plate Soil Compacted I

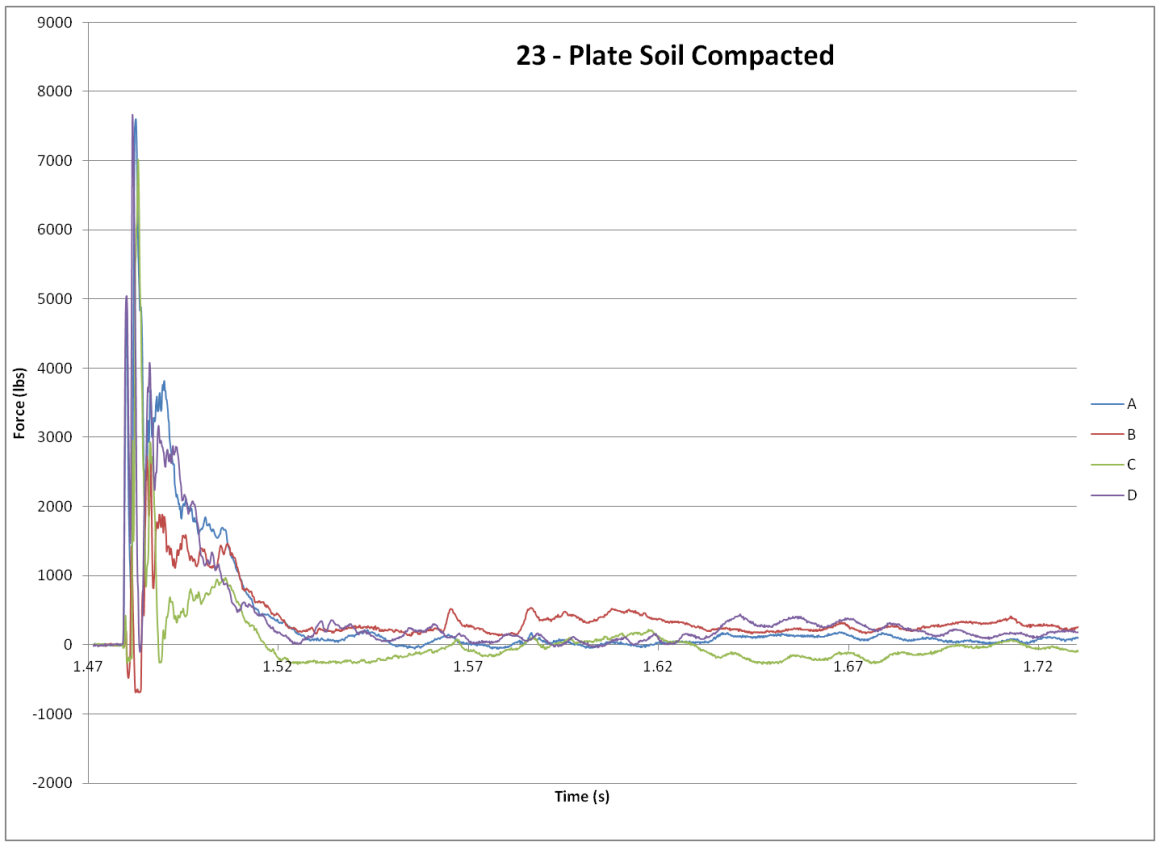

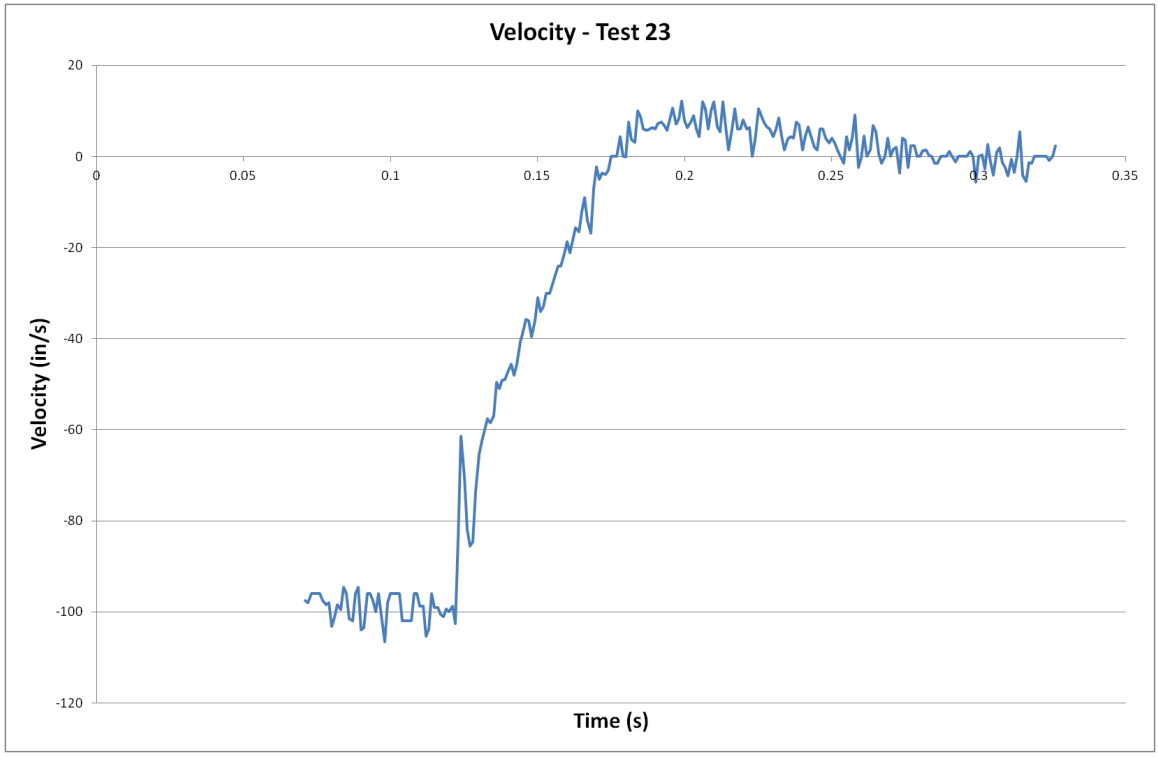
Velocity - Test 23
Velocity (in/s)
Time (s)
20
0
-20
-40
-60
-80
-100
-120
0
0.05
0.1
0.15
0.2
0.25
0.3
0.35

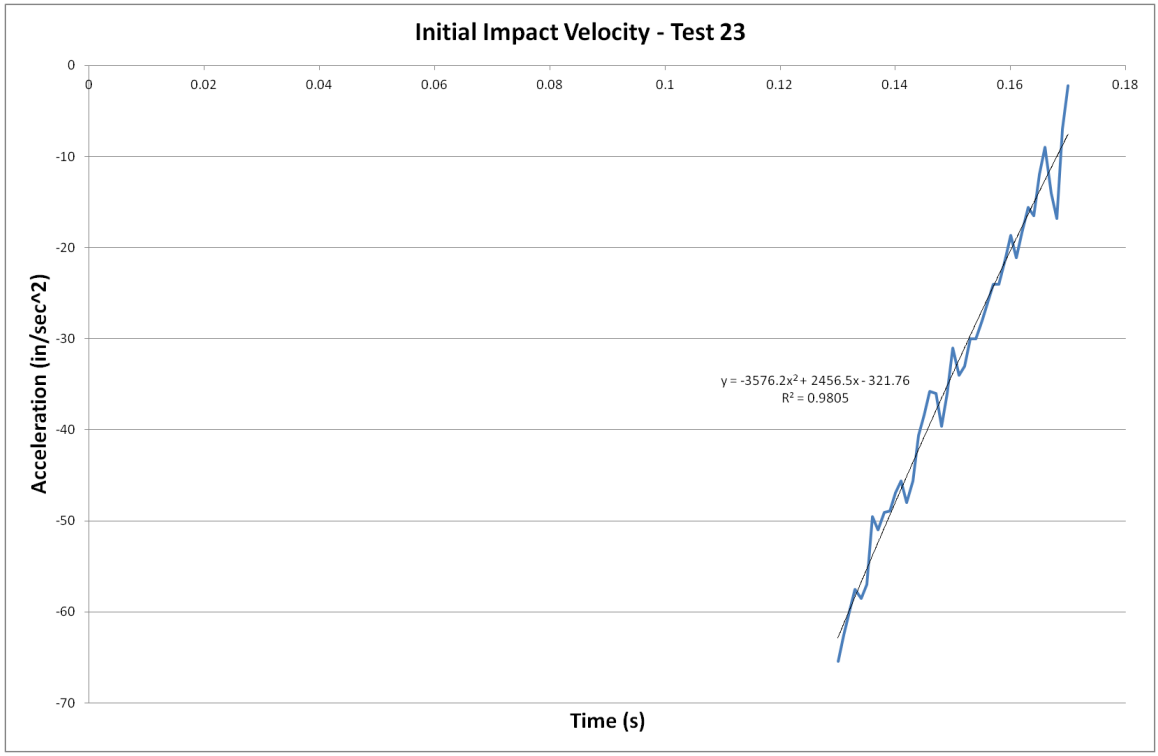
Initial Impact Velocity - Test 23
Acceleration (in/sec^2)
Time (s)
y = -3576.2x² + 2456.5x - 321.76
R² = 0.9805
0
-10
-20
-30
-40
-50
-60
-70
0
0.02
0.04
0.06
0.08
0.1
0.12
0.14
0.16
0.18

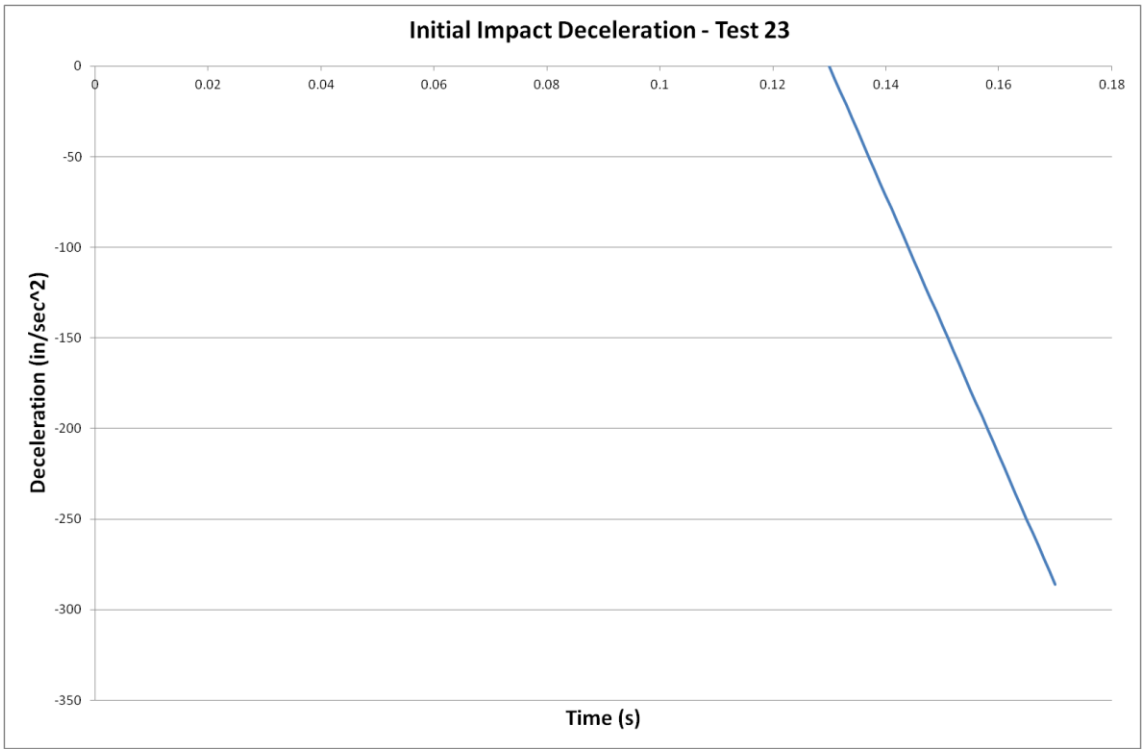
Initial Impact Deceleration - Test 23
Deceleration (in/sec^2)
Time (s)
0
-50
-100
-150
-200
-250
-300
-350
0
0.02
0.04
0.06
0.08
0.1
0.12
0.14
0.16
0.18

A.2.14 Plate Soil Compacted II

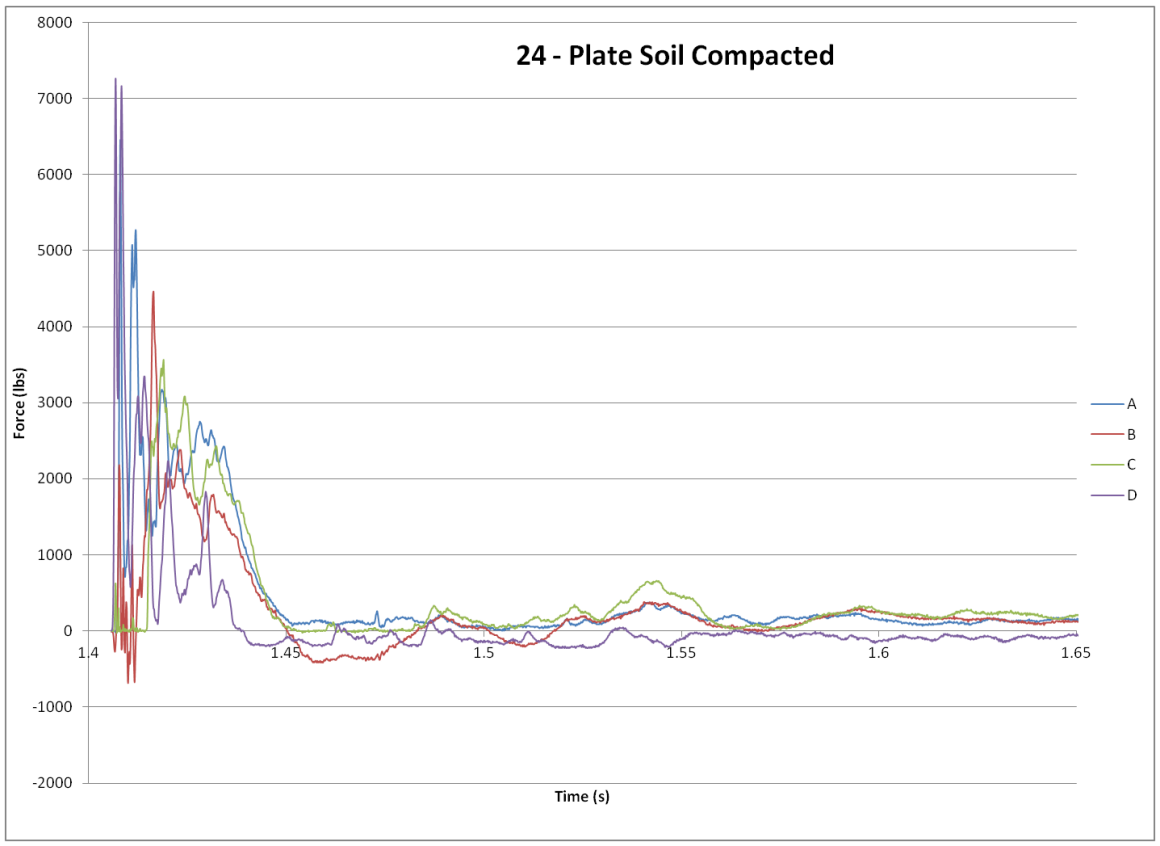

Below, two sets of acceleration and velocity graphs are given for test #24. Two tracking dots were put on the impact carriage. The reason for this is to calibrate the tracking software. The dots were placed 3 inches apart. Looking at the graphs, it shows that consistency was achieved and either tracking dot produces very similar results.

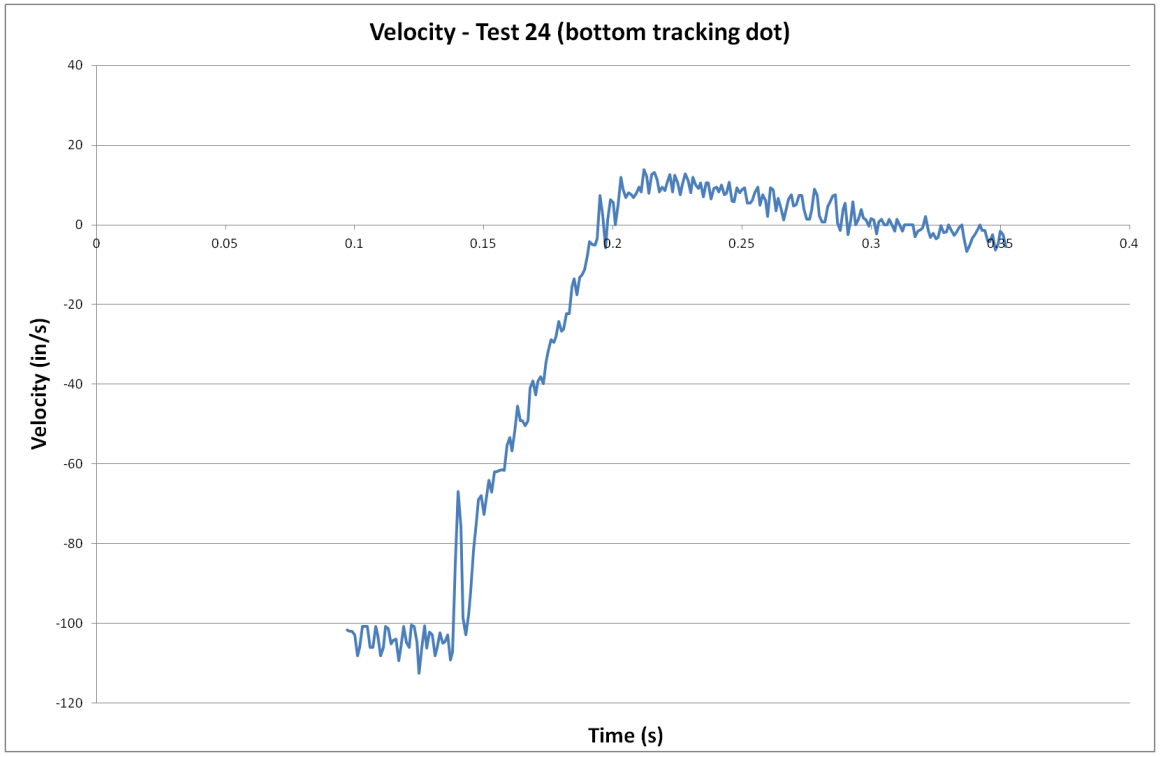
Velocity - Test 24 (bottom tracking dot)
Velocity (in/s)
Time (s)
40
20
0
-20
-40
-60
-80
-100
-120
0
0.05
0.1
0.15
0.2
0.25
0.3
0.35
0.4

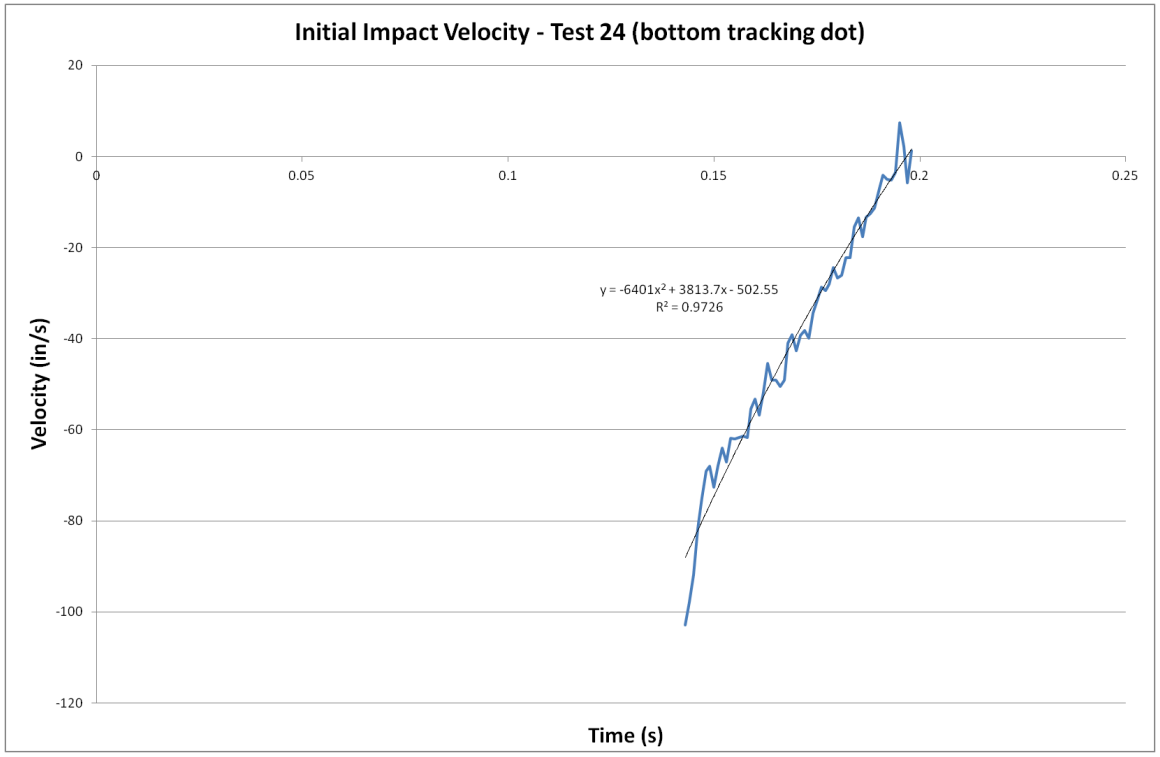
Initial Impact Velocity - Test 24 (bottom tracking dot)
Velocity (in/s)
Time (s)
y = -6401x² + 3813.7x - 502.55
R² = 0.9726
20
0
-20
-40
-60
-80
-100
-120
0
0.05
0.1
0.15
0.2
0.25

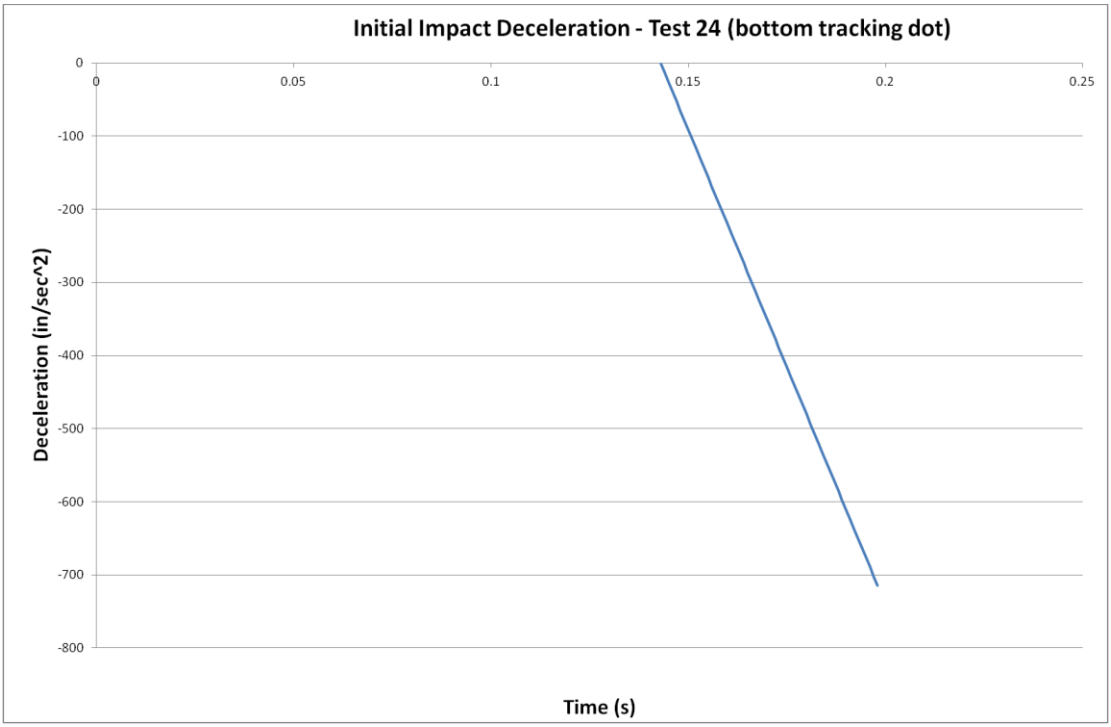
Initial Impact Deceleration - Test 24 (bottom tracking dot)
Deceleration (in/sec^2)
0
-100
-200
-300
-400
-500
-600
-700
-800
0
0.05
0.1
0.15
0.2
0.25
Time (s)

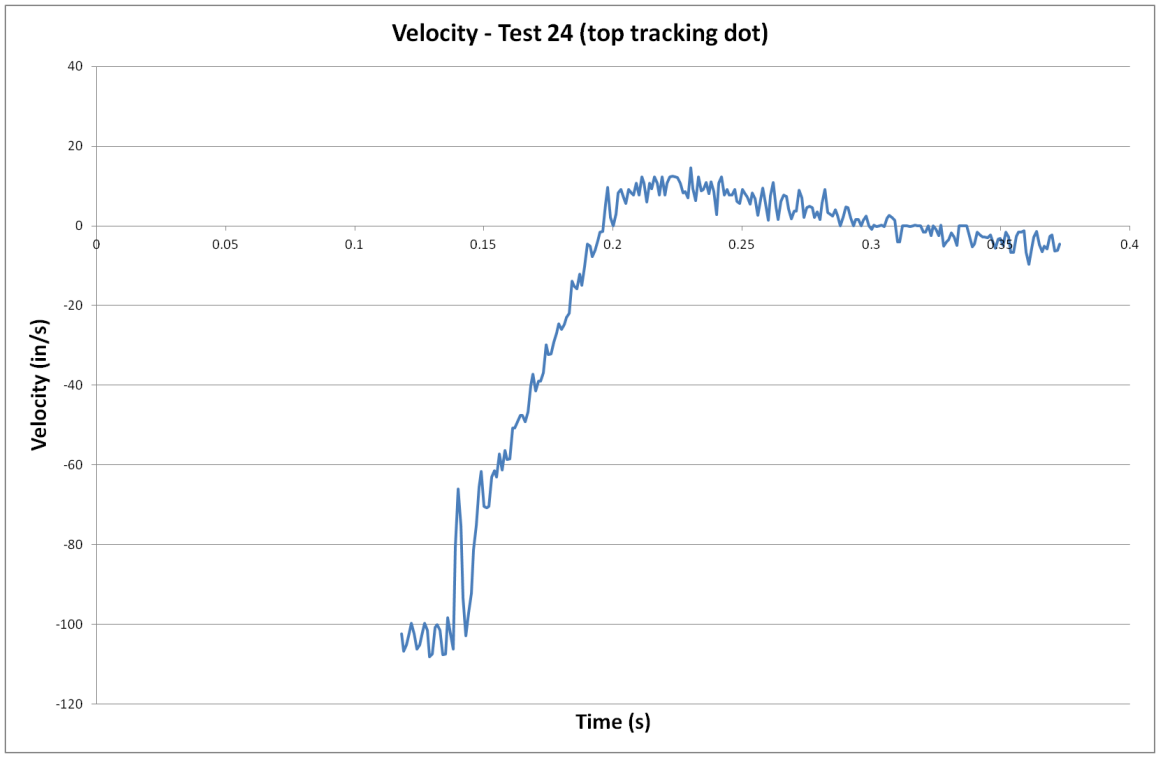
Velocity - Test 24 (top tracking dot)
Velocity (in/s)
40
20
0
-20
-40
-60
-80
-100
-120
0
0.05
0.1
0.15
0.2
0.25
0.3
0.35
0.4
Time (s)

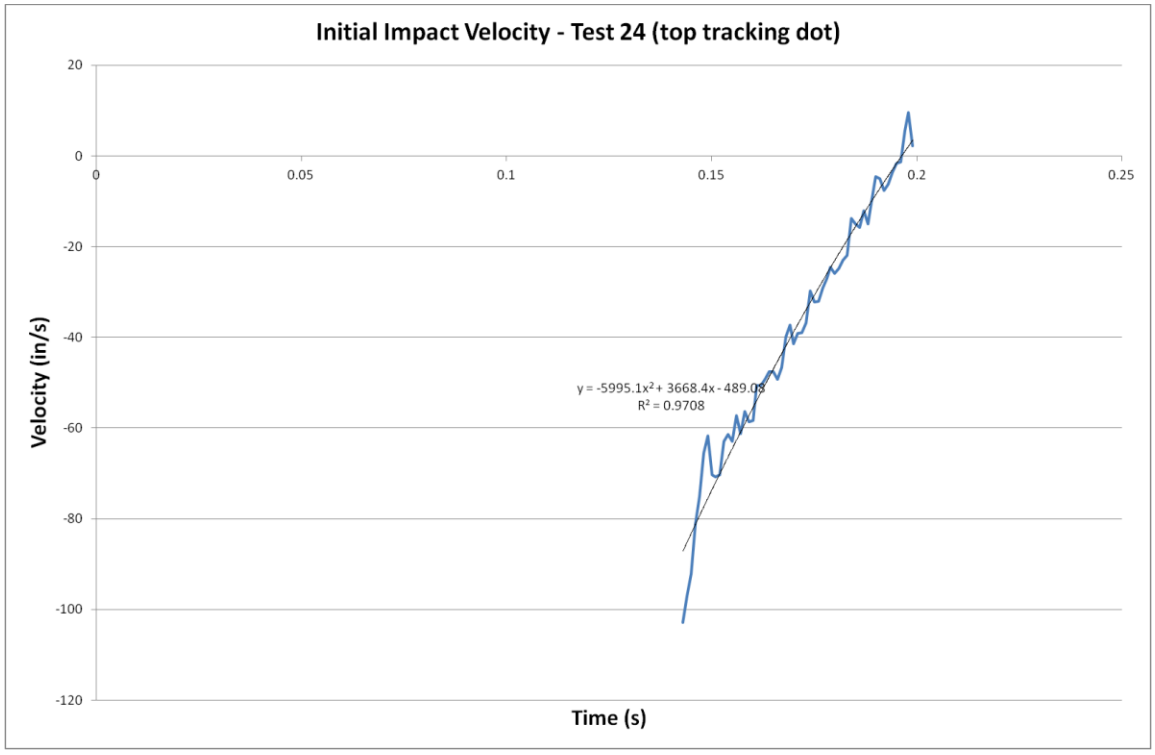
Initial Impact Velocity - Test 24 (top tracking dot)
Velocity (in/s)
Time (s)
y = -5995.1x² + 3668.4x - 489.03
R² = 0.9708
20
0
-20
-40
-60
-80
-100
-120
0
0.05
0.1
0.15
0.2
0.25

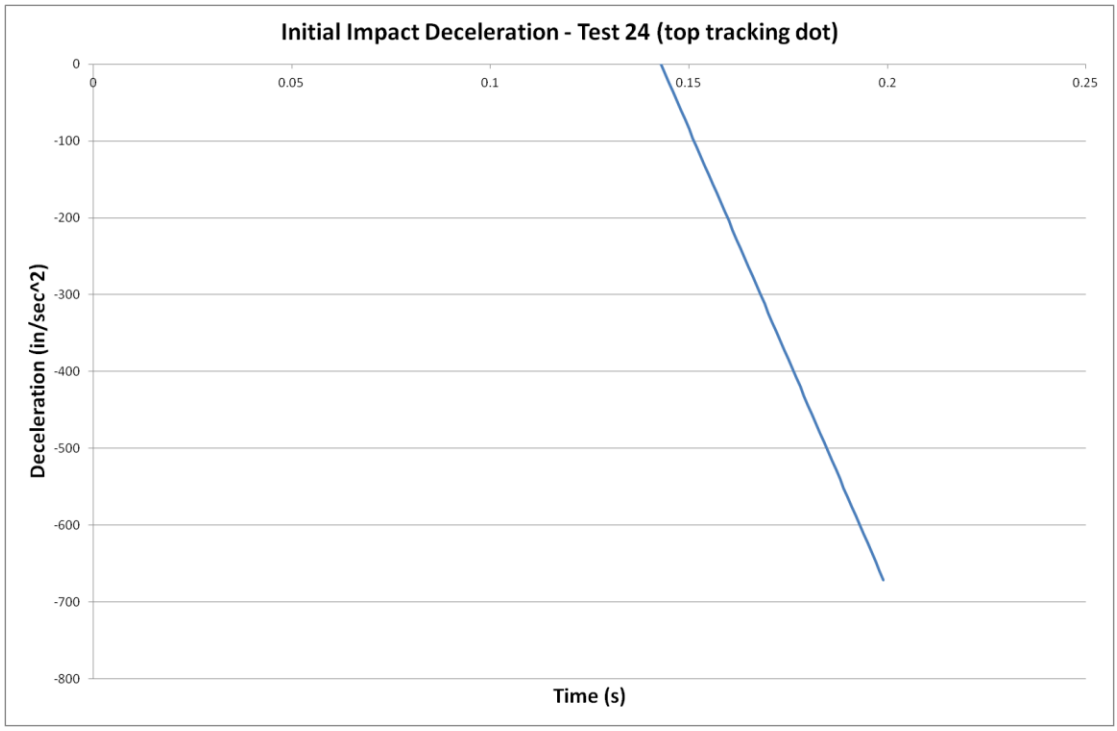
Initial Impact Deceleration - Test 24 (top tracking dot)
Deceleration (in/sec^2)
Time (s)
0
-100
-200
-300
-400
-500
-600
-700
-800
0
0.05
0.1
0.15
0.2
0.25

A.2.15 Plate River Gravel I

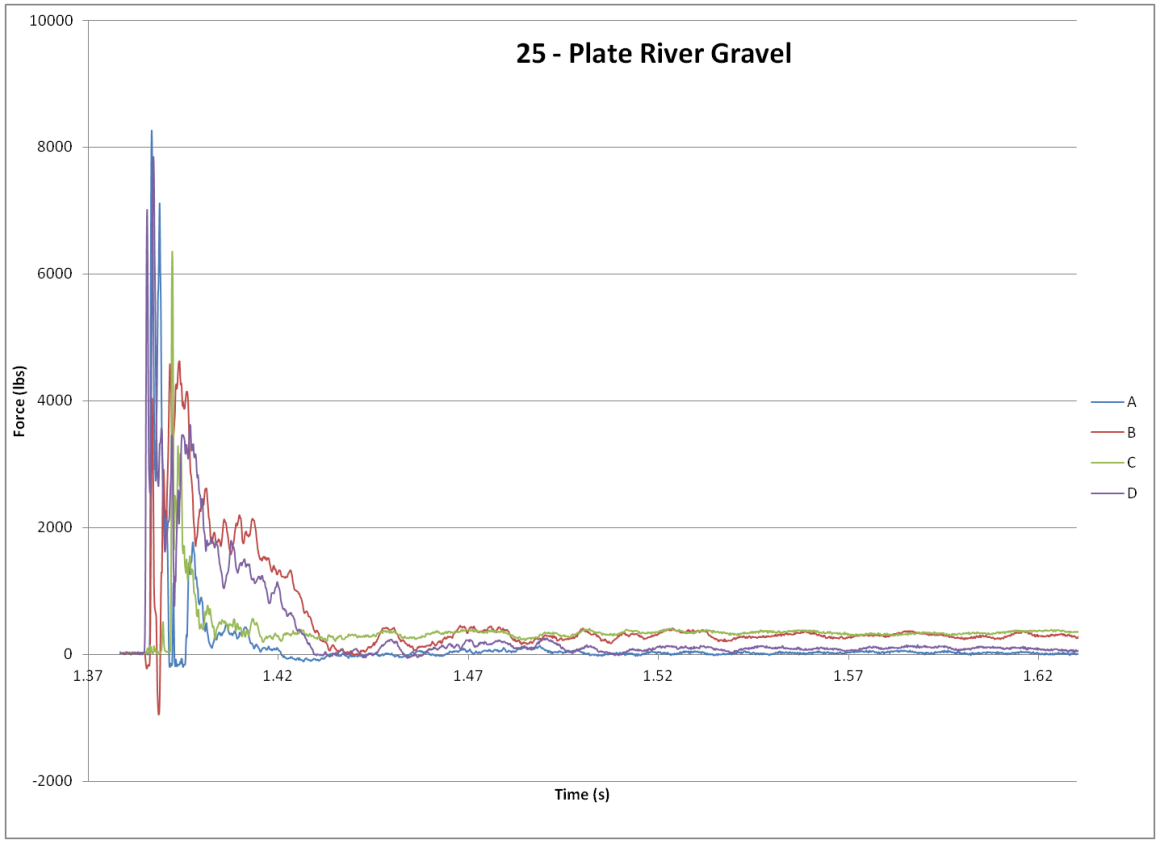

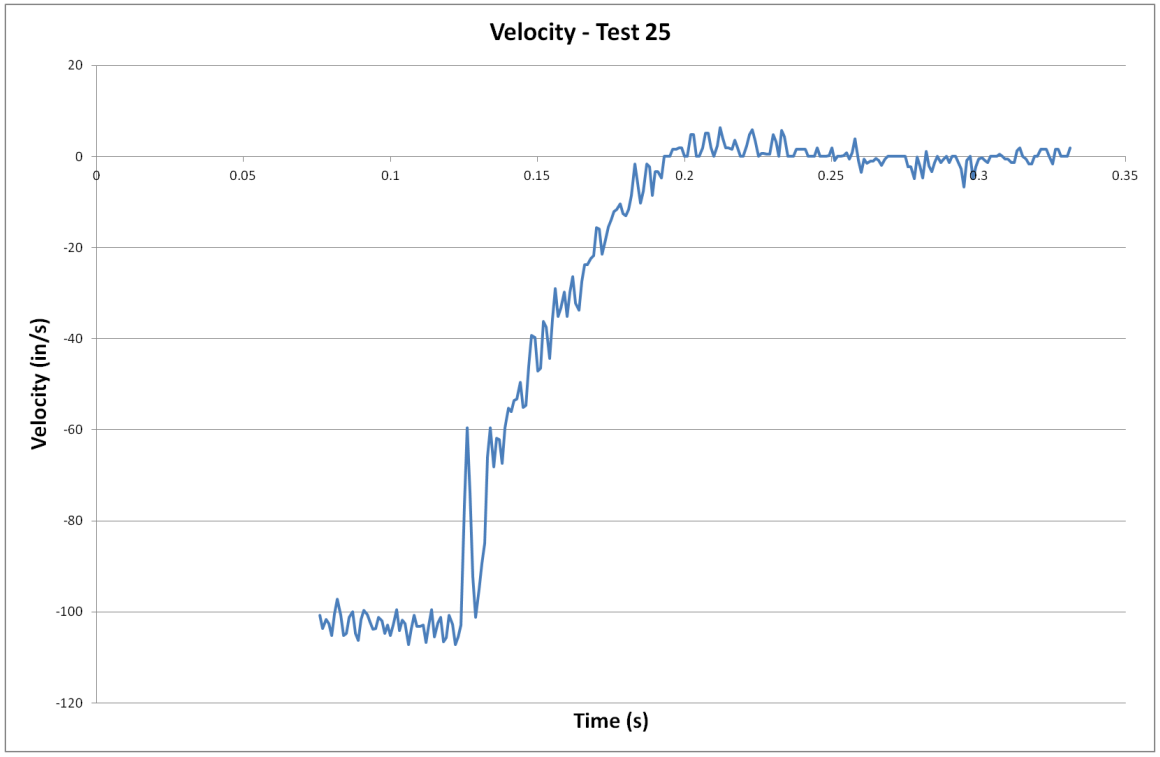
Velocity - Test 25
Velocity (in/s)
Time (s)
20
0
-20
-40
-60
-80
-100
-120
0
0.05
0.1
0.15
0.2
0.25
0.3
0.35

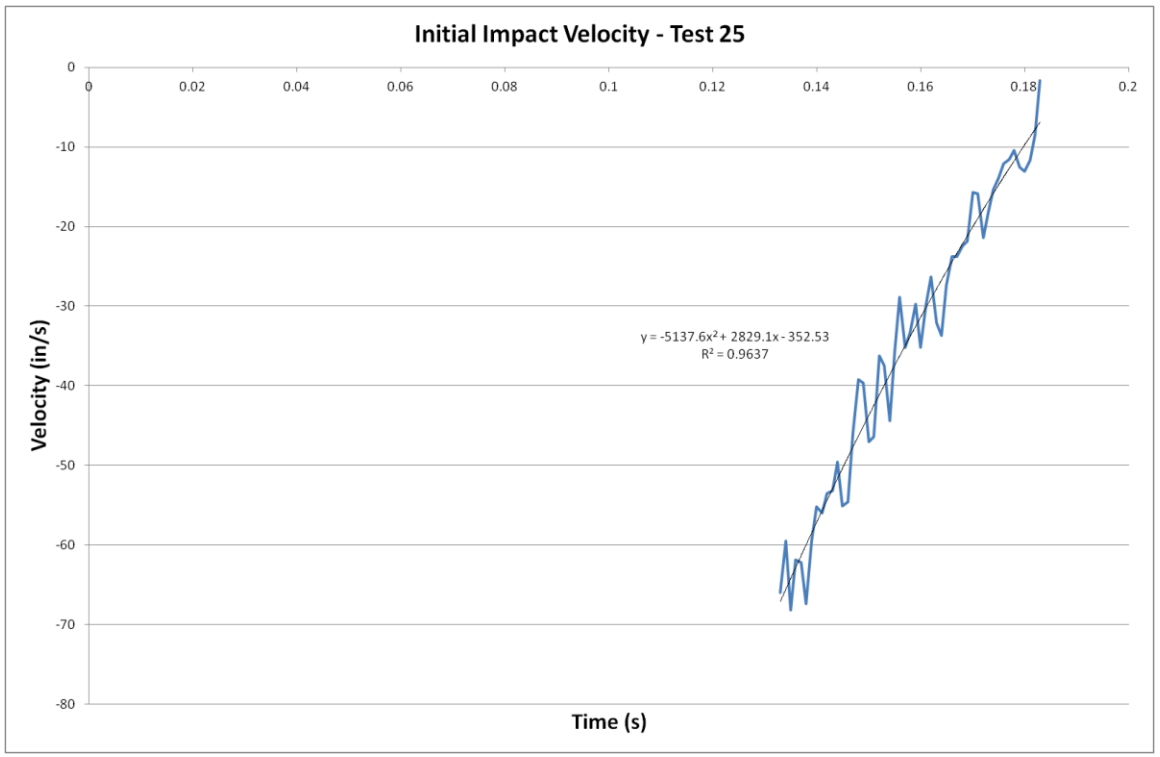
Initial Impact Velocity - Test 25
Velocity (in/s)
Time (s)
y = -5137.6x² + 2829.1x - 352.53
R² = 0.9637
0
-10
-20
-30
-40
-50
-60
-70
-80
0
0.02
0.04
0.06
0.08
0.1
0.12
0.14
0.16
0.18
0.2

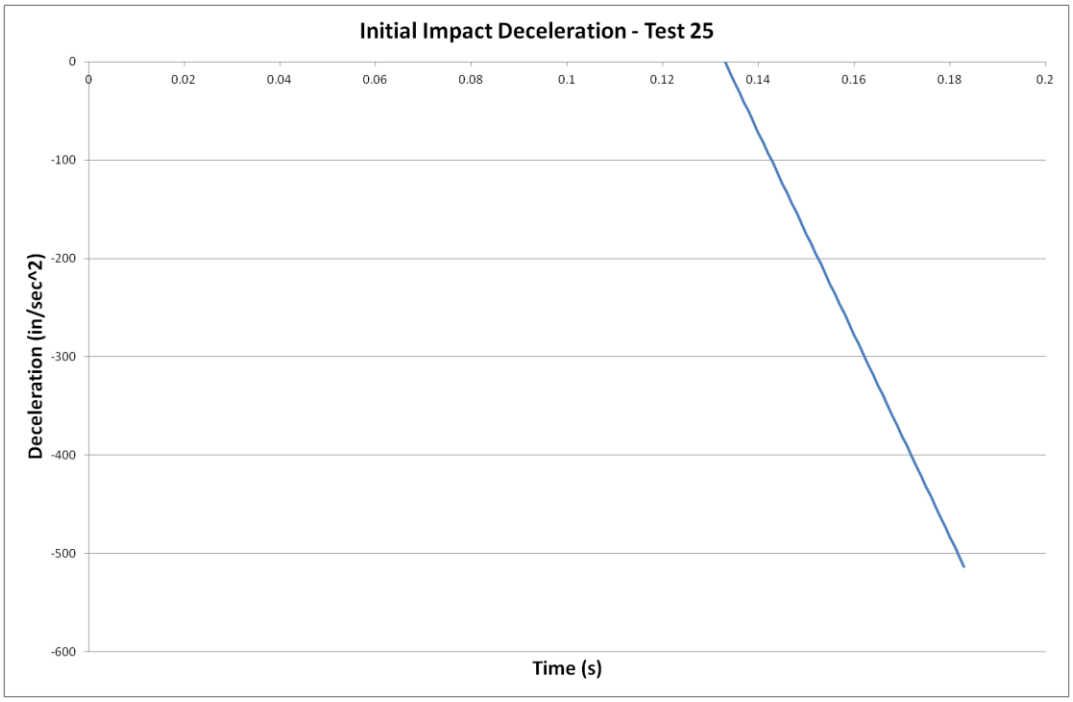
Initial Impact Deceleration - Test 25
Deceleration (in/sec^2)
Time (s)
0
-100
-200
-300
-400
-500
-600
0
0.02
0.04
0.06
0.08
0.1
0.12
0.14
0.16
0.18
0.2

A.2.16 Plate River Gravel II

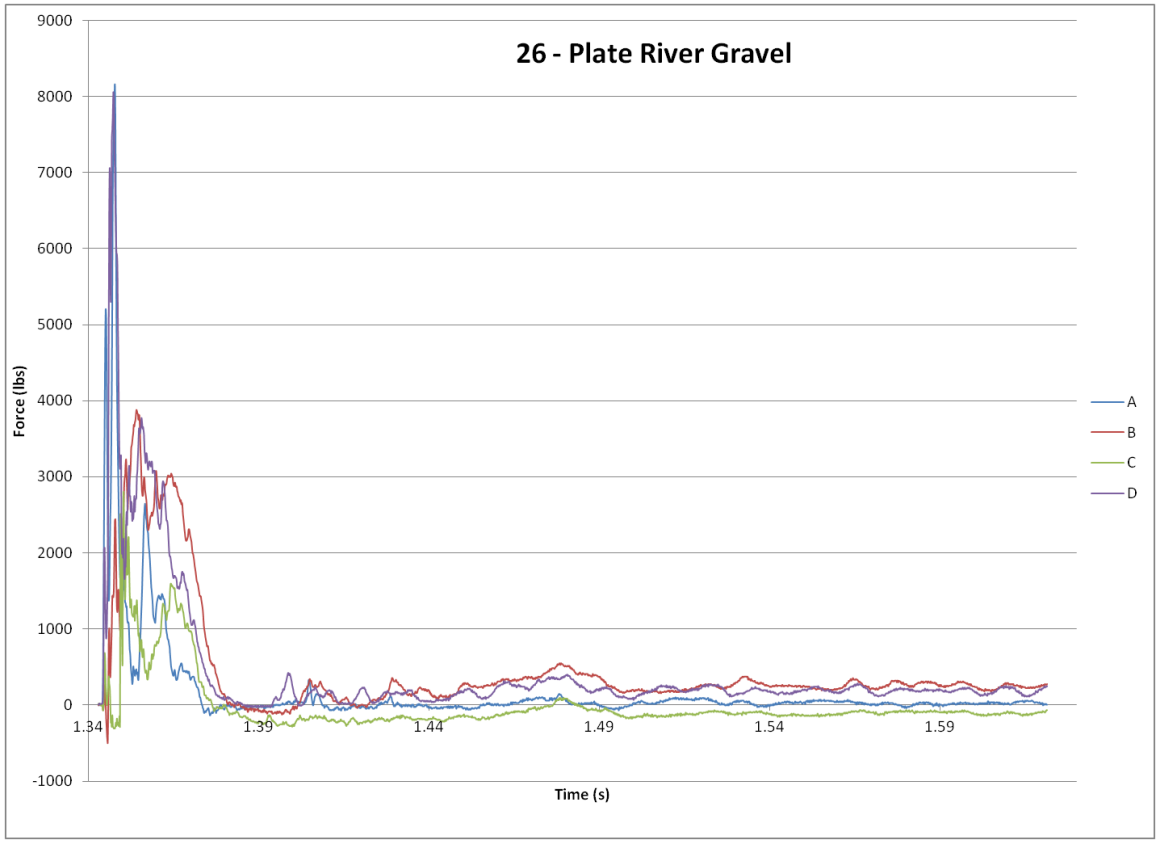

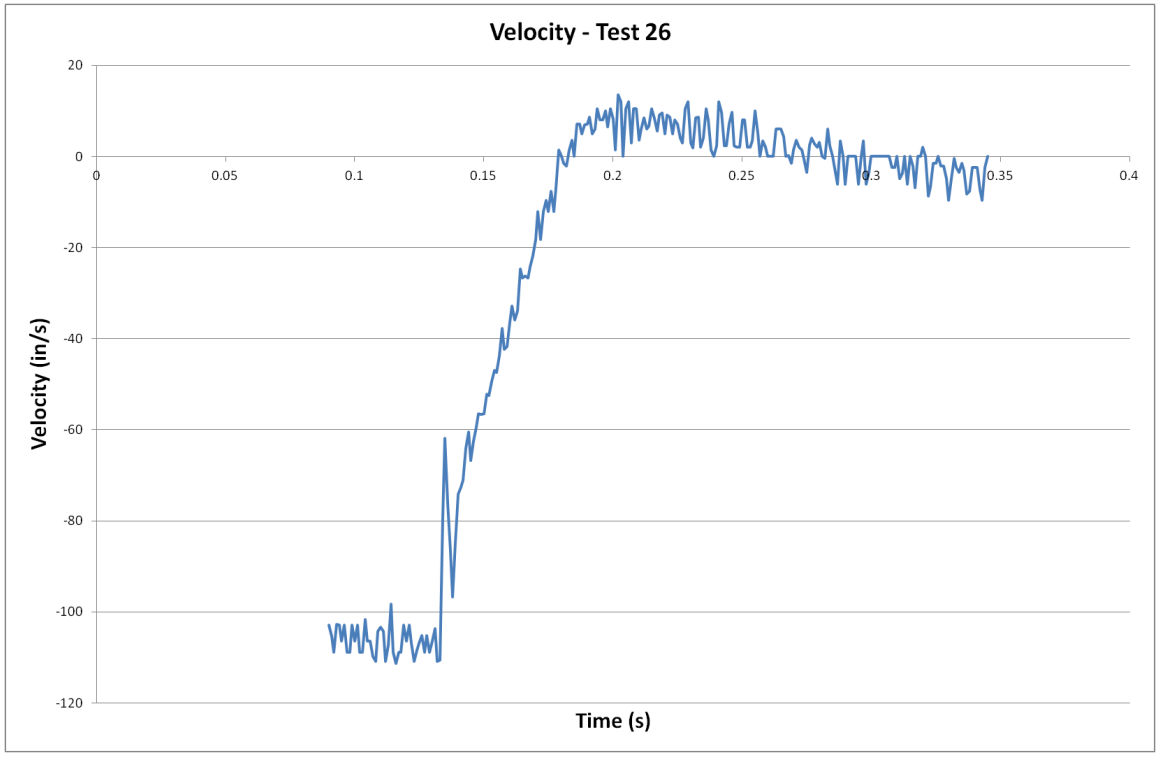
Velocity - Test 26
Velocity (in/s)
Time (s)
20
0
-20
-40
-60
-80
-100
-120
0
0.05
0.1
0.15
0.2
0.25
0.3
0.35
0.4

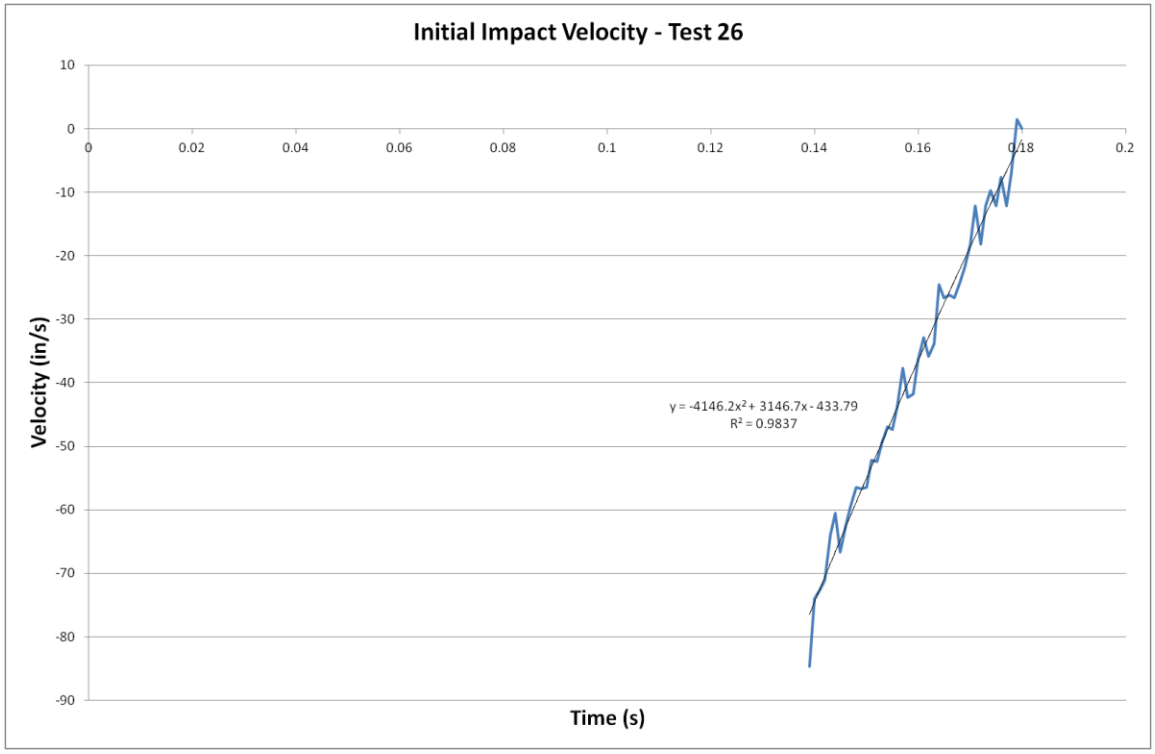
Initial Impact Velocity - Test 26
Velocity (in/s)
Time (s)
y = -4146.2x² + 3146.7x - 433.79
R² = 0.9837
10
0
-10
-20
-30
-40
-50
-60
-70
-80
-90
0
0.02
0.04
0.06
0.08
0.1
0.12
0.14
0.16
0.18
0.2

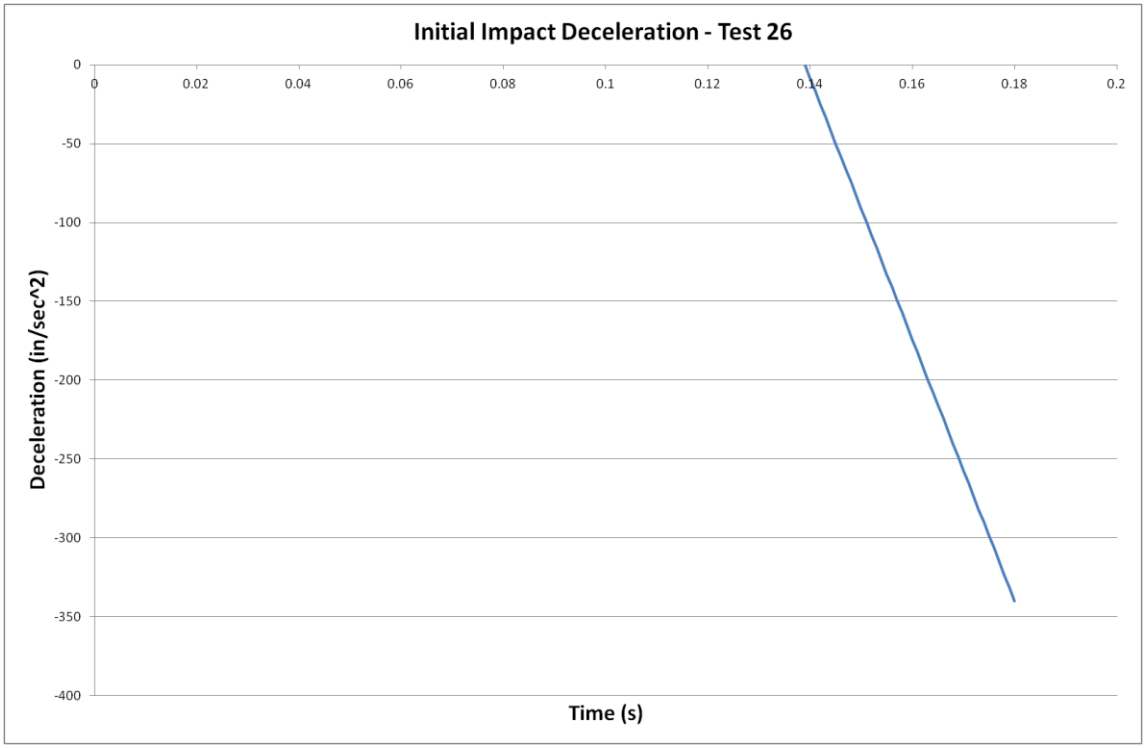
Initial Impact Deceleration - Test 26
Deceleration (in/sec^2)
0
-50
-100
-150
-200
-250
-300
-350
-400
0
0.02
0.04
0.06
0.08
0.1
0.12
0.14
0.16
0.18
0.2
Time (s)